République Algérienne Démocratique et Populaire

UNIVERSITE SAAD DAHLEB BLIDA 1

Institut d'Aéronautique et des Études Spatiales

MEMOIRE DE MASTER

Spécialité : Aéronautique
Option : CNS/ATM

Thème:

Modeling and Simulation of a Strap-Down Inertial Navigation System's Errors due to the Inertial Sensors

Realisé par :

- Mlle. Azzoune Imane
- Mlle. Benaouda Hamida

Jury:

- Encadré par: Dr. Rahmouni Mohammed.
- Président du Jury:.....
- Examinateur: .....

IAES BLIDA 2019-2020

DEDICATION

Let me first thank Allah the Almighty for having

enlightened my path and for guiding my steps.

I dedicate this work:

To those who sacrificed their lives for me

To those who never stopped encouraging and supporting me,

To those whom their love has given me

the will to always go forward,

My very dear parents, may God the Almighty protect them.

Soulmates Sara, Cherifa and maria

and my brother Mohamed Rida.

To my colleague Said Cheroudi Bouzidi

My colleagues and my friends

in the Aeronautics specialty,

Especially my partner Hamida for the nice moments we

spent together

IMANE

DEDICATION

I want to give thanks to the most merciful God

for granting me health, morale and his blessing

for the success of my studies

Until this culmination.

I dedicate this work:

To my dear parents,

my treasure in this life.

For their patience, love,

support and encouragement.

To my sisters and brothers.

My colleagues in the Aeronautics specialty,

and all who participated in the development

of this work, and my partner Imane.

HAMIDA

T H A N K S

First of all, we thank God, the Almighty,

for giving us the courage, patience and will

to complete this work.

We would like to sincerely thank, the jury members for this thesis, Dr. RAHMOUNI Mohammed Lecturer at the Institute of Aeronautics at Saad Dahlab University,

who as our promoter, has always been attentive and available throughout the realization of this THESIS

for inspiration, his valuable advices and encouragements

and the time he was kind enough to devote to us.

We do not forget to thank all our teachers for their attributions in our training throughout our university courses

Our thanks go to all those who contributed

from far or near to the realization of this thesis and to all the friends and colleges

To all who have supported us from near or far to carry out this work, we tell them:

THANK YOU

Imane & Hamida

ABSTRACT

ملخص

تحديد الموقع هو مسألة مطروحة بشده في عصرنا الحالي، مثلا للطائرات بدون طيار وبعض المركبات الذكية ولهذا تمحورت دراستنا حول ثلاث جوانب: أولا تحديد موقع متحرك خلال تنقّلها ومن أجل هذا اعتمدنا على نظام الملاحة بالقصور الذاتي

من جانب ثاني إنشاء نموذج يمثل مولد مسار مثالي بدون أخطاء، وآخر مع حقن أخطاء مختلفة على مستوى أجهزة الاستشعار من أجل ملاحظة تباعد المسارين الناتجين عن كلا النموذجين وأخيرا تحقيق واجهة رسومية لحساب وعرض عدد من المعلومات الخاصة بالملاحة انطلاقا من معطيات نظام الملاحة بالقصور الذاتي وحاسوب المتن.

La localisation est une problematique en plein essor avec, par exemple, l expansion des drones civils et autres vehicules intelligents. Raison pour laquelle cette etude va se focaliser sur trois aspects. Dans un premier temps, un effort sera porte sur l aspect positionnement d un mobile au cour de son deplacement. Pour cela il est necessaire de se pencher sur le systeme de navigation inertielle INS. Dans un deuxieme temps, Nous allons creer un modele representant un generateur de trajectoire qui ne fournit aucune erreur sur la position, un autre modele(INS) qui differe du premier par l injection de plusieurs types d erreurs au niveaux des capteurs inertielle pour faire diverger la trajectoire de celle du reference, finalement la visualisation de la position et de l erreur en position qui s influent par le type de capteur inertiel choisi. A la fin, la realisation d une logiciel simulink permettant de calculer et d afficher un certain nombre de parametres de navigation a partir de donnees INS *Abstract :*• The location is a problematic booming with, for example , the expansion of the drones civilians and other intelligent vehicles. Reason for which this study will focus on three aspects. In a first time, an effort will be focused on the aspect of positioning a mobile at court of its travel. For this it is necessary to look on the inertial navigation system INS. In a second time, we are going to create a model representing a generator of trajectory that provides no error on the position, another model(INS) which differs from the first by the injection of several types of errors at the levels of the inertial sensors for to diverge the trajectory of that of the reference, finally the visualization of the position and of the error in position which is influential by the type of inertial sensor chosen.In the end, the achievement of a graphical interface allowing to calculate and display a number of Navigation settings from data INS and ADC (Air Data Computer).

Table 1: List of Acronyms

ARW	Angle Random Walk
CTP	Conventional Terrestrial Pole
DR	Dead Reckoning
DCM	Direction Cosine Matrices
DTG	Dynamically Tuned Gyroscopes
ECI	Earth-Centered Inertial Frame
ECEF	Earth-Centered Earth-Fixed Frame
ENU	East-North-UP navigation frame
GPS	Global Positioning System
GNSS	Global Navigation Satellite Systems
GRS	Geographic Reference System
HRG	Hemispherical Resonant Gyroscopes
INS	Inertial Navigation System
IMU	Inertial Measurement Unit
IFOG	Interferometric FIber-Optic Gyroscopes
IEEE	
LLF	Local-Level Frame
MEMS	Micro-Electro-Mechanical-Systems
NEMS	Nano-Electro-Mechanical- Systems
RF	Radio Frequency
RLG	Ring Laser Gyroscopes
SINS	Strapdown Inertial Navigation System
UAV	
VRW	Velocity Random Walk
VBAs	Vibrating Beam Accelerometers
b	Body frame
e	Earth frame
i	Inertial frame
n	Navigation frame
O	Center of the Earth
P	Center of the vehicle
p	Wander azimuth frame

Table 2: Nomenclature

x, y, z	3 orthogonal axes or the 3 components of a Cartesian coordinate
A^T	Transpose of matrix A
a	Vehicle acceleration
g^p	Gravity vector measured in p-frame
g	Local gravity scalar
g_0	Local gravity scalar at sea level
F	The force
f	specific force
m	The mass of the body
e	Major eccentricity of the ellipsoid of the Earth
ψ_G	Grid azimuth angle of the vehicle in b-frame with respect to p-frame
α	Wander azimuth angle of p-frame with respect to n-frame
φ	
ω	Angular Speed (disturbed signal) expressed in deg/s
ψ	Heading angle of the vehicle in b-frame with respect to n-frame
θ	
	Grid pitch angle of the vehicle in b-frame with respect to n-frame or p-frame
γ	Grid roll angle of the vehicle in b-frame with respect to n-frame or p-frame
$\Delta\psi$	Increase of the heading angle ψ
$\Delta\theta$	Increase of the grid pitch angle θ
$\Delta\gamma$	Increase of the grid roll angle γ
λ	Longitude of the vehicle
ΦL	Latitude of the vehicle
h	Altitude of the vehicle above the sea level of the Earth
Φ_0, λ_0, h_0	Initial vehicle position (latitude, longitude, height)
V_0	Initial vehicle velocity (east, north, up)
V	Vehicle velocity (east, north, up)
V_g	Vehicle ground velocity
R_e	Length of the semi-major axis of the Earth
R_N	Meridian radius of curvature of the Earth

T_circle	Period of the circle trajectory in simulation
T_sshape	Period of the s-shape trajectory in simulation
A_sshape	Amplitude of the s-shape trajectory in simulation
PV	Position and velocity
N	sensitivity axis misalignment (in radians)
B	bias (expressed in percent of span)
k_c	crossaxis sensitivity (expressed in percent ofSpan of a
ν	sensor noise (given by its density v_d expressed in $\mu g/Hz^(1/2)$
K	scale factor (expressed in mV/g)
ΔK	scale factor error (percents of K)
S	Sensitivity to the acceleration
r_e^n	Vehicle position measured in n-frame with respect to e-frame
$V_e^(p)$	Velocity vector measured in p-frame with respect to e-frame
C_b^p	Vehicle attitude DCM used to transform the measured angle in b frame to p-frame, with its
$C_(p)^b$	Transpose ofC_b^p is used to transform the measured vector in p-frame to b-frame
R_E	Transverse radius of curvature of the Earth
R_xp, R_yp	Free curvature radiuses
Q	Quaternion q1, q2, q3, q4: Four components of the quaternion Q
t	The time
Δt	Time step
$C_e^(p)$	Vehicle position DCM used to transform the measured vector in e-frame to p-frame, with its
C_p^e	Transposeof C_e^p is used to transform the measured vector in p-frame to e-frame
C_b^n	Vehicle attitude DCM used to transform the measured angle in b-frame to n-frame
f^p	Specific force vector measured in p-frame
f^n	Specific force vector measured in n-frame
f^b	Specific force vector measured in b-frame; the output of the 3 accelerometers

ω^i	Constant value of the turn rate of the Earth, $\omega_e^i = 7.2921151467 \cdot 10^{-5} rad/s$
$\omega_i e^n$	Turn rate of the Earth measured in n-frame
$\omega_i b^b$	Turn rate of the b-frame with respect to i-frame, which is measured in b-frame
$\omega_e n^n$	Transport rate of the n-frame with respect to e-frame, which is measured in n-frame
$\omega_i e^e$	Turn rate of the e-frame with respect to i-frame, which is measured in e-frame
$\omega_e p^p$	Turn rate of the p-frame with respect to e-frame, which is measured in p-frame
$\omega_p e^e$	Turn rate of the e-frame with respect to p-frame, which is measured in e-frame
$\omega_p b^b$	Turn rate of the b-frame with respect to p-frame, which is measured in b-frame
$\omega_n b^b$	Turn rate of the b-frame with respect to n-frame, which is measured in b-frame
$\Omega(\omega)$	Skew matrix form of ω

Contents

List of Figures

List of Tables

General Itroduction

Navigation primarily dealt with vessels traveling in sea. However, it has now permeated into every imaginable form of transportation as well as various other applications including location-based services, search and rescue, law enforcement, road and air travel, remote asset tracking, fleet management, intelligence gathering, sports, public safety, and environmental assessment and planning. Advances in microelectronics and miniaturization of integrated circuits have facilitated the production of inexpensive inertial sensors, global positioning system (GPS) receivers and powerful computers. A navigation system can either be autonomous or be dependent on external sources, or in some cases a combination of the two. The fusion of the two systems is traditionally based on the technique of Kalman filtering.

There are two fundamental methods for finding a navigation solution: position fixing and dead reckoning (DR).

Position fixing is based on the information of external sources with known locations, with GPS being a typical example, On the other hand, dead reckoning is autonomous and relies on knowledge of the initial location, speed and heading information.

Inertial navigation is a dead reckoning system which uses accelerometers and gyroscopes to monitor translational motion and rotational motion respectively. [1].

General Classification of Positioning Techniques

Techniques Using Relative Measurements (Known as DR)

Odometry The odometry data is obtained by using sensors that measure the rotation of the wheel axes and the steer axes This employs inertial sensors (gyroscopes and accelerometers) which measure the rotation rates and the specific forces from which acceleration can be obtained.

Inertial navigation systems are autonomous,Starting from a known position and orientation, measurements are integrated once for gyroscopes and twice for accelerometers to provide orientation and position respectively Inertial navigation alone, especially with low cost sensors, is thus unsuitable for accurate positioning over an extended period of time.

Techniques Using Absolute Measurements (Known as Reference-based Systems)

Electronic Compasses an electronic compass is a device which uses magnetometers to provide heading measurements relative to the Earth's magnetic north by observing the direction of the local magnetic field.

Active Beacons This approach can be used if the moving platform is to navigate in an already known environment, and can provide accurate positioning information.There are several positioning algorithms that can be used with different active beacon systems, such as the trilateration-based algorithm, the triangulation-based algorithms, and the fingerprinting algorithms. Trilateration is the calculation of a vehicle's position based on distance measurements relative to a known beacon using, for example, time-of-flight information. Triangulation is the calculation of a vehicle's position and possibly its orientation based on the angles at which beacons are seen relative to the moving platform's longitudinal axis.

Global Navigation Satellite SystemsGNSS is mainly a technology for outdoor navigation. Currently, the most popular example is GPS, which is a constellation of satellites that transmit encoded radio frequency (RF) signals. By means of trilateration, ground receivers can calculate their position using the travel time of the satellites's signals and information about their current location, this being included in the transmitted signal.

Landmark Navigation This approach can be used if the moving platform is to navigate in an environment that is well known. Landmarks are distinct objects or features such as geometric shapes that can be detected and distinguished by appropriate sensors on a vehicle.

Map-Based Positioning (Or Model Matching) This approach can be used if the moving platform is to navigate in a specific mapped environment. In this approach, the moving platform uses its sensors to perceive its local environment, and this perception is then compared to a map previously stored in its memory. If a match is found, then the vehicle can calculate its position and orientation in this specific environment. Cameras and laser range finders are examples of sensors that can be used with this type of positioning.

Combined Systems

For the category that uses relative measurements (i.e. dead reckoning) the determination of the current vehicle position uses the knowledge of the previous position and the measurement of its latest movements. For the category of absolute measurements (i.e. reference-based systems) the current vehicle position is calculated by measuring known reference points but without knowledge of its previous trajectory. Usually two methods or more, involving at least, one from each group, are combined in order to obtain a reliable navigation solution.

Chapter 1

Basic Navigational Mathematics, Reference Frames and the Earth's Geometry

Navigation algorithms involve various coordinate frames and the transformation of coordinates between them. For example, inertial sensors measure motion with respect to an inertial frame which is resolved in the host platform's body frame. This information is further transformed to a navigation frame. A GPS receiver initially estimates the position and velocity of the satellite in an inertial orbital frame. Since the user wants the navigational information with respect to the Earth, the satellite's position and velocity are transformed to an appropriate Earth-fixed frame. Since measured quantities are required to be transformed between various reference frames during the solution of navigation equations, it is important to know about the reference frames and the transformation of coordinates between them. Assume r^k vector r in k-frame and r^m vector r in m-frame

$$r^k = \begin{pmatrix} x^k \\ y^k \\ z^k \end{pmatrix}$$

$$r^m = {R_k}^m r^k \tag{1.1}$$

$$\overset{k}{r} = \left(\overset{m}{R_k}\right)^{-1} \overset{m}{r} = \overset{k}{R_m} \overset{m}{r}$$

where R_k^m represents the matrix that transforms vector r from the k-frame to the m-frame. where $\overset{k}{R_m}$ represents the matrix that transforms vector r from the m-frame to the k-frame . If the two

coordinate frames are mutually orthogonal, their transformation matrix will also be orthogonal and its inverse is equivalent to its transpose

$$\overset{m}{R}_k = \left(\overset{k}{R}_m\right)^{-1} = \left(\overset{k}{R}_m\right)^{T}$$

The angular velocity of the k-frame relative to the m-frame, as resolved in the p-frame, is represented by

$$\overset{p}{\omega}_{mk} = \begin{pmatrix} \omega_x \\ \omega_y \\ \omega_z \end{pmatrix}$$

The rotation between two coordinate frames can be performed in two steps and expressed as the sum of the rotations between two different coordinate frames, as shown in Eq. 1.2

$$\overset{k}{\omega}_{pk} = \overset{k}{\omega}_{pm} + \overset{k}{\omega}_{mk} \tag{1.2}$$

The rotation of the k-frame with respect to the p-frame can be performed in two steps: firstly a rotation of the m-frame with respect to the p-frame and then a rotation of the k-frame with respect to the m-frame

Skew-Symmetric Matrix The angular rotation between two reference frames can also be expressed by a skew-symmetric matrix instead of a vector. In fact this is sometimes desired in order to change the cross product of two vectors into the simpler case of matrix multiplication. A vector and the corresponding skew-symmetric matrix forms of an angular velocity vector are denoted as $\overset{p}{\omega}_{mk}$

$$\overset{p}{\omega}_{mk} = \begin{pmatrix} \omega_x \\ \omega_y \\ \omega_z \end{pmatrix} \quad \Rightarrow \quad \overset{p}{\Omega}_{mk} = \begin{pmatrix} 0 & -\omega_z & \omega_y \\ \omega_z & 0 & -\omega_x \\ -\omega_y & \omega_x & 0 \end{pmatrix} \tag{1.3}$$

Basic Operations with Skew-Symmetric Matrices Since a vector can be expressed as a corresponding skew-symmetric matrix, the rules of matrix operations can be applied to most vector operations. If **a, b and c** are three-dimensional vectors with corresponding skew-symmetric matrices **A, B and C**, then following relationships hold

[**Ab**] depicts the skew-symmetric matrix of vector **Ab**

Table 1.1: Operations with Skew-Symmetric Matrices

$\mathbf{a} \cdot \mathbf{b} = \mathbf{a}^T\mathbf{b} = \mathbf{b}^T\mathbf{a}$
$\mathbf{a} \times \mathbf{b} = \mathbf{A}\mathbf{b} = \mathbf{B}^T\mathbf{a} = -\mathbf{B}\mathbf{a}$
$[\mathbf{A}\mathbf{b}] = \mathbf{A}\mathbf{B} - \mathbf{B}\mathbf{A}$
$(\mathbf{a} \times \mathbf{b}) \cdot \mathbf{c} = \mathbf{a} \cdot (\mathbf{b} \times \mathbf{c}) = \mathbf{a}^T\mathbf{B}\mathbf{c}$
$\mathbf{a} \times (\mathbf{b} \times \mathbf{c}) = \mathbf{A}\mathbf{B}\mathbf{c}$
$(\mathbf{a} \times \mathbf{b}) \times \mathbf{c} = \mathbf{A}\mathbf{B}\mathbf{c} - \mathbf{B}\mathbf{A}\mathbf{c}$

Hence the transformation of an angular velocity vector $\overset{p}{\omega}_{mk}$ from the k-frame to the$p$-frame can be expressed as

$$\overset{p}{\omega}_{mk} = \overset{p}{R}_k \overset{k}{\omega}_{mk} \tag{1.4}$$

The equivalent transformation between two skew-symmetric matrices has the special form

$$\overset{p}{\Omega}_{mk} = \overset{p}{R}_k \overset{k}{\Omega}_{mk} \overset{k}{R}_p \tag{1.5}$$

1.1 Coordinate Frames

1.1.1 Earth-Centered Inertial Frame

An inertial frame is defined to be either stationary in space or moving at constant velocity (i.e. no acceleration). All inertial sensors produce measurements relative to an inertial frame resolved along the instrument's sensitive axis [2].

- The origin is at the center of mass of the Earth.
- The z-axis is along axis of the Earth's rotation through the conventional terrestrial pole (CTP).
- The x-axis is in the equatorial plane pointing towards the vernal equinox.
- The y-axis completes a right-handed system.

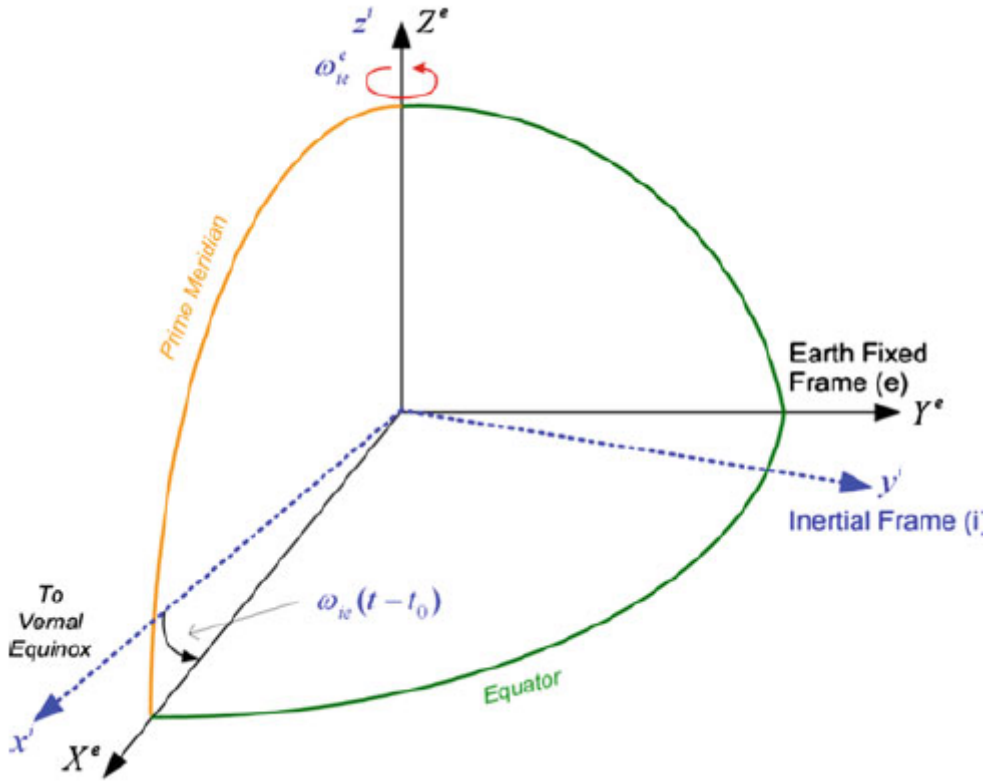

Figure 1.1: An illustration of the ECI and ECEF coordinate frames

1.1.2 Earth-Centered Earth-Fixed Frame

This frame is similar to the i-frame because it shares the same origin and z-axis as the i-frame, but it rotates along with the Earth

- The origin is at the center of mass of the Earth.
- The z-axis is through the CTP.
- The x-axis passes through the intersection of the equatorial plane and the reference meridian (i.e. the Greenwich meridian).
- The y-axis completes the right-hand coordinate system in the equatorial plane.

1.1.3 Local-Level Frame

A local-level frame (LLF) serves to represent a vehicle's attitude and velocity when on or near the surface of the Earth. This frame is also known as the local geodetic or navigation frame.

- The origin coincides with the center of the sensor frame (origin of inertial sensor triad).
- The y-axis points to true north.
- The x-axis points to east.
- The z-axis completes the right-handed coordinate systems by pointing up, perpendicular to reference ellipsoid.

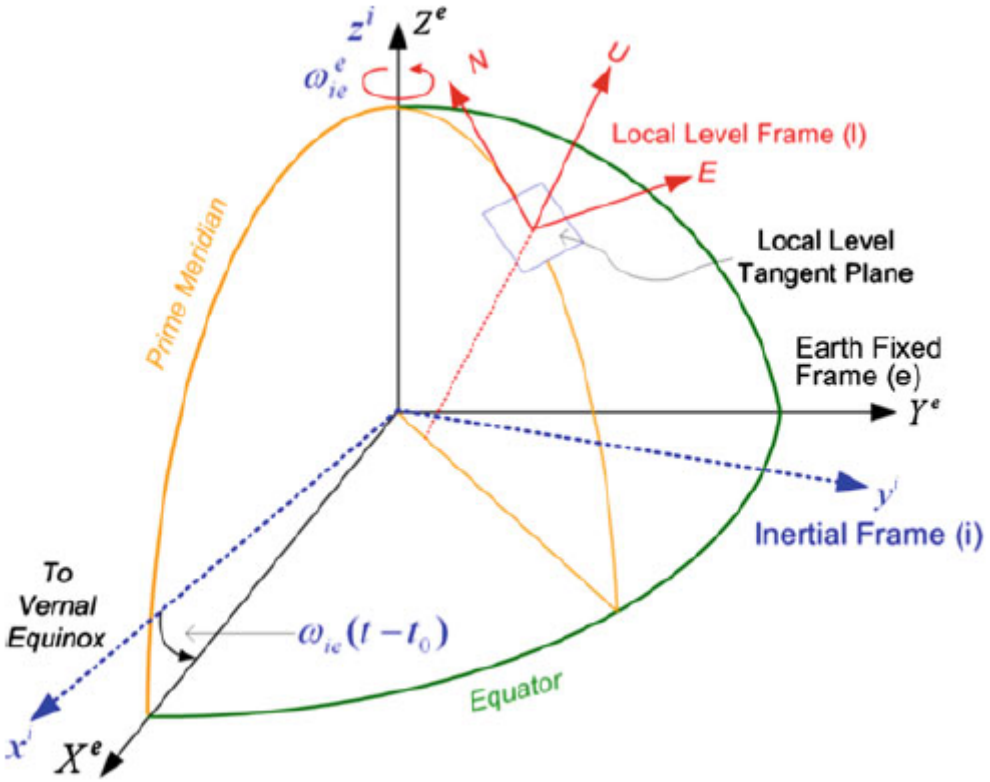

Figure 1.2: The local-level ENU reference frame in relation to the ECI and ECEF frames

This frame is referred to as ENU since its axes are aligned with the east, north and up directions

1.1.4 Wander Frame w-frame.

In the l-frame the y-axis always points towards true north, so higher rotation rates about the z-axis are required in order to maintain the orientation of the l-frame in the polar regions (higher latitudes) than near the equator (lower latitudes). As is apparent in Fig. 2.3b, the l-frame

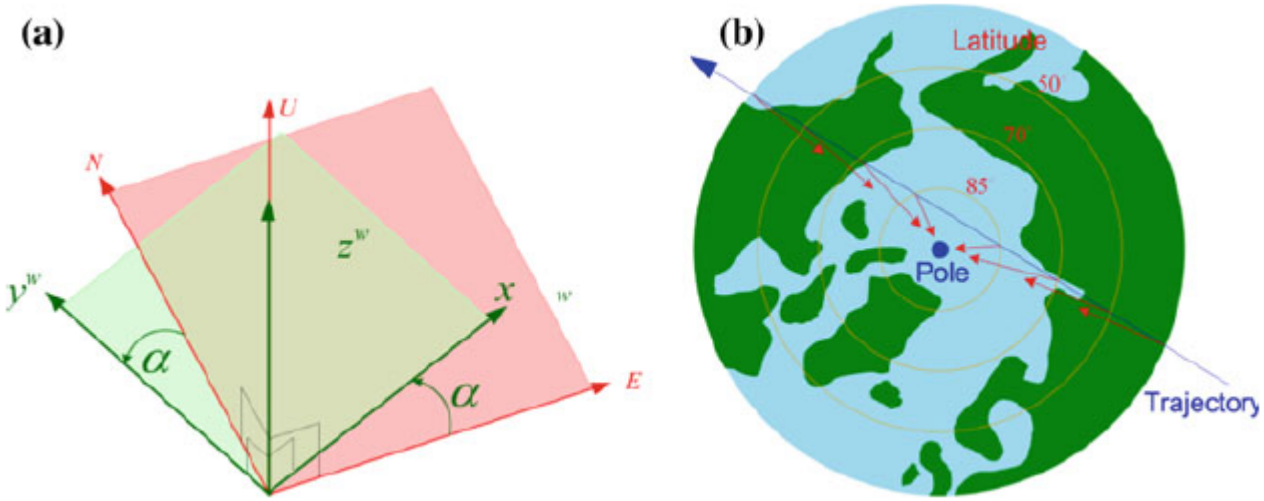

Figure 1.3: **a** The wander frame shown with respect to the local-level frame. **b** Rotation of the y-axis of the local-level frame (shown with red/dark arrows) for a near polar crossing trajectory at various latitudes

must rotate at higher rates to maintain its orientation when moving towards the pole, reaching its maximum when it crosses the north pole. This rate can even become infinite (a singularity condition) if the l-frame passes directly over the pole. The wander frame avoids higher rotation rates and singularity problems. Instead of always pointing northward, this rotates about the z-axis with respect to the l-frame. The angle between the y-axis of the wander frame and north is known as the wander angle α: The rotation rate of this angle is given as

$$\dot{\alpha} = -\dot{\lambda} \sin \varphi \tag{1.6}$$

The wander frame (in relation to the l-frame) is shown in Fig.1.3 **a**, and is defined as

- The origin coincides with the center of the sensor frame (origin of inertial sensor triad).
- The z-axis is orthogonal to the reference ellipsoid pointing upward.
- The y-axis rotates by an angle α anticlockwise from north.
- The x-axis is orthogonal to the y and z axes and forms a right-handed coordinate frame.

1.1.5 Body Frame

In most applications, the sensitive axes of the accelerometer sensors are made to coincide with the axes of the moving platform in which the sensors are mounted. These axes are usually known as the body frame. The body frame is defined as

- The origin usually coincides with the center of gravity of the vehicle (this simplifies derivation of kinematic equations).
- The y-axis points towards the forward direction. It is also called the roll axis as the roll angle is defined around this axis using the right-hand rule.
- The x-axis points towards the transverse direction. It is also called the pitch axis, as the pitch angle corresponds to rotations around this axis using the righthand rule.
- The z-axis points towards the vertical direction completing a right-handed coordinate system. It is also called the yaw axis as the yaw angle corresponds to rotations around this axis using the right-hand rule.

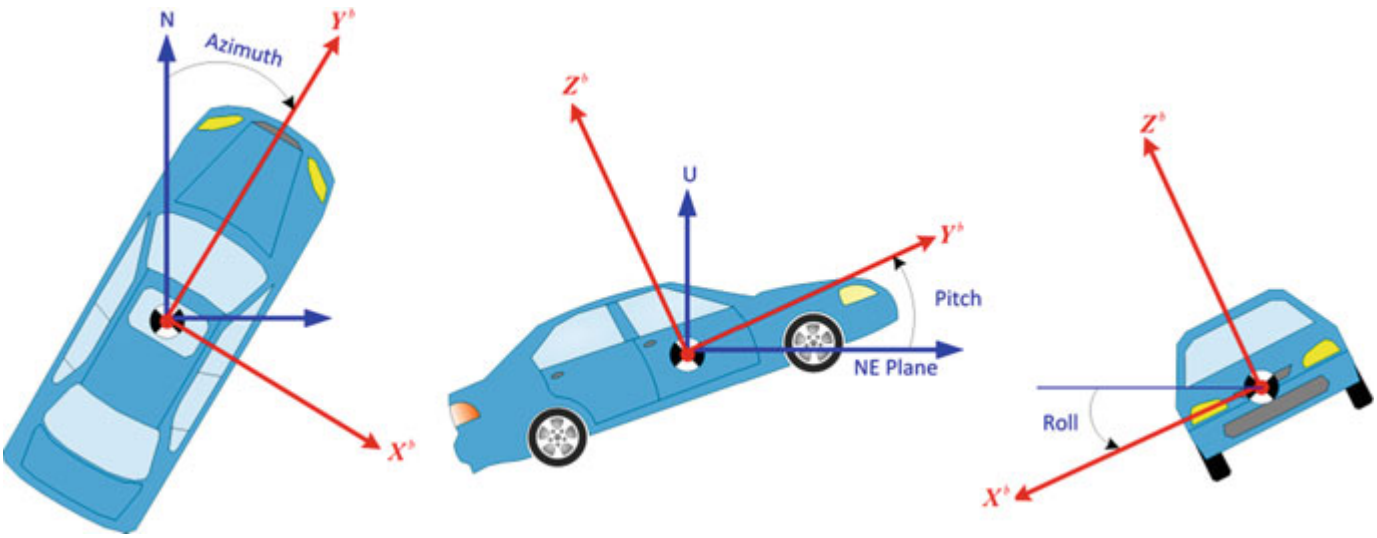

Figure 1.4: A depiction of a vehicle's azimuth, pitch and roll angles. The body axes are shown in red

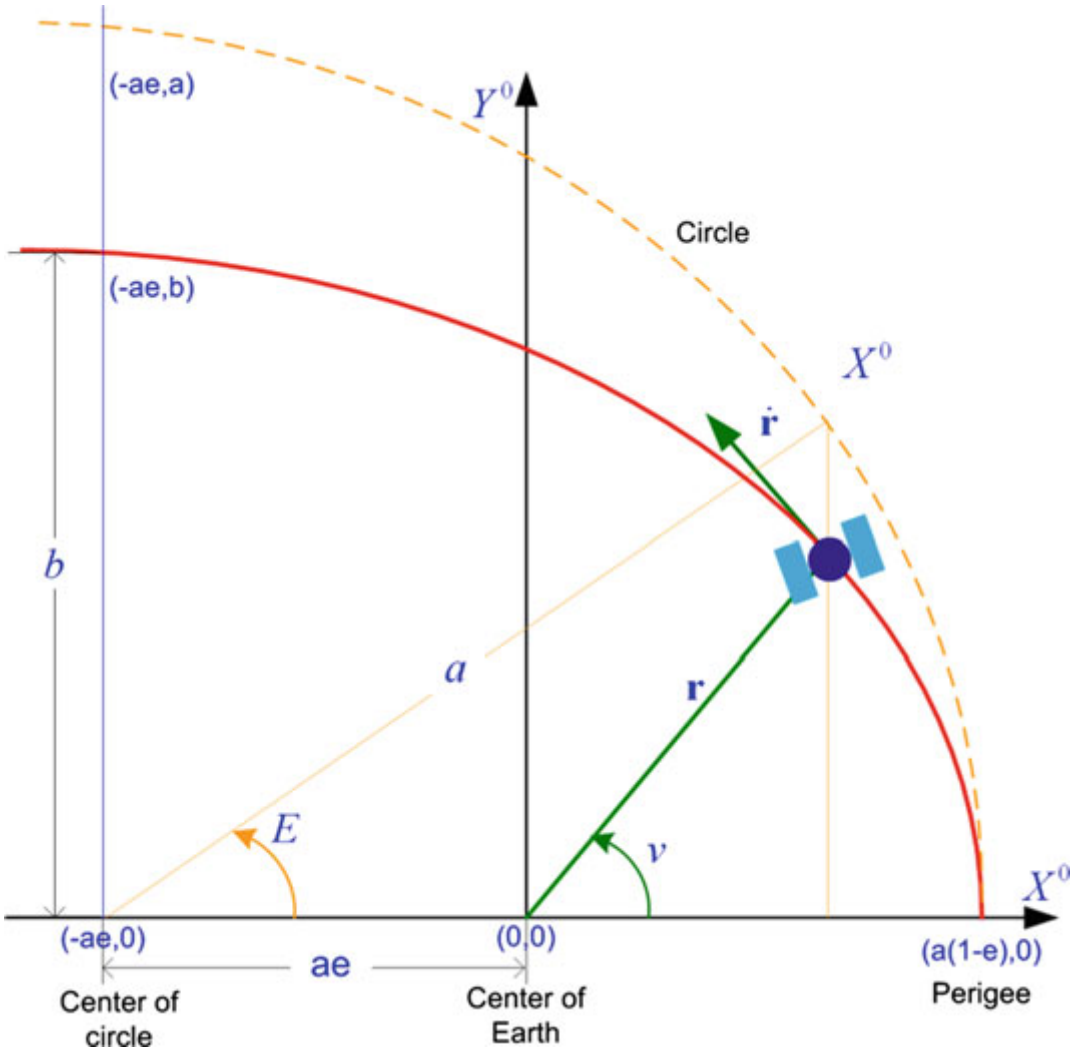

Figure 1.5: The orbital coordinate system for a satellite

Orbital Coordinate System

This is a system of coordinates with Keplerian elements to locate a satellite in inertial space. It is defined as follows

- The origin is located at the focus of an elliptical orbit that coincides with the center of the mass of the Earth.
- The y-axis points towards the descending node, parallel to the minor axis of the orbital ellipse.
- The x-axis points to the perigee (the point in the orbit nearest the Earth's center) and along the major axis of the elliptical orbit of the satellite.

- The z-axis is orthogonal to the orbital plane.

1.2 Coordinate Transformations

The techniques for transforming a vector from one coordinate frame into another can use direction cosines, rotation (Euler) angles or quaternions. They all involve a rotation matrix which is called either the transformation matrix or the direction cosine matrices (DCM), and is represented as $\overset{l}{R}_k$ where the subscript represents the frame from which the vector originates and the superscript is the target frame.

1.2.1 Euler Angles and Elementary Rotational Matrices

A transformation between two coordinate frames can be accomplished by carrying out a rotation about each of the three axes. For example, a transformation from the reference frame a to the new coordinate frame b involves first making a rotation of angle α about the z-axis, then a rotation of an angle β about the new x-axis, and finally a rotation of an angle γ about the new y-axis. In these rotations,α, β and γ are the Euler angles.

To transform a vector $\overset{a}{r} = \left[\overset{a}{x}; \overset{a}{y}; \overset{a}{z}\right]$ from frame a to frame d where the two frames are orientated differently in space, we align frame a with frame d using the three rotations specified above, each applying a suitable direction cosine matrix. The individual matrices can be obtained by considering each rotation, one by one.

$$\begin{bmatrix} \overset{b}{x} \\ \overset{b}{y} \\ \overset{b}{z} \end{bmatrix} = \begin{bmatrix} \cos\gamma & \sin\gamma & 0 \\ -\sin\gamma & \cos\gamma & 0 \\ 0 & 0 & 1 \end{bmatrix} \begin{bmatrix} \overset{a}{x} \\ \overset{a}{y} \\ \overset{a}{z} \end{bmatrix} = \overset{b}{R}_a \begin{bmatrix} \overset{a}{x} \\ \overset{a}{y} \\ \overset{a}{z} \end{bmatrix} \tag{1.7}$$

where $\overset{b}{R}_a$ is the elementary DCM which transforms the coordinates $\overset{a}{x}$; $\overset{a}{y}$; $\overset{a}{z}$ to $\overset{b}{x}$; $\overset{b}{y}$; $\overset{b}{z}$ in a frame rotated by an angle γ around the z-axis of frame a:

For the second rotation, we consider the $(y-z)$ plane of the new coordinate frame b, and rotate it by an angle β around its x-axis to an intermediate frame c as shown in Fig.

$$\begin{bmatrix} \overset{c}{x} \\ \overset{c}{y} \\ \overset{c}{z} \end{bmatrix} = \begin{bmatrix} 1 & 0 & 0 \\ 0 & \cos\beta & \sin\beta \\ 0 & -\sin\beta & \cos\beta \end{bmatrix} \begin{bmatrix} \overset{b}{x} \\ \overset{b}{y} \\ \overset{b}{z} \end{bmatrix} = \overset{c}{R}_b \begin{bmatrix} \overset{b}{x} \\ \overset{b}{y} \\ \overset{b}{z} \end{bmatrix} \tag{1.8}$$

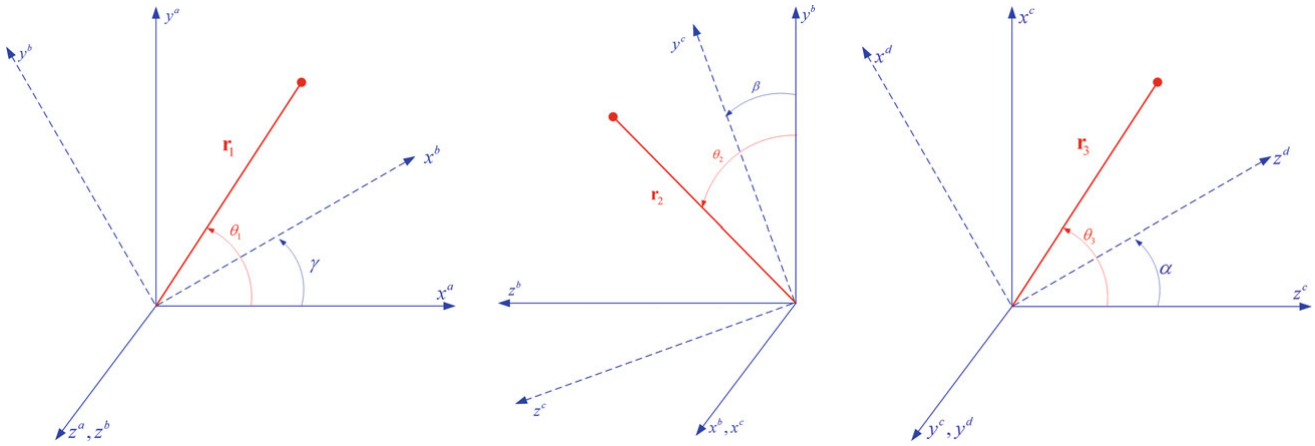

Figure 1.6: Euler Angles and Elementary Rotational sequences

For the third **rotation**, we consider the $x-z$ plane of new coordinate frame c; and rotate it by an angle a about its y-axis to align it with coordinate frame d as shown in Fig.1.6.

$$\begin{bmatrix} \overset{d}{x} \\ \overset{d}{y} \\ \overset{d}{z} \end{bmatrix} = \begin{bmatrix} \cos\beta & 0 & -\sin\alpha \\ 0 & 1 & 0 \\ \sin\alpha & 0 & \cos\alpha \end{bmatrix} \begin{bmatrix} \overset{c}{x} \\ \overset{c}{y} \\ \overset{c}{z} \end{bmatrix} = \overset{c}{R}_b \begin{bmatrix} \overset{c}{x} \\ \overset{c}{y} \\ \overset{c}{z} \end{bmatrix} \tag{1.9}$$

We can combine all three rotations by multiplying the cosine matrices into a single transformation matrix as

$$\overset{d}{R}_a = \overset{d}{R}_c \overset{c}{R}_b \overset{b}{R}_a$$

The final DCM for these particular set of rotations can be given as

$$\overset{d}{R}_a = \begin{bmatrix} \cos\alpha\cos\gamma - \sin\beta\sin\alpha\sin\gamma & \cos\alpha\sin\gamma + \cos\gamma\sin\beta\sin\alpha & -\cos\beta\sin\alpha \\ -\cos\beta\sin\gamma & \cos\beta\cos\gamma & \sin\beta \\ \cos\gamma\sin\alpha + \cos\alpha\sin\beta\sin\gamma & \sin\alpha\sin\gamma - \cos\alpha\cos\gamma\sin\beta & \cos\beta\cos\alpha \end{bmatrix} \tag{1.10}$$

The inverse transformation from frame d to a is therefore

$$\overset{a}{R}_d = \left(\overset{d}{R}_a\right)^{-1} = \left(\overset{d}{R}_a\right)^T = \left(\overset{d}{R}_c \overset{c}{R}_b \overset{b}{R}_a\right)^T = \left(\overset{b}{R}_a\right)^T \left(\overset{c}{R}_b\right)^T \left(\overset{d}{R}_c\right)^T \tag{1.11}$$

For small values of α; β and γ we can use the following approximations

$$\cos\theta \approx 1, \sin\theta \approx \theta \tag{1.12}$$

we can reduce the DCM to

$$\overset{d}{R}_a = \begin{bmatrix} 1 & 0 & 0 \\ 0 & 1 & 0 \\ 0 & 0 & 1 \end{bmatrix} - \begin{bmatrix} 1 & -\gamma & \alpha \\ \gamma & 0 & -\beta \\ -\alpha & \beta & 0 \end{bmatrix} = I - \Psi \tag{1.13}$$

where $\Psi$is the skew-symmetric matrix for the small Euler angles. For the small angle approximation, **the order of rotation is no longer important** since in all cases the final result will always be the matrix of the Eq.1.13 . Similarly, it can be verified that

$$\overset{a}{R}_d \approx \begin{bmatrix} 1 & -\gamma & \alpha \\ \gamma & 0 & -\beta \\ -\alpha & \beta & 0 \end{bmatrix}^T = I - \Psi^T \tag{1.14}$$

1.2.2 Transformation Between ECI and ECEF

The angular velocity vector between the i-frame and the e-frame as a result of the rotation of the Earth is

$$\overset{e}{\omega}_{ie} = (0, 0, \omega_e)^T$$

where ω_e denotes the magnitude of the Earth's rotation rate. The transformation from the i-frame to the e-frame is a simple rotation of the i-frame about the z-axis by an angle $\omega_e t$ where t is the time since the reference epoch (Fig.1.7).

$$\overset{e}{R}_i = \begin{bmatrix} \cos\omega_e t & sin\omega_e t & 0 \\ -sin\omega_e t & \cos\omega_e t & 0 \\ 0 & 0 & 1 \end{bmatrix}^T \tag{1.15}$$

1.2.3 Transformation Between LLF and ECEF

From Fig.1.8 it can be observed that to align the l-frame with the e-frame, the l-frame must be rotated by $\varphi - 90$ degrees around its x-axis (east direction) and then by $(-90 - \lambda)$ degrees about its z-axis (up direction). For the definition of elementary direction cosine matrices, the transformation from the l-frame to the e-frame is

$$\overset{e}{R}_l = \overset{b}{R}_a (-\lambda - 90) \overset{c}{R}_b (\varphi - 90) \tag{1.16}$$

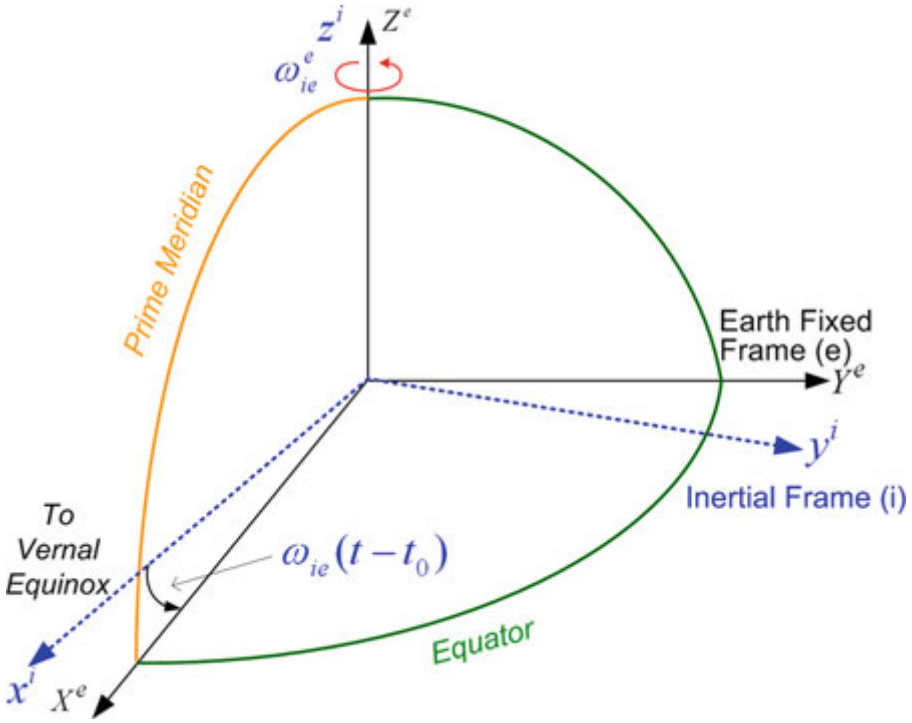

Figure 1.7: Transformation between the e-frame and the i-frame

$$\overset{e}{R}_i = \begin{bmatrix} \cos(-\lambda - 90) & \sin(-\lambda - 90) & 0 \\ -sin(-\lambda - 90) & \cos(-\lambda - 90) & 0 \\ 0 & 0 & 1 \end{bmatrix} \begin{bmatrix} 1 & 0 & 0 \\ 0 & \cos(\varphi - 90) & \sin(\varphi - 90) \\ 0 & -\sin(\varphi - 90) & \cos(\varphi - 90) \end{bmatrix} \tag{1.17}$$

$$\overset{e}{R}_i = \begin{bmatrix} -\sin\lambda & -\sin\varphi\cos\lambda & \cos\varphi\cos\lambda \\ \cos\lambda & -\sin\varphi\sin\lambda & \cos\varphi\sin\lambda \\ 0 & \cos\varphi & \sin\varphi \end{bmatrix} \tag{1.18}$$

1.2.4 Transformation Between LLF and Wander Frame

The wander frame has a rotation about the z-axis of the l-frame by a wander angle α; as depicted in Fig.1.9 Thus the transformation matrix from the w-frame frame to the l-frame corresponds to the elementary matrix $\overset{b}{R}_a$ with an angle $(-\alpha)$; and is expressed as

$$\overset{l}{R}_w = \begin{bmatrix} \cos\alpha & -\sin\alpha & 0 \\ \sin\alpha & \cos\alpha & 0 \\ 0 & 0 & 1 \end{bmatrix} \tag{1.19}$$

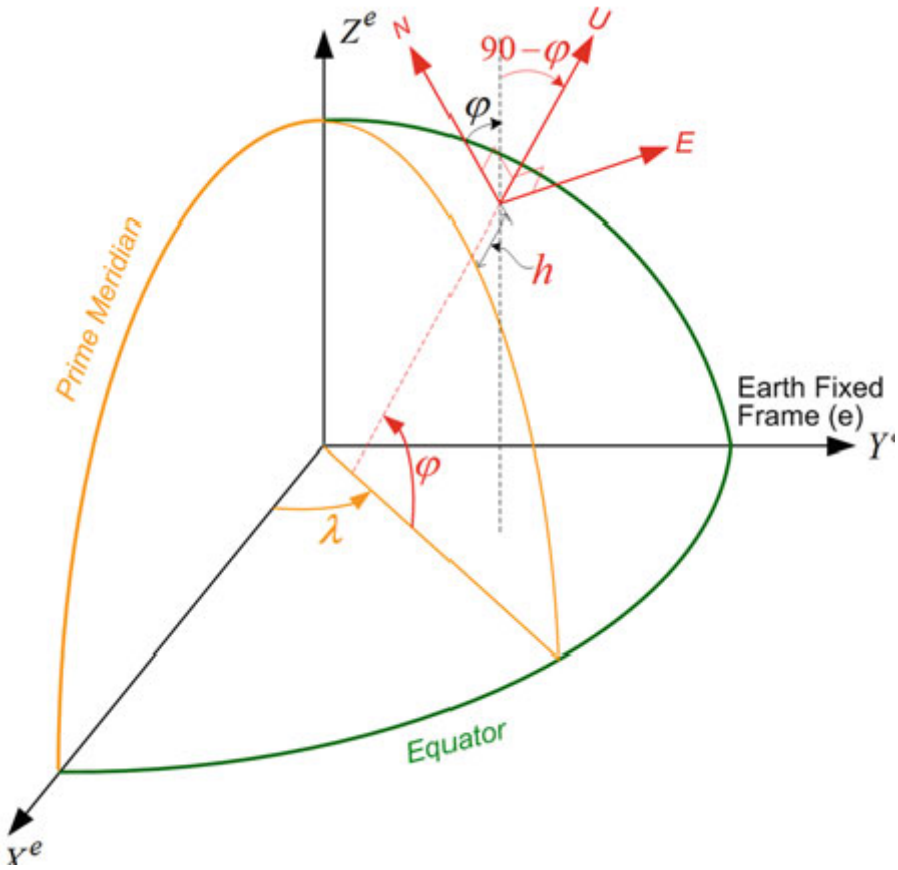

Figure 1.8: The LLF in relation to the ECEF frame

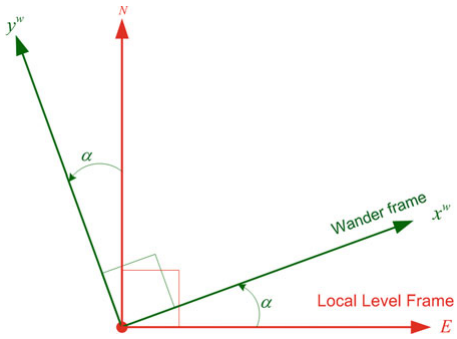

Figure 1.9: The relationship between the l-frame and the w-frame (the third axes of these the frames are not shown because they coincide and point out of the page towards the reader)

1.2.5 Transformation Between ECEF and Wander Frame

This transformation is obtained by first going from the w-frame to the l-frame and then from the l-frame to the e-frame

$$\overset{e}{R}_w = \overset{e}{R}_l \overset{l}{R}_w \tag{1.20}$$

$$\overset{e}{R}_w = \begin{bmatrix} -\sin\lambda\cos\alpha - \cos\lambda\sin\varphi\sin\alpha & \sin\lambda\sin\alpha - \cos\lambda\sin\varphi\cos\alpha & \cos\lambda\cos\varphi \\ \cos\lambda\cos\alpha - \sin\lambda\sin\varphi\sin\alpha & -\cos\lambda\sin\alpha - \sin\lambda\sin\varphi\cos\alpha & \sin\lambda\cos\varphi \\ \cos\varphi\sin\alpha & \cos\varphi\cos\alpha & \sin\varphi \end{bmatrix} \tag{1.21}$$

1.2.6 Transformation Between Body Frame and LLF

One of the important direction cosine matrices is $\overset{l}{R}_b$ which transforms a vector from the b-frame to the l-frame, a requirement during the mechanization process. This is expressed in terms of yaw, pitch and roll Euler angles. According to the definitions of these specific angles and the elementary direction cosine matrices, $\overset{l}{R}_b$ can be expressed as

$$\overset{l}{R}_b = \left(\overset{b}{R}_l\right)^{-1} = \left(\overset{b}{R}_l\right)^T = \left(\overset{n}{R}_l\right)^T \left(\overset{m}{R}_n\right)^T \left(\overset{b}{R}_m\right)^T \tag{1.22}$$

Substituting the elementary matrices into this equation gives

$$\overset{l}{R}_b = \begin{bmatrix} \cos y & \sin y & 0 \\ -\sin y & \cos y & 0 \\ 0 & 0 & 1 \end{bmatrix}^T \begin{bmatrix} 1 & 0 & 0 \\ 0 & \cos p & \sin p \\ 0 & -\sin p & \cos p \end{bmatrix}^T \begin{bmatrix} \cos r & 0 & -\sin r \\ \sin r & 0 & \cos r \\ 0 & 0 & 1 \end{bmatrix}^T \tag{1.23}$$

where 'p', 'r' and 'y' are the pitch, roll and yaw angles. With a known $\overset{l}{R}_b$ these angles can be calculated as

$$\overset{l}{R}_b = \begin{bmatrix} \cos y\cos r - \sin y\sin p\sin r & -\sin y\cos p & \cos y\sin r + \sin y\sin p\cos r \\ \sin y\cos r + \cos y\sin p\sin r & \cos y\cos p & \sin y\sin r - \cos y\sin p\cos r \\ -\cos p\sin r & \sin p & \cos p\cos r \end{bmatrix} \tag{1.24}$$

$$p = \tan^{-1}\left(\frac{\overset{l}{R}_b(3,2)}{\sqrt[2]{\left[\overset{l}{R}_b(1,2)\right]^2 + \left[\overset{l}{R}_b(2,2)\right]^2}}\right) \tag{1.25}$$

$$y = -\tan^{-1}\left(\frac{\overset{l}{R}_b(1,2)}{\overset{l}{R}_b(2,2)}\right) \tag{1.26}$$

$$r = -\tan^{-1}\left(\frac{\overset{l}{R}_b(3,1)}{\overset{l}{R}_b(3,3)}\right) \tag{1.27}$$

1.2.7 Transformation From Body Frame to ECEF and ECI Frame

Two other important transformations are from the b-frame to the e-frame and the i-frames. Their rotation matrices can be computed from those already defined as follows. For the body frame to the e-frame

$$\overset{e}{R}_b = \overset{e}{R}_l \overset{l}{R}_b \tag{1.28}$$

For the body frame to the i-frame

$$\overset{i}{R}_b = \overset{i}{R}_e \overset{e}{R}_b \tag{1.29}$$

1.3 Time Derivative of the Transformation Matrix

If a coordinate reference frame k rotates with angular velocity ω relative to another frame m, the transformation matrix between the two is composed of a set of time variable functions. The time rate of change of the transformation matrix $\dot{\overset{e}{R}}_b$ can be described using a set of differential equations. The frame in which the time differentiation occurs is usually identified by the superscript of the variable. equation for the rate of change of the DCM is

$$\dot{\overset{m}{R}}_k = \overset{m}{R}_k \overset{k}{\Omega}_{mk} \tag{1.30}$$

$\overset{k}{\Omega}_{mk}$is the skew-symmetric form of the angular velocity vector of the m-frame with respect to the k-frame This implies that the time derivative of the rotation matrix is related to the angular velocity vector ω of the relative rotation between the two coordinate frames. If we have the initial transformation matrix between the body and inertial frames $\overset{i}{R}_b$ then we can update the change of the rotation matrix using gyroscope output $\overset{b}{\Omega}_{ib}$

1.3.1 Time Derivative of the Position Vector in the Inertial Frame

For a position vector $\overset{b}{r}$ the transformation of its coordinates from the b-frame to the inertial frame is

$$\overset{i}{r} = \overset{i}{R}_b \overset{b}{r} \tag{1.31}$$

A rearrangement of the terms gives

$$\dot{\overset{i}{r}} = \overset{i}{R}_b \left(\dot{\overset{b}{r}} + \overset{b}{\Omega}_{ib} \overset{b}{r} \right) \tag{1.32}$$

which describes the transformation of the velocity vector from the b-frame to the inertial frame. ***This is often called the Coriolis equation.***

1.3.2 Time Derivative of the Velocity Vector in the Inertial Frame

The time derivative of the velocity vector is obtained by differentiating Eq. 1.32 as follows

$$\ddot{r}^i = \overset{i}{R}_b \left(\ddot{r}^b + 2\overset{b}{\Omega}_{ib}\dot{r}^b + \dot{\Omega}^b_{ib} r^b + \Omega^b_{ib}\Omega^b_{ib} r^b \right) \tag{1.33}$$

where

where:

$\ddot{r}^b$	is the acceleration of the moving object in the b-frame
Ω^b_{ib}	is the angular velocity of the moving object measured by a gyroscope
$2\overset{b}{\Omega}_{ib}\dot{r}^b$	is the Coriolis acceleration
$\dot{\Omega}^b_{ib} r^b$	is the tangential acceleration
$\Omega^b_{ib}\Omega^b_{ib} r^b$	is the centripetal acceleration

1.4 The Geometry of the Earth

Although the Earth is neither a sphere nor a perfect ellipsoid, it is approximated by an ellipsoid for computational convenience. here are some of the important definitions

- **Physical Surface** "Terrain": This is defined as the interface between the solid and fluid masses of the Earth and its atmosphere.
- **Geometric Figure** "Geoid": This is the equipotential surface. It can be thought of as the idealized mean sea level extended over the land portion of the globe. The geoid is a smooth surface but its shape is irregular and it does not provide the simple analytic expression needed for navigational computations.
- **Reference Ellipsoid** "Ellipsoid": This mathematically defined surface approximates the geoid by an ellipsoid that is made by rotating an ellipse about its minor axis, which is coincident

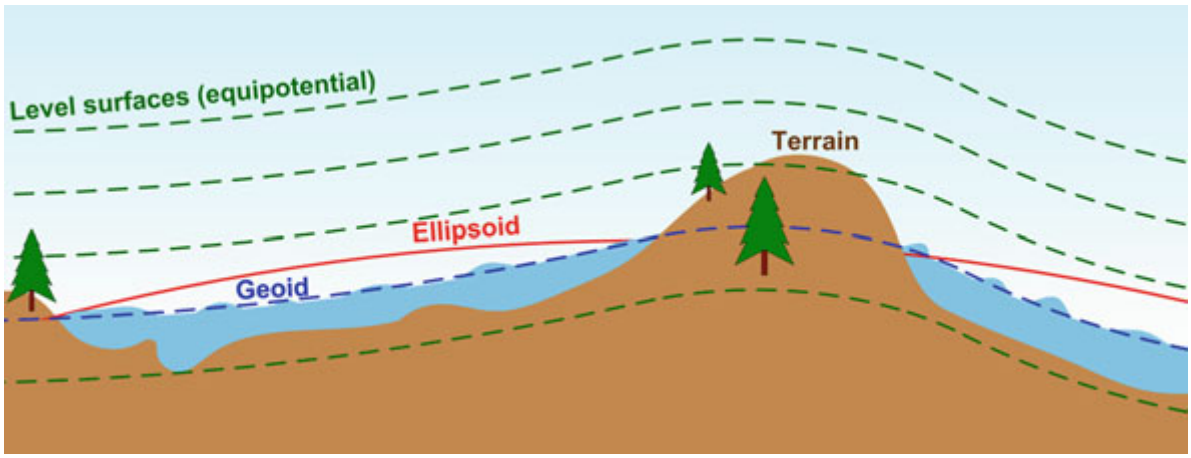

Figure 1.10: A depiction of various surfaces of the Earth.

with the mean rotational axis of the Earth. The center of the ellipsoid is coincident with the Earth's center of mass.

Various parameter sets have been defined to model the ellipsoid.below shown some parameters **Normal and Meridian Radii**In navigation two radii of curvature are of particular interest, the

Table 1.2: Earth's parameter sets to model the ellipsoid

Semimajor axis (equatorial radius) $a = 6378137m$
Reciprocal flattening $\frac{1}{f} = 298,257223563$
Earth's rotation rate $\omega_e = 7,292115\ 10^{-5} rad/s$
Gravitational constant $GM = 3,986004418\ 10^{14} \frac{m^3}{s^2}$
Flatness $f = \frac{a-b}{a} = 0,00335281$
Semiminor axis $b = a\,(1-f) = 6356752,3142m$
Eccentricity $e = \sqrt{\frac{a^2-b^2}{a^2}} = \sqrt{f\,(2-f)} = 0,08181919$

normal radius and the meridian radius. These govern the rates at which the latitude and longitude change as a navigating platform moves on or near the surface of the Earth. The normal radius R_N is defined for the east-west direction, and is also known as the great normal or the radius of curvature of the prime vertical The meridian radius of curvature is defined for the north-south direction and is the radius of the ellipse

$$R_N = \frac{a}{\sqrt{\left(1 - e^2 \sin^2 \varphi\right)}} \tag{1.34}$$

$$R_M = \frac{a\left(1-e^2\right)}{\left(1-e^2\sin^2\varphi\right)^{3/2}} \tag{1.35}$$

1.4.1 Types of Coordinates in the ECEF Frame

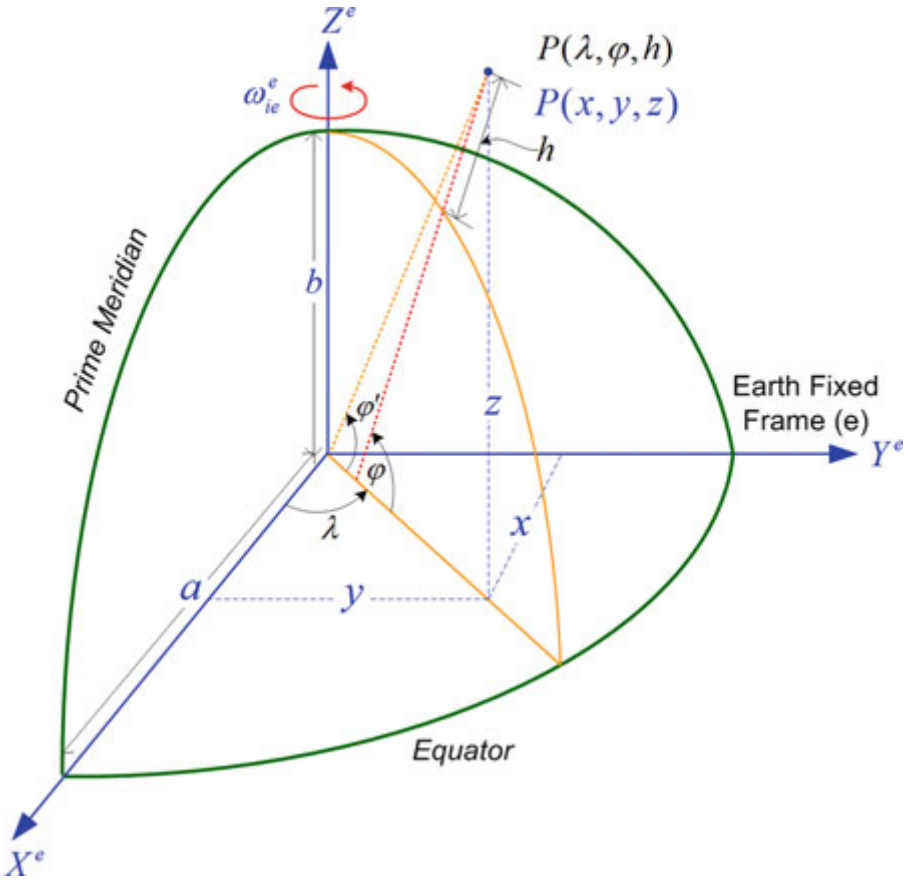

Figure 1.11: Two types of ECEF coordinates and their interrelationship

1.4.2 Rectangular Coordinates in the ECEF Frame

Rectangular coordinates are like traditional Cartesian coordinates, and represent the position of a point with its x, y and z vector components aligned parallel to the corresponding e-frame axes (Fig. 1.11).

1.4.3 Geodetic Coordinates in the ECEF Frame

Geodetic coordinates are defined in a way that is more intuitive for positioning applications on or near the Earth. Latitude(φ), Longitude(λ) and Altitude(h)

1.4.4 Conversion From Geodetic to Rectangular Coordinates in the ECEF Frame

In navigation, it is often necessary to convert from geodetic e-frame coordinates to rectangular e-frame coordinates.

$$[x^e, y^e, z^e] = \begin{bmatrix} (R_N + h)\cos\varphi\cos\lambda \\ (R_N + h)\cos\varphi\sin\lambda \\ [R_N(1-e^2) + h]\sin\varphi \end{bmatrix} \tag{1.36}$$

1.4.5 Conversion From Rectangular to Geodetic Coordinates in the ECEF Frame

Converting rectangular to geodetic coordinates is not straightforward, because the analytical solution results in a fourth-order equation. There are approximate closed form solutions but an iterative scheme is usually employed:

- Initialize the altitude as

$$h_0 = 0$$

- Choose an arbitrary value of latitude

$$\varphi_0 = \tan^{-1}\left[\frac{z^e}{P^e(1-e^2)}\right]$$

- The ellipsoidal height

$$P^e = \left(R^N + h\right)\cos\varphi$$

- The geodetic longitude is calculated as

$$\lambda = \tan^{-1}\left(\frac{y^e}{x^e}\right)$$

- Starting from $i = 1$ iterate as follows

$$R_{Ni} = \frac{a}{\sqrt{\left(1 - e^2\sin^2\varphi_{i-1}\right)}}$$

- $$h_i = \frac{\sqrt{\left(x^e\right)^2 + \left(y^e\right)^2}}{\cos\varphi_{i-1}} - R_{Ni}$$

- $$\varphi_i = \tan^{-1}\left(\frac{z^e}{\sqrt{(x^e)^2 + (y^e)^2}} \cdot \frac{R_{Ni} + h_i}{R_{Ni}\,(1 - e^2) + h_i}\right)$$
- Compare φ_i, φ_{i-1} and h_i; h_{i-1} if convergence has been achieved then stop, otherwise repeat step 5 using the new values.

1.5 Earth Gravity

The gravity field vector is different from the gravitational field vector. Due to the Earth's rotation, the gravity field is used more frequently and is defined as

$$g = \bar{g} - \Omega_{ie}\Omega_{ie}r \tag{1.37}$$

where

$\bar{g}$ is the gravitational vector, Ω_{ie} is the skew-symmetric representation of the Earth's rotation vector ω_{ie} with respect to the i-frame, and r is the geocentric position vector. The **second term** in the above equation **denotes the centripetal acceleration** due to the rotation of the Earth around its axis. Usually, the gravity vector is given in the l-frame. Because the normal gravity vector on the ellipsoid coincides with the ellipsoidal normal, the east and the north components of the normal gravity vector are zero and only third component is non-zero

$$g^l = [0 \quad 0 \quad -g]^T \tag{1.38}$$

The magnitude of the normal gravity vector over the surface of the ellipsoid can be computed as a function of latitude and height by a closed form expression known as the Somigliana formula

$$\gamma = a_1\left(1 + a_2\sin^2\varphi + a_3\sin^4\varphi\right) + \left(a_4 + a_5\sin^2\varphi + a_3\sin^4\varphi\right)h + a_6h^2 \tag{1.39}$$

where h is the height above the Earth's surface and the coefficients a_1 through a_6 for the 1980 geographic reference system (GRS) are defined as

$$\begin{aligned} a_1 &= 9,7803267714\tfrac{m}{s^2} & a_4 &= 0,0000030876910891\tfrac{m}{s^2} \\ a_2 &= 0,0052790414\tfrac{m}{s^2} & a_5 &= 0,0000000043977311\tfrac{m}{s^2} \\ a_3 &= 0,0000232718\tfrac{m}{s^2} & a_6 &= 0,0000000000007211\tfrac{m}{s^2} \end{aligned}$$

Conclusion : A navigation system can be autonomous or be dependent on external sources, That depends on in order to locate the vehicle through a techniques using Relative Measurements (Known as DR) which uses accelerometers and gyroscopes to provide orientation and position respectively. And techniques using Absolute Measurements (Known as Reference-based Systems), It is classified into several applications; Electronic Compasses, Active Beacons, Global Navigation Satellite Systems (GNSS), Landmark Navigation and Map-Based Positioning.

Chapter 2

Principle & Mathematical Model of Inertial Navigation

2.1 Inertial Navigation System Principle

The principle of inertial navigation is based upon Newton's first law of motion, which states:
A body continues in its state of rest, or uniform motion in a straight line, unless it is compelled to change that state by forces impressed on it.
Newton's second law of motion shares importance with his first law in the inertial navigation system, and states
Acceleration is proportional to the resultant force and is in the same direction as this force.

$$F = ma \tag{2.1}$$

where F is the force
m is the mass of the body
a is the acceleration of the body due to the applied force F.

The physical quantity pertinent to an inertial navigation system is acceleration, because both velocity v and displacement s can be derived from acceleration by the process of integration.

$$v = \int adt; s = \int vdt; s = \int\int adtdt \tag{2.2}$$

An inertial navigation system is an integrating system consisting of a detector and an integrator.

It detects acceleration, integrates this to derive the velocity and then integrates that to derive the displacement. By measuring the acceleration of a vehicle in an inertial frame of reference and then transforming it to the navigation frame and integrating with respect to time, it is possible to obtain velocity, attitude and position differences. Measurement of the vehicle's rotation is needed for the transformation from the inertial to the navigation frame and for the computation of the attitude of the vehicle.

Physical Implementation of an INS There are two implementation approaches to an INS:

- Stable platform system,
- Strapdown system.also known as a gimbaled system.

The components of these systems are shown in Fig. 2.1. In the stable platform, the inertial sensors are mounted on a set of gimbals such that the platform always remains aligned with the navigation frame. This is done by having a set of torque motors rotate the platform in response to rotations sensed by the gyroscopes. Thus the output of the accelerometers is directly integrated for velocity and position in the navigation frame. Since gimbaled systems are mechanically complex and expensive, their use is limited.

Advances in electronics gave rise to strapdown systems. In these, the inertial sensors are rigidly mounted onto the body of the moving platform and the gimbals are replaced by a computer that simulates the rotation of the platform by software frame transformation. Rotation rates measured by the gyroscopes are applied to continuously update the transformation between the body and navigation frames. The accelerometer measurements are then passed through this transformation to obtain the acceleration in the navigation frame. Strapdown systems are favored for their reliability, flexibility, low power usage, being lightweight and less expensive than stable platforms. The transition to strapdown systems was facilitated by the introduction of optical gyros to replace rotor gyros, and by the rapid development of the processor technology required to perform the computations.

An INS can be thought of as consisting of three principal modules: an inertial measurement unit (IMU), a pre-processing unit, and a mechanization module. An IMU uses three mutually orthogonal accelerometers and three mutually orthogonal gyroscopes. The signals are pre-processed by some form of filtering to eliminate disturbances prior to the mechanization algorithm which converts the signals into positional and attitude information

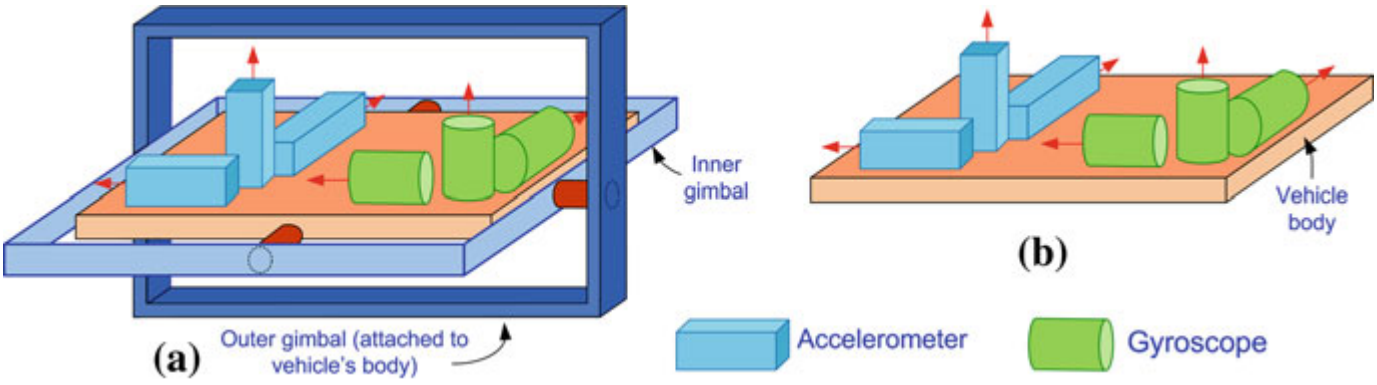

Figure 2.1: Arrangement of the components of a gimbaled IMU (left) and a strapdown IMU (right)

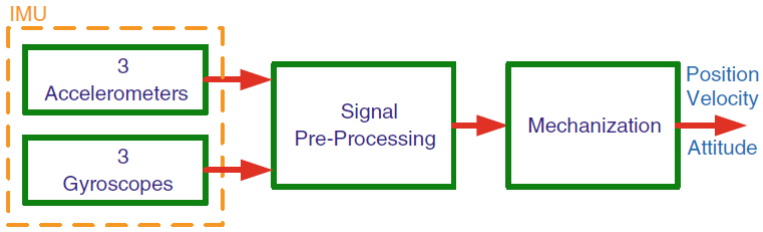

Figure 2.2: The principal modules of an inertial navigation system

2.1.1 Inertial Sensors

Accelerometers

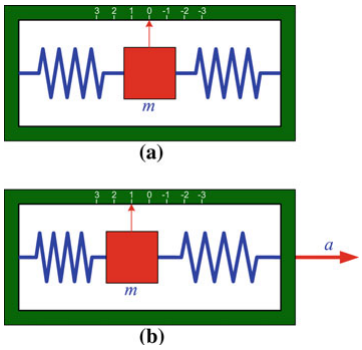

Figure 2.3: **a** An accelerometer in the null position with no force acting on it, **b** the same accelerometer measuring a linear acceleration of the vehicle in the positive direction (to the right)

Acceleration will displace the proof mass from its equilibrium position, with the amount of

displacement proportional to the acceleration. The displacement from the equilibrium position is sensed by a pickoff and is then scaled to provide an indication of acceleration along this axis. The equilibrium position is calibrated for zero acceleration. Acceleration to the right will cause the proof mass to move left in relation to the case and (as shown by the scale) indicates positive acceleration. the output of an accelerometer due to a gravitational field is the negative of the field acceleration. The output of an accelerometer is called the specific force, and is given by

$$f = a - \vec{g} \tag{2.3}$$

where f is the specific force a is the acceleration with respect to the inertial frame g is the gravitational acceleration which is $+9.8\ \frac{m}{s^2}$. To navigate with respect to the inertial frame we need a, therefore in the navigation equations we convert the output of an accelerometer from f to a by adding g. The acceleration a can be expressed as the double derivative of the position vector r, as

$$\mathbf{a} = \left(\frac{d^2r}{dt^2}\right)_i = \ddot{r} \tag{2.4}$$

using eq. Substituting Eqs. 1.37 and (2.4) into Eq. (2.3) provides

$$\mathbf{f} = \left(\frac{d^2r}{dt^2}\right)_i - g - \Omega_{ie}\Omega_{ie}r \tag{2.5}$$

Gyroscopes

Gyros measure the angular rate of a body with respect to the navigation frame, the rotation of the navigation frame with respect to the Earth-fixed frame (as it traces the curvature of the Earth), and the rotation of the Earth as it spins on its axis with respect to inertial space. These quantities are all expressed in the body frame and can be given as

$$\omega_{ib}^b = \omega_{ie}^b + \omega_{en}^b + \omega_{nb}^b \tag{2.6}$$

where

- ω_{ib}^b is the rotation rate of the body with respect to the i-frame

- ω_{nb}^{b} is the rotation rate of the body with respect to the navigation frame
- ω_{en}^{b} is the rotation rate of the navigation frame with respect to the e-frame
- ω_{ie}^{b} is the rotation rate of the Earth with respect to the i-frame.

Traditional gyroscopes were mechanical and based on angular momentum, but more recent ones are based on either the Coriolis effect on a vibrating mass or the Sagnac interference effect. There are three main types of gyroscope (Lawrence 1998): mechanical gyroscopes, optical gyroscopes, and micro-electro-mechanical system (MEMS) gyroscopes.

2.2 Notes on Inertial Sensor Measurements

for strapdown systems the b-frame can take essentially any arbitrary direction because the accelerometers and gyros are strapped onto the vehicle, which can adopt any orientation with respect to the navigation frame. The establishment of the relationship between the INS body frame and the local level (navigation) frame is usually done at the beginning of the survey by a stationary alignment process. In this process, the initial attitude angles (pitch, roll and azimuth) between the b-frame and the n-frame require to be estimated. The attitude angles are used in generating the rotation matrix R_b^n for the transformation from the b-frame to the n-frame. The rotation rates measured by the gyros are used to constantly update this matrix. Once this transformation has been made, the process of integrating an acceleration measurement twice will provide the IMU's position difference relative to the initial point.

However, accelerometers cannot separate the total platform acceleration from that caused by the presence of gravity. In fact, accelerometers provide the sum of the platform's acceleration in space and its acceleration due to gravity. The accelerometer measurements must be combined with knowledge of the ambient gravitational field in order to determine the acceleration of the vehicle with respect to a non-inertial reference frame.

Obviously, the inertial navigation is fundamentally dependent on an accurate specification of the position, velocity and attitude of the moving platform prior to the start of navigation.

2.2.1 Inertial Sensor Errors

Inertial sensors are prone to various errors which get more complex as the price of the sensor goes down. The errors limit the accuracy to which the observables can be measured. They are classified according to two broad categories of systematic and stochastic (or random) errors.

2.2.2 Systematic Errors

These types of errors can be compensated by laboratory calibration, especially for high-end sensors. Some common systematic sensor errors (Grewal et al. 2007) are described below:

Systematic Bias Offset It is defined as the output of the sensor when there is zero input,

Scale Factor Error This is the deviation of the input–output gradient from unity.

Non-linearity This is non-linearity between the input and the output,

Scale Factor Sign Asymmetry This is due to the different scale factors for positive and negative inputs

Dead Zone This is the range where there is no output despite the presence of an input

Quantization Error This type of error is present in all digital systems which generate their inputs from analog signals

Non-orthogonality Error occur when any of the axes of the sensor triad depart from mutual orthogonality. This usually happens at the time of manufacturing. Figure 2.4 depicts the case of the z-axis being misaligned by an angular offset of θ_{zx} from xz-plane and θ_{zy} from the yz-plane.

Misalignment Error This is the result of misaligning the sensitive axes of the inertial sensors relative to the orthogonal axes of the body frame as a result of mounting imperfections.

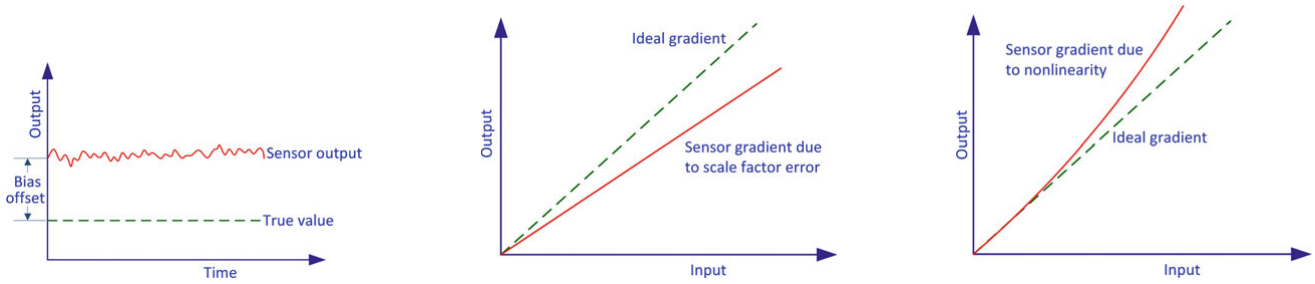

Figure 2.4: Sensor bias,sensor scale factor and Non-linearity errors

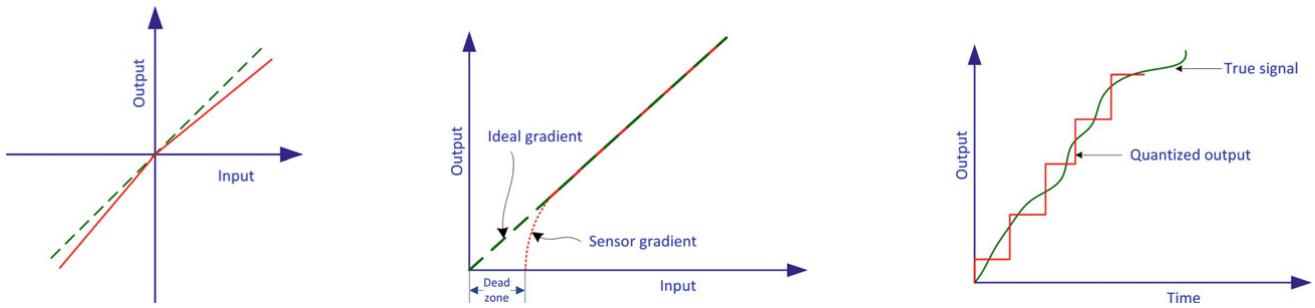

Figure 2.5: Scale factor sign bias,Dead zone and quantization errors

2.2.3 Random Errors

Inertial sensors suffer from a variety of random errors which are usually modeled stochastically in order to mitigate their effects.

Run-to-Run Bias Offset If the bias offset changes for every run, this falls under the bias repeatability error, and is called the run-to-run bias offset.

Bias Drift This is a random change in bias over time during a run, it is the instability in the sensor bias for a single run, and is called bias drift, it is illustrated in Fig. **??**. Bias is deterministic but bias drift is stochastic. One cause of bias drift is a change in temperature.

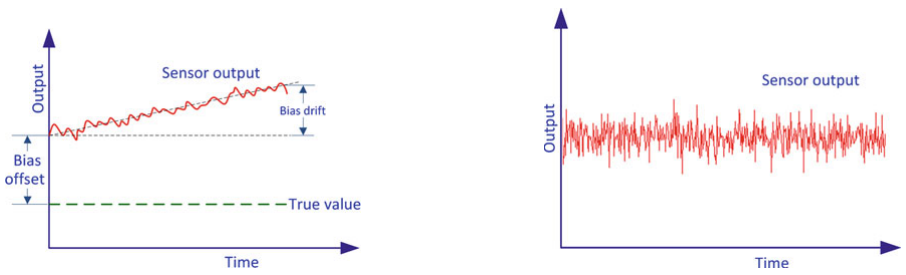

Figure 2.6: Bias Drift and White noiser sign bias,Dead zone and quantization errors

Scale Factor Instability Random changes in scale factor during a single run. This is usually the result of temperature variations. The scale factor can also change from run to run, but stay constant during a particular run. This demonstrates the repeatability of the sensor and is also called the run-to-run scale factor.

White Noise This is an uncorrelated noise that is evenly distributed in all frequencies. This type of noise can be caused by power sources but can also be intrinsic to semiconductor devices.

Notes on Random Errors Most manufacturers express the randomness associated with their inertial sensors by the concept of random walk. The angle random walk (ARW) for gyroscopes is usually specified in terms of $(deg/hr/\sqrt{Hz})$ or $(deg/\sqrt{hr})$ and the velocity random walk (VRW) for accelerometers is given in terms of $(\mu g/\sqrt{Hz}$ or $m/s/\sqrt{hr})$

This definition requires knowledge of the data rate (sampling frequency) at which the sensor measurements are acquired by the data acquisition systems. The data rate is related to the bandwidth of the sensor, which is another important parameter. The inertial sensor bandwidth (specified in Hz) defines the range of frequencies that can be monitored by the sensor. For example a gyroscope with 100 Hz bandwidth is capable of monitoring the dynamics of frequencies less than 100 Hz. Any higher frequencies will not be detected. Table 2.1 shows some important performance specifications for various KVH gyroscopes [3].

Table 2.1: Performance specification of various KVH gyroscopes.

	KVH DSP-300 (single axis FOG)	KVH DSP-3100 (single axis FOG)	DSP-3400 single axis FOG
Bandwidth	100 Hz	1000 Hz	1000 Hz
Bias drift	$< 3^{\text{deg}}/h$	$< 1^{\text{deg}}/h$	$< 1^{\text{deg}}/h$
ARW	$< 6^{\text{deg}}/h/\sqrt{Hz}$	$< 4^{\text{deg}}/h/\sqrt{Hz}$	$< 4^{\text{deg}}/h/\sqrt{Hz}$
Scale factor	$< 0.05\%$	$< 0.05\%$	$< 0.05\%$

2.2.4 Mathematical Models of Inertial Sensor Errors

2.2.5 Gyroscope Measurement Model

Measurements of angular rate can be modeled by the observation equation

$$\widetilde{\omega}_{ib}{}^{b} = \overset{b}{\omega}_{ib} + \mathbf{b}_g + S_g \overset{b}{\omega}_{ib} + N_g \overset{b}{\omega}_{ib} + \varepsilon_g \tag{2.7}$$

where

Table 2.2: Gyroscope Measurement Model.

$\widetilde{\omega}_{ib}{}^{b}$	the gyroscope measurement vector (deg/h)
$\overset{b}{\omega}_{ib}$	is the true angular rate velocity vector (deg/h)
$\mathbf{b}_g$	is the gyroscope instrument bias vector (deg/h)
S_g	is a matrix representing the gyro scale factor
N_g	is a matrix representing non-orthogonality of the gyro triad
ε_g	is a vector representing the gyro sensor noise (deg/h)

$$N_g = \begin{bmatrix} 1 & \theta_{g,xy} & \theta_{g,xz} \\ \theta_{g,yx} & 1 & \theta_{g,yz} \\ \theta_{g,zx} & \theta_{g,zy} & 1 \end{bmatrix} \tag{2.8}$$

$$S_g = \begin{bmatrix} S_{g,x} & 0 & 0 \\ 0 & S_{g,y} & 0 \\ 0 & 0 & S_{g,z} \end{bmatrix} \tag{2.9}$$

where $\theta_{(.),(.)}$ are the small angles defining the misalignments between the different gyro axes and $S_{(.),(.)}$ are the scale factors for the three gyros.

2.2.6 Accelerometer Measurement Model

Measurements of the specific force can be modeled by the observation equation

$$\widetilde{\mathbf{f}}_{ib}{}^{b} = \overset{b}{\mathbf{f}}_{ib} + \mathbf{b}_a + S_1 \overset{b}{\mathbf{f}}_{ib} + S_2 \overset{b}{\mathbf{f}}_{ib} + N_a \overset{b}{\mathbf{f}}_{ib} + \delta_g + \varepsilon_a \tag{2.10}$$

where

Table 2.3: Accelerometer Measurement Model.

$\widetilde{\mathbf{f}}_{ib}^{\ b}$	is the accelerometer measurement vector (m/s2)
$\mathbf{f}_{ib}^{b}$	is the true specific force vector (i.e. observable) (m/s2)
$\mathbf{b}_a$	is the accelerometer instrument bias vector (m/s2)
S_1	is a matrix of the linear scale factor error
S_2	is a matrix of the non-linear scale factor error
N_a	is a matrix representing non-orthogonality of the accelerometer triad
δ_g	is the anomalous gravity vector (i.e. the deviation from the theoretical gravity value) (m/s2)
ε_a	is a vector representing the accelerometer sensor noise (m/s2).

2.3 Classification of Inertial Sensors

A rough comparison of different inertial navigation sensors/systems is outlined in Table 2.4 with data obtained from (Groves Dec 2007), (Petovello et al. Jun 2007), (Barbour and Schmidt 2001) and (Wang and Williams 2008). Usually the cost of an IMU is dictated by the type of inertial sensors. IMUs are categorized according to their intended applications, which mainly depend on the gyroscope bias expressed in $(deg/hour)$. A secondary measure of performance is the gyroscope random walk, which is usually expressed in terms of $(deg/root-hour)$ and accelerometer bias.

2.3.1 Gyroscope Technologies and their Applications

There are several gyroscope technologies, including ring laser gyroscopes (RLG), dynamically tuned gyroscopes (DTG), hemispherical resonant gyroscopes (HRG), and interferometric fiber-optic gyroscopes (IFOG). Spinning mass and ring laser gyroscopes offer high performance but at high cost, and find their application in strategic/tactical and submarine navigation systems. DTG offer a medium level of performance and share some applications with RLG (Prasad and Ruggieri 2005). IFOG and Coriolis-based gyroscopes are of lower performance but cost less and are typically used in torpedoes, tactical missile midcourse guidance, flight control and smart munitions guidance and robotics. There has been a recent trend towards MEMS gyroscopes that are being researched for low cost navigation applications such as car navigation and portable navigation devices. Details of all these sensor technologies can be found in (Barbour and Schmidt 2001, Lawrence 1998).

Table 2.4: Classification of inertial measurement units.

Performance	Strategic grade	Navigation grade	Tactical grade	Commercial grade
Positional error	$< 100m/h$	1 Nm/h	10–20 Nm/h	Large variation
Gyroscope drift	0.0001 0.001°/h	$< 0.01°/h$	1 10°/h	0.1°/s
Gyroscope random walk	—-	$< 0.002°/\sqrt{h}$	0.05 0.02°/$\sqrt{h}$	several °/$\sqrt{h}$
Accelerometer bias	0.1 - 1 μg	$< 100\mu g$	$1 - 5\ mg$	$100 - 1000\mu g$
Applications	Intercontinental ballistic missile, Submarines.	General navigation, high precision georeferencing mapping.	Integrated with GPS for mapping, Weapons (short time).	Research, Low cost navigation pedometers, Antilock breaking, active suspension, airbags.

2.3.2 Accelerometer Technologies and their Applications

The main accelerometer technologies are mechanical pendulous force-rebalance accelerometers, vibrating beam accelerometers (VBAs) and gravimeters. The best performance is provided by mechanically floated instruments, and these are used in strategic missiles. Mechanical pendulous rebalance accelerometers are used in submarine navigation, land and aircraft navigation and space applications. Quartz resonator accelerometers are low grade sensors typically found in tactical missile midcourse guidance.

2.4 Calibration of Inertial Sensors

Calibration is defined as the process of comparing instrument outputs with known reference information to determine coefficients that force the output to agree with the reference information across the desired range of output values. Calibration is used to compute deterministic errors of sensors in the laboratory. The calibration parameters to be determined can change according to the specific technology in an IMU. To accurately determine all of the parameters, special

calibration devices are needed, such as three-axial turntables, to perform either a six-position static test or an angle rate test.

2.5 Initialization and Alignment of Inertial Sensors

An INS takes acceleration and rotation rates from sensors to calculates velocity and attitudes by integrating them once, and then integrates the velocity in order to obtain the position. The navigation equations require starting values for position, velocity and attitude. These are readily available from the last epoch of an ongoing iteration, but for the first epoch the INS must be specifically provided with this information before it can begin to function. This process is called initialization for position and velocity, and is called alignment for attitude (Groves Dec 2007).

Position and Velocity Initialization Position can be initialized using a vehicle's last known position before it started to move. For a system where the INS is integrated with other systems, typically GPS, a position can easily be provided by the external navigation system. In some cases the starting point is known a priori (for example a pre-surveyed location). If the vehicle is stationary then the velocity initialization can be made with zero input. If it is moving, the initial velocity can be provided by an external navigation source such as GPS, Doppler or an odometer.

Attitude Alignment Attitude alignment involves two steps. **First**, the platform is leveled by initializing the pitch (p) and roll (r) angles, and **then** gyro-compassing to provide an initial value of the heading (alternatively known as the yaw angle 'y' or azimuth 'A').

2.6 Inertial Navigation System Modeling

Modeling requires representing real world phenomena by mathematical language. To keep the problem tractable the goal is not to produce the most comprehensive descriptive model but to produce the simplest possible model which incorporates the major features of the phenomena of interest. The model is also restricted by the ability of mathematics to describe a phenomenon. Here we deal with models which describe the motion of an object on or near the surface of the Earth. This kind of motion is greatly influenced by the geometry of the Earth. There are two

broad categories for modeling motion: dynamic and kinematic.in this further we will use the second one.

2.6.1 INS Mechanization

Mechanization is the process of converting the output of an IMU into position, velocity and attitude information. The outputs include rotation rates about three body axes ω_{ib}^{b} measured by the gyroscopes triad and three specific forces $\mathbf{f}^{b}$ along the body axes measured by the accelerometer triad, all of which are with respect to the inertial frame. Mechanization is a recursive process that starts with a specified set of initial values and iterates on the output. A general diagram of INS mechanization is shown in Fig. 2.7.

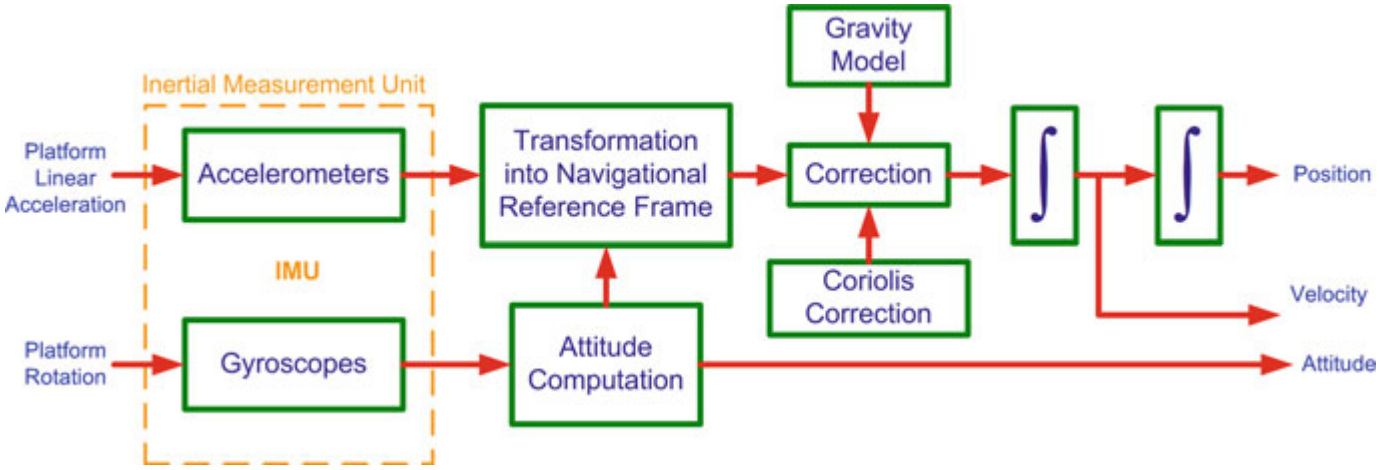

Figure 2.7: A block diagram depicting the mechanization process of an INS in the inertial frame

INS Mechanization in an Inertial Frame of Reference

The output of an accelerometer is called the specific force, and is given as

$$\mathbf{f}^{\,i} = \mathbf{a}^{\,i} - \vec{\mathbf{g}}^{i} \tag{2.11}$$

where $\mathbf{f}$ is the specific force, $\mathbf{a}$ is the acceleration of the body, and $\vec{\mathbf{g}}$ is the gravitational vector. By letting $\mathbf{a}^{i} = \ddot{\mathbf{r}}^{i}$

$$\ddot{\mathbf{r}}^{i} = \mathbf{f}^{\,i} + \vec{\mathbf{g}}^{i} \tag{2.12}$$

$\ddot{\mathbf{r}}^{i}$ is the second derivative of the position vector measured from the origin of the inertial frame to the moving platform

$\mathbf{f}^{i}$ is the specific force

$\vec{\mathbf{g}}^{i}$ is the gravitational vector

For ease of solution, the set of three second-order differential equations can be transformed to a set of first-order differential equations as follows

$$\dot{\mathbf{r}}^{i} = \mathbf{v}^{i} \tag{2.13}$$

$$\dot{\mathbf{v}}^{i} = \mathbf{f}^{i} + \vec{\mathbf{g}}^{i} \tag{2.14}$$

The measurements are usually made in the body frame. By assuming that the body frame coincides with the sensor triad frame these measurements can be transformed into the inertial frame using the transformation matrix ${R_b}^{i}$ between the body frame and the inertial frame

$$f^{i} = {R_b}^{i} f^{b} \tag{2.15}$$

$$\vec{g}^{i} = {R_e}^{i} \vec{g}^{e} \tag{2.16}$$

$$\dot{\mathbf{v}}^{i} = {R_b}^{i} f^{b} + {R_e}^{i} \vec{g}^{e} \tag{2.17}$$

As discussed

$$\dot{R}_b^i = R_b^i \Omega_{ib}^b \tag{2.18}$$

where Ω_{ib}^b is the skew-symmetric matrix form of the vector of angular velocities ω_{ib}^b output by the gyroscope.

$$\overset{p}{\omega}_{mk} = \begin{pmatrix} \omega_x \\ \omega_y \\ \omega_z \end{pmatrix} \quad \Rightarrow \quad \overset{p}{\Omega}_{mk} = \begin{pmatrix} 0 & -\omega_z & \omega_y \\ \omega_z & 0 & -\omega_x \\ -\omega_y & \omega_x & 0 \end{pmatrix} \tag{2.19}$$

where $\omega_x, \omega_y, \omega_z,$ are the gyroscope measurements in the b-frame. Solving Eq.2.18 yields the desired transformation matrix R_b^i. Once the elements of the rotation matrix are known, it is possible to calculate the attitude of the body using Euler angles

The mechanization equations for the i-frame can therefore be summarized as

$$\begin{bmatrix} \dot{\mathbf{r}} \\ \dot{\mathbf{v}} \\ \dot{\mathbf{R}}_b^i \end{bmatrix} = \begin{bmatrix} \mathbf{v}^i \\ R_b{}^i f^b + R_e{}^i \vec{g}^e \\ R_b^i \Omega_{ib}^b \end{bmatrix} \tag{2.20}$$

where the specific force vector $\mathbf{f}^b$ and the angular velocity vector ω_{ib}^b are sensor measurements. The gravity model in the e-frame $\vec{g}^e$ is known in advance.

INS Mechanization in ECEF Frame

A position vector r^e in the e-frame can be transformed into the i-frame by using the rotation matrix R_e^i as follows

$$r^i = R_e{}^i f^e \tag{2.21}$$

After differentiating twice and rearranging the terms we get

$$\ddot{r}^i = R_e{}^i \left(\ddot{r}^e + 2\Omega_{ie}^e \dot{r}^e + \dot{\Omega}_{ie}^e r^e + \Omega_{ie}^e \Omega_{ie}^e r^e \right) \tag{2.22}$$

$$R_e{}^i \left(\ddot{r}^e + 2\Omega_{ie}^e \dot{r}^e + \dot{\Omega}_{ie}^e r^e + \Omega_{ie}^e \Omega_{ie}^e r^e \right) = f^i + \vec{g}^i \tag{2.23}$$

$$R_e{}^i \left(\ddot{r}^e + 2\Omega_{ie}^e \dot{r}^e + \dot{\Omega}_{ie}^e r^e + \Omega_{ie}^e \Omega_{ie}^e r^e \right) = R_b^i f^b + R_e^i \vec{g}^e \tag{2.24}$$

by letting $R_b^i = R_e^i R_b^e$ and $\dot{\Omega}_{ie}^e r^e = 0$

$$R_e{}^i \left(\ddot{r}^e + 2\Omega_{ie}^e \dot{r}^e + \Omega_{ie}^e \Omega_{ie}^e r^e \right) = R_e^i R_b^e f^b + R_e^i \vec{g}^e \tag{2.25}$$

$$\ddot{r}^e + 2\Omega_{ie}^e \dot{r}^e + \Omega_{ie}^e \Omega_{ie}^e r^e = R_b^e f^b + \vec{g}^e \tag{2.26}$$

and because the gravity vector is defined as $g^e - \Omega_{ie}^e \Omega_{ie}^e r^e$ this can be further reduced to

$$\ddot{r}^e = R_b^e f^b - 2\Omega_{ie}^e \dot{r}^e + g^e \tag{2.27}$$

which is second-order and can be broken into the following first-order equations

$$\dot{r}^e = v^e \tag{2.28}$$

$$\dot{v}^e = R_b^e f^b - 2\Omega_{ie}^e v^e + g^e \tag{2.29}$$

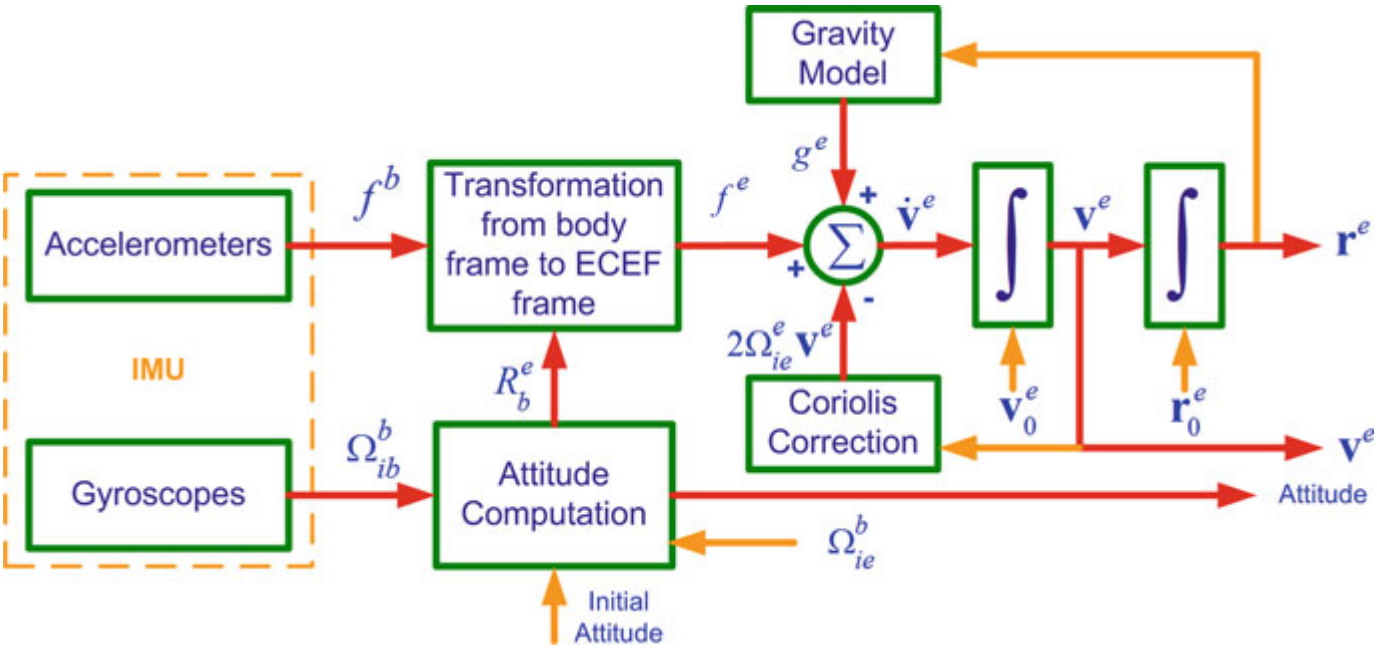

Figure 2.8: A block diagram depicting the mechanization process of an INS in the ECEF frame

The rate of change of the rotation matrix R^e_b can be given as

$$\dot{R}^e_b = R^e_b \Omega^b_{eb} \tag{2.30}$$

As we wish to write the above expression in terms of sensed angular rate ω^b_{ib} monitored by the gyroscopes then we use the following relationship

$$\Omega^b_{eb} = \Omega^b_{ei} + \Omega^b_{ib} \tag{2.31}$$

then

$$\dot{R}^e_b = R^e_b \left(\Omega^b_{ei} + \Omega^b_{ib}\right) \tag{2.32}$$

The e-frame mechanization equations can be summarized as

$$\begin{bmatrix} \dot{r}^e \\ \dot{v}^e \\ \dot{R}^e_b \end{bmatrix} = \begin{bmatrix} v^e \\ R^e_b f^b - 2\Omega^e_{ie} v^e + g^e \\ R^e_b \left(\Omega^b_{ei} + \Omega^b_{ib}\right) \end{bmatrix} \tag{2.33}$$

which represents the mechanization equations in the e-frame where the inputs are the sensed accelerations f^b from the accelerometers and rotation rates ω^b_{ib} from the gyroscopes. The outputs are the position vector r, the velocity vector v, and the Euler angles, all expressed in the e-frame.

INS Mechanization in the Local-Level Frame

Position Mechanization Equations

In many applications the mechanization equations are desired in the LLF

$$r^l = [\varphi, \lambda, h]^T \tag{2.34}$$

the rate of change of platform position is expressed in terms of the velocity in the east, north and up directions

$$\dot{\varphi} = \frac{v_N}{R_M + h} \tag{2.35}$$

$$\dot{\lambda} = \frac{v_e}{(R_N + h)\cos\varphi} \tag{2.36}$$

$$\dot{h} = v_u \tag{2.37}$$

the time rate of change of the position components is related to the velocity components as follows

$$\begin{bmatrix} \dot{\varphi} \\ \dot{\lambda} \\ \dot{h} \end{bmatrix} = \begin{bmatrix} 0 & \frac{1}{R_M+h} & 0 \\ \frac{1}{(R_N+h)\cos\varphi} & 0 & 0 \\ 0 & 0 & 1 \end{bmatrix} \begin{bmatrix} v_e \\ v_n \\ v_u \end{bmatrix}^l \tag{2.38}$$

$$\dot{r}^l = D^{-1} v^l \tag{2.39}$$

in which D^{-1} transforms the velocity vector from rectangular coordinates into curvilinear coordinates in the ECEF frame.

Velocity Mechanization Equations

The acceleration of the moving body is measured in the b-frame by an accelerometer These measurements are known as specific force measurements and are given in the b-frame as

$$f^b = \begin{bmatrix} f_x \\ f_y \\ f_z \end{bmatrix} \tag{2.40}$$

They can be transformed to the local-level frame using the rotation matrix R_b^l

$$f^l = \begin{bmatrix} f_e \\ f_n \\ f_u \end{bmatrix} = R_b^l f^r = R_b^l \begin{bmatrix} f_x \\ f_y \\ f_z \end{bmatrix} \tag{2.41}$$

However, for three reasons the acceleration components expressed in the local level frame cannot directly yield the velocity components of the moving body:

- The rotation of the Earth about its spin axis $\omega^e = 15^\circ/hr$ is interpreted in the local-level frame as the angular velocity vector ω_{ie}^l

$$\omega_{ie}^l = \begin{bmatrix} 0 \\ \omega^e \cos\varphi \\ \omega^e \sin\varphi \end{bmatrix} \tag{2.42}$$

- A change of orientation of the local-level frame with respect to the Earth

$$\omega_{el}^l = \begin{bmatrix} -\varphi \\ \dot{\lambda}\cos\varphi \\ \dot{\lambda}\sin\varphi \end{bmatrix} = \begin{bmatrix} -\frac{v_n}{R_M+h} \\ \frac{v_e}{R_N+h} \\ \frac{v_e \tan\varphi}{R_N+h} \end{bmatrix} \tag{2.43}$$

- The Earth's gravity field is

$$g^l = \begin{bmatrix} 0 \\ 0 \\ -g \end{bmatrix} \tag{2.44}$$

Taking these three factors into the consideration we can derive the expression for the time rate of change of the velocity components of the moving body.

$$\dot{v}^l = R_b^l f^b - \left(2\Omega_{ie}^l + \Omega_{el}^l v^l + g^l\right) \tag{2.45}$$

$$\omega_{ie}^l = \begin{bmatrix} 0 \\ \omega^e \cos\varphi \\ \omega^e \sin\varphi \end{bmatrix} \rightarrow \Omega_{ie}^l = \begin{bmatrix} 0 & -\omega^e \sin\varphi & \omega^e \cos\varphi \\ \omega^e \sin\varphi & 0 & 0 \\ -\omega^e \cos\varphi & 0 & 0 \end{bmatrix} \tag{2.46}$$

$$\omega_{el}^l = \begin{bmatrix} -\varphi \\ \dot{\lambda}\cos\varphi \\ \dot{\lambda}\sin\varphi \end{bmatrix} = \begin{bmatrix} -\frac{v_n}{R_M+h} \\ \frac{v_e}{R_N+h} \\ \frac{v_e \tan\varphi}{R_N+h} \end{bmatrix} \rightarrow \Omega_{el}^l = \begin{bmatrix} 0 & -\frac{v_e \tan\varphi}{R_N+h} & \frac{v_e}{R_N+h} \\ \frac{v_e \tan\varphi}{R_N+h} & 0 & \frac{v_n}{R_M+h} \\ -\frac{v_e}{R_N+h} & -\frac{v_n}{R_M+h} & 0 \end{bmatrix} \tag{2.47}$$

Attitude Mechanization Equations

The attitude (orientation) of the moving body is determined by solving the time derivative equation of the transformation matrix R_b^l that relates the body frame to the local-level frame. For local-level mechanization the following time derivative equation of the transformation matrix should be considered

$$\dot{R}_b^l = R_b^l \Omega_{lb}^b \tag{2.48}$$

$$\Omega_{lb}^b = \Omega_{ib}^b - \Omega_{il}^b \tag{2.49}$$

$$\dot{R}_b^l = R_b^l \left(\Omega_{ib}^b - \Omega_{il}^b\right) \tag{2.50}$$

The rotation matrix can be obtained by solving Eq. (2.50) for the attitude angles.

The quantity Ω_{ib}^b, which is the rate of rotation of the b-frame with respect to the i-frame, is directly measured by the gyroscopes. However, in addition to the angular velocities of the moving body the gyroscopic measurements contain both the Earth's rotation Ω_{ie}^b and the change in orientation of the LLF. So Ω_{il}^b must be subtracted from Ω_{ib}^b to remove these affects. Ω_{il}^b is composed of two parts: Ω_{ie}^b ,which is the Earth's rotation rate with respect to the i-frame expressed in the body frame and Ω_{el}^b, which is the change in the orientation of the LLF with respect to the $ECEF$ frame as expressed in *body* frame. Therefore

$$\Omega_{il}^b = R_l^b \left(\Omega_{ie}^l + \Omega_{el}^l\right) R_b^l \tag{2.51}$$

By substituting this into Eq. (2.50) we get

$$\dot{R}_b^l = R_b^l \left[\Omega_{ib}^b - R_l^b \left(\Omega_{ie}^l + \Omega_{el}^l\right) R_b^l\right] \tag{2.52}$$

The results of the previous subsections can be summarized as follows

$$\begin{bmatrix} \dot{r}^l \\ \dot{v}^l \\ \dot{R}_b^l \end{bmatrix} = \begin{bmatrix} D^{-1} v^l \\ R_b^l f^b - \left(2\Omega_{ie}^l + \Omega_{el}^l\right) v^l + g^l \\ R_b^l \left\{\Omega_{ib}^b - R_l^b \left(\Omega_{ie}^l + \Omega_{el}^l\right) R_b^l\right\}) \end{bmatrix} \tag{2.53}$$

which expresses the mechanization in the local-level frame. The position output is expressed in ECEF curvilinear coordinates ϕ, λ, h, the velocity output is in l-frame coordinates $v_e; v_n; v_u$, and

the attitude angles (roll, pitch and yaw) are measured with respect to the l-frame. Figure 2.9 is a block diagram of local-level frame mechanization.

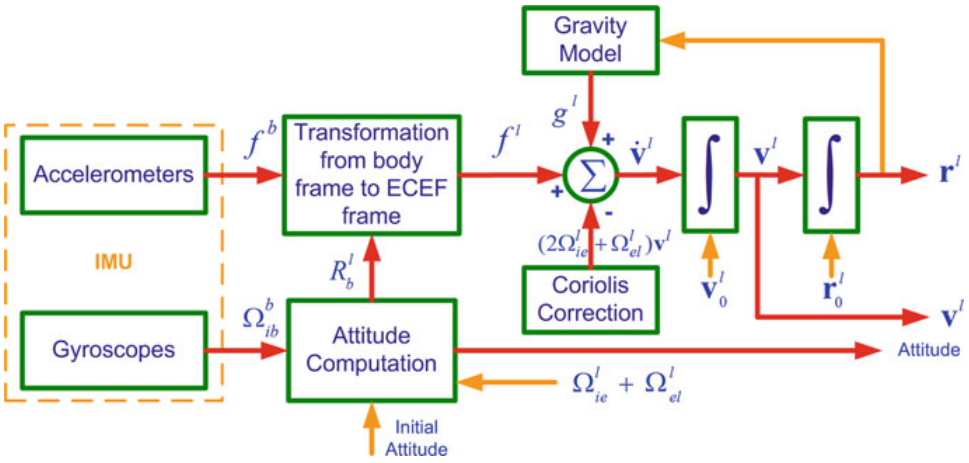

Figure 2.9: A block diagram depicting the mechanization of an INS in the local-level frame

INS Mechanization in Wander Frame

The l-frame rotates continuously as it moves over the curved surface of the Earth because its y-axis always pointing toward the north (tangential to the meridian).this rate of rotation becomes ever greater as the l-frame approaches the pole and will become infinite if the l-frame passes directly over the pole.

The rotational rate of the navigation l-frame over the Earth's surface (known as the transport rate) is

$$\omega_{el}^{l} = \begin{bmatrix} -\varphi \\ \dot{\lambda}\cos\varphi \\ \dot{\lambda}\sin\varphi \end{bmatrix} = \begin{bmatrix} \omega_e \\ \omega_n \\ \omega_u \end{bmatrix} = \begin{bmatrix} -\frac{v_n}{R_M+h} \\ \frac{v_e}{R_N+h} \\ \frac{v_e \tan\varphi}{R_N+h} \end{bmatrix} \tag{2.54}$$

where ω_e, ω_n and ω_u are the east, north and up angular velocity components as in Fig. (2.10).

It is evident from Eq. (2.54) that the third component of the above vector will introduce numerical instabilities as φ approaches $\pi/2$ and will actually be indeterminate at the pole. This condition is avoided by using the wander azimuth frame in which the third component of Eq. (2.54) is forced to zero and the y-axis of the w-frame will deviate from true north by an angle α, referred to as the wander azimuth angle ([4]). This angle is initialized when initiating the

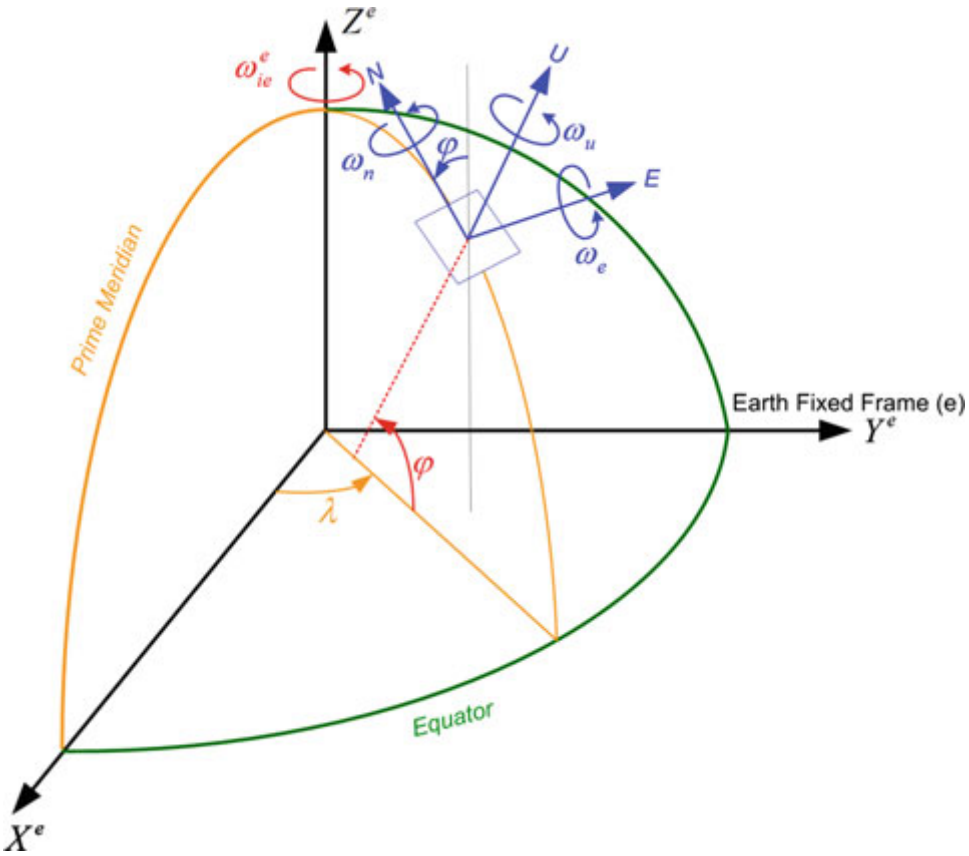

Figure 2.10: A depiction of the rotational velocity components experienced in the l-frame

trajectory. In the *wander* frame, the wander azimuth angle between the true north and the y-axis of the frame varies as the vehicle moves. The output parameters of the w-frame mechanization are eventually transformed into the l-frame. The angular rate vector of the wander frame with respect to the l-frame can be expressed ([5]) as

$$\omega_{lw}^l = [0\ 0\ \dot{\alpha}]^T \tag{2.55}$$

and the angular rate of the wander frame with respect to the e-frame is

$$\omega_{ew}^l = \omega_{el}^l + \omega_{lw}^l \tag{2.56}$$

$$\omega_{ew}^l = \begin{bmatrix} -\dot{\varphi} \\ \dot{\lambda}\cos\varphi \\ \dot{\lambda}\sin\varphi \end{bmatrix} + \begin{bmatrix} 0 \\ 0 \\ \dot{\alpha} \end{bmatrix} = \begin{bmatrix} -\dot{\varphi} \\ \dot{\lambda}\cos\varphi \\ \dot{\lambda}\sin\varphi + \dot{\alpha} \end{bmatrix} \tag{2.57}$$

and therefore the rotation rate of the w-frame with respect to the e-frame, resolved in the w-frame, is

$$\omega_{ew}^w = R_l^w \omega_{ew}^l \tag{2.58}$$

transpose of the matrix R_l^w

$$R_w^l \begin{bmatrix} \cos\alpha & -\sin\alpha & 0 \\ \sin\alpha & \cos\alpha & 0 \\ 0 & 0 & 1 \end{bmatrix} \tag{2.59}$$

To force the third component ω_u of Eq. (2.54) to be zero we must ensure that

$$\dot{\alpha} = -\lambda \sin\varphi \tag{2.60}$$

The mechanization equations are equivalent to those of the l-frame except that all the notations are for the w-frame rather than for the l-frame

$$\begin{bmatrix} \dot{r}^w \\ \dot{v}^w \\ \dot{R}_b^w \end{bmatrix} = \begin{bmatrix} D^{-1} v^w \\ R_b^w f^b - \left(2\Omega_{ie}^w + \Omega_{ew}^w\right) v^w + g^w \\ R_b^w \left(\Omega_{ib}^b - \Omega_{iw}^b\right) \end{bmatrix} \tag{2.61}$$

2.7 Parameterization of the Rotation Matrix

The solution of the mechanization equations requires the parameterization of the rotation matrix R_b^l. The three most common methods are Euler angles, direction cosines and the quaternion. Euler angles require only three independent parameters. Direction cosines require nine parameters, six of which are independent. Both of these methods are computationally expensive and therefore inappropriate for real-time computations. Furthermore, Euler angles are prone to singularities. The six independent kinematic equations involved in the derivative of the rotation matrix $\dot{R}_x^y = R_x^y \Omega_{yx}^x$ cannot be solved in closed form, and require numerical integration. The most effective way of parameterizing the transformation matrix is therefore to use the quaternion method.**[Appendix]**

2.8 Quaternions

Solving the mechanization equations requires the parameterization of the rotation matrix R_b^l. The most popular method is the quaternion approach ([6]). Euler's theorem states that the rotation of a rigid body (represented by the body frame) with respect to a reference frame (in this case the

computational frame) can be expressed in terms of a rotation angle θ about a fixed axis and the direction cosines of the rotation axis that define the rotation direction. Figure (2.11) represents a quaternion where θ is the magnitude of the rotation and α, β and γ define the orientation of the unit vector '**n**' that lies along the axis of rotation. A quaternion is a four-parameter representation of a transformation matrix that is defined ([7]) as follows

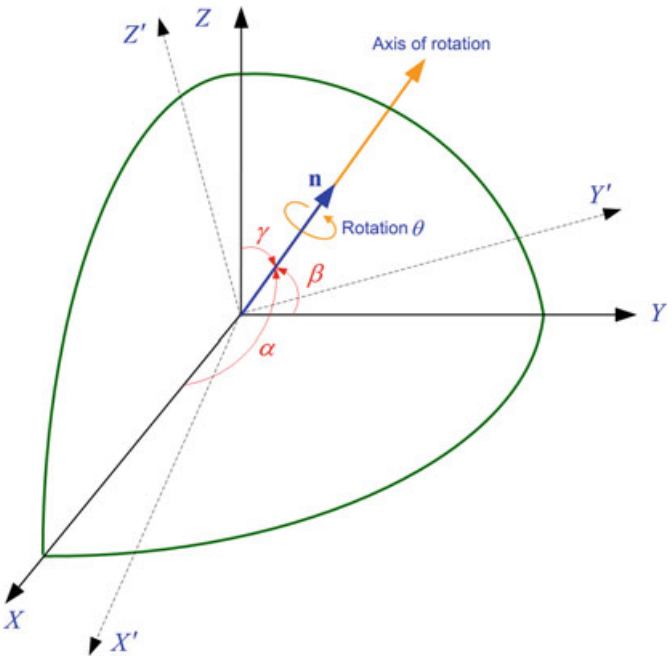

Figure 2.11: Spatial representation of a quaternion in relation to the reference frame XYZ

$$q = \begin{bmatrix} q_1 \\ q_2 \\ q_3 \\ q_4 \end{bmatrix} = \begin{bmatrix} \frac{\theta_x}{\theta} \sin\frac{\theta}{2} \\ \frac{\theta_y}{\theta} \sin\frac{\theta}{2} \\ \frac{\theta_z}{\theta} \sin\frac{\theta}{2} \\ \frac{\cos\theta}{2} \end{bmatrix} \tag{2.62}$$

where $\theta = \sqrt{\theta_x^2 + \theta_y^2 + \theta_z^2}$ is the rotation angle, and $\frac{\theta_x}{\theta}$, $\frac{\theta_y}{\theta}$ and $\frac{\theta_z}{\theta}$ are direction cosines of the rotation axis with respect to the computational frame. The components of a quaternion are related by the constraint $q_1^2 + q_2^2 + q_3^2 + q_4^2 = 1$ The quaternion parameters are functions of time, and the associated differential equation is

$$\dot{q} = \frac{1}{2}\vec{\Omega}(\omega)\, q \tag{2.63}$$

where $\vec{\Omega}(\omega)$ is the skew-symmetric matrix of the following form

$$\vec{\Omega}(\omega) = \begin{bmatrix} 0 & \omega_z & -\omega_y & \omega_x \\ -\omega_y & 0 & \omega_x & \omega_y \\ \omega_y & -\omega_x & 0 & \omega_z \\ -\omega_x & -\omega_y & -\omega_z & 0 \end{bmatrix} \tag{2.64}$$

2.8.1 Relationship Between the Transformation Matrix and Quaternion Parameters

Once the quaternion parameters are known at a certain time, the rotation matrix R can be obtained using the following direct relationship

$$R = \begin{bmatrix} R(1,1) & R(1,2) & R(1,3) \\ R(2,1) & R(2,2) & R(2,3) \\ R(3,1) & R(3,2) & R(3,3) \end{bmatrix} = \begin{bmatrix} q_1^2 - q_2^2 - q_3^2 + q_4^2 & 2(q_1q_2 - q_3q_4) & 2(q_1q_3 + q_2q_4) \\ 2(q_1q_2 + q_3q_4) & -q_1^2 + q_2^2 - q_3^2 + q_4^2 & 2(q_2q_3 - q_1q_4) \\ 2(q_1q_3 - q_2q_4) & 2(q_2q_3 + q_1q_4) & -q_1^2 - q_2^2 + q_3^2 + q_4^2 \end{bmatrix} \tag{2.65}$$

After determining the initial rotation matrix from the attitude angles measured during the alignment process, the initial values of the quaternion are calculated as A.3

$$\begin{bmatrix} q_1 \\ q_2 \\ q_3 \\ q_4 \end{bmatrix}_{t_0} = \begin{bmatrix} 0.25\left(\frac{R(3,2)-R(2,3)}{q_4}\right) \\ 0.25\left(\frac{R(1,3)-R(3,1)}{q_4}\right) \\ 0.25\left(\frac{R(2,1)-R(1,2)}{q_4}\right) \\ 0.25\sqrt{1 + R(1,1) + R(2,2) + R(3,3)} \end{bmatrix} \tag{2.66}$$

2.9 Step by Step Computation of Navigation Parameters in the l-Frame

Owing to the advantages offered by mechanization in the l-frame, many applications prefer to implement mechanization in this frame of reference. steps of the mechanization process in the l-frame are as follow.

- Obtain rotation rates $(\omega_x, \omega_y, \omega_z)$ from the gyroscopes and accelerations $(f_x; f_y; f_z)$ from the accelerometers. These measurements are in relation to the inertial frame resolved into the body frame, and they constitute the IMU outputs.

- Calculate the attitude angles of pitch, roll and azimuth (p, r, A) in terms of the rotation rates $(\omega_x, \omega_y, \omega_z)$. This involves the computation of R_b^l
- Use R_b^l. computed by the previous step to transform the specific forces in the body frame to the navigation frame, yielding the accelerations in the local-level frame (f_e, f_n, f_u).
- Since accelerometers also measure gravity and Coriolis forces, we must compensate for these effects.
- Calculate the east, north and up velocities (V_e, V_n, V_u) by integrating the transformed specific forces (f_e, f_n, f_u).
- Calculate the geodetic coordinates of the position (φ, λ, h) by integrating the velocities.

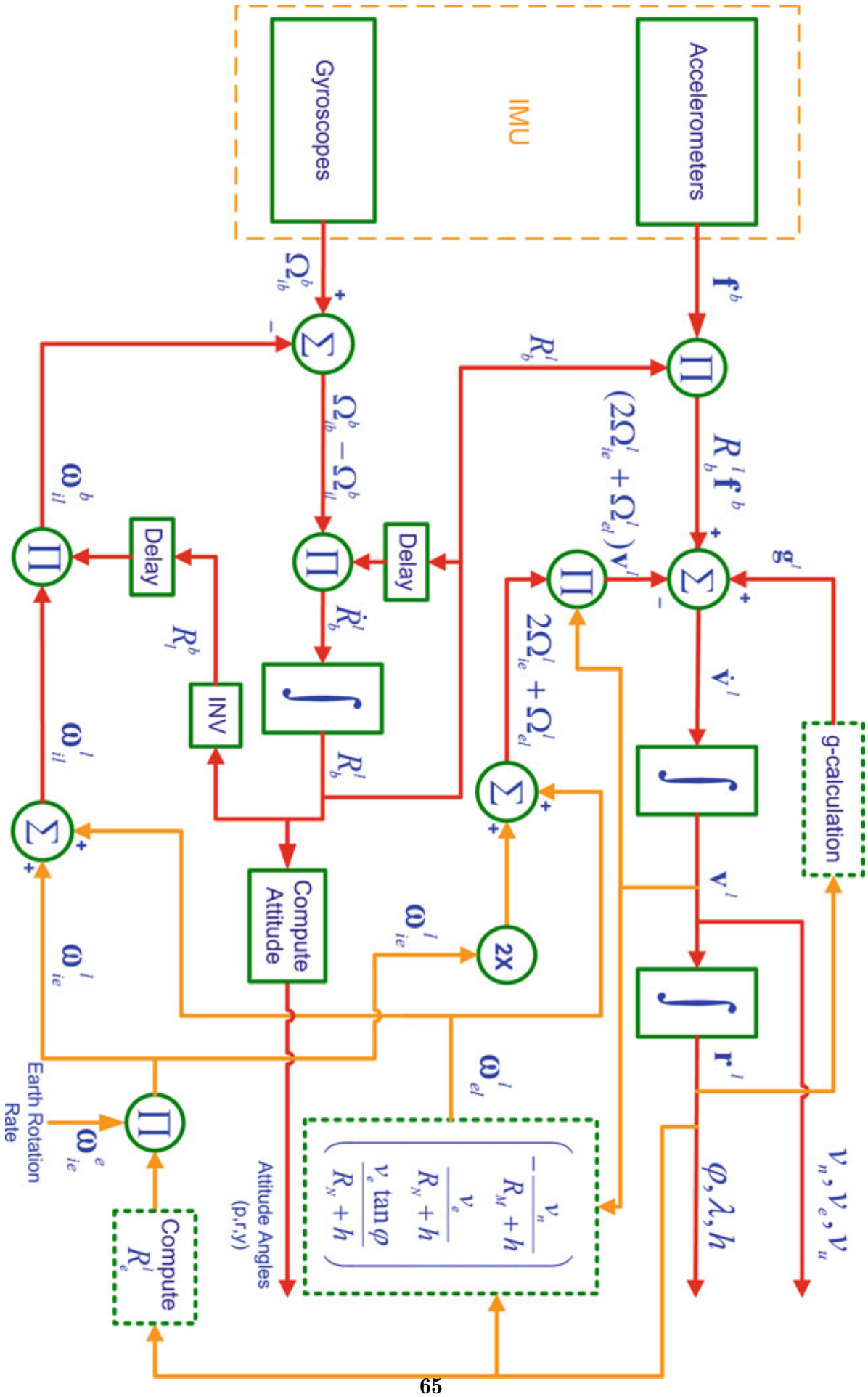
IMU
Gyroscopes
Accelerometers
Delay
Delay
Delay
INV
Compute Attitude
2X
g-calculation
Earth Rotation Rate
Compute R_e^l
Attitude Angles (p,r,y)
φ, λ, h
v_n, v_e, v_u

It should be noted that the rotation rate of the l-frame due to the Earth's rotation rate ω_{ie}^{i} and movement on the curved surface of the Earth ω_{el}^{l} must be compensated from the measured angular rate of the body ω_{ib}^{b} prior to integration. Similarly, the Coriolis acceleration due to the Earth's rotation Ω_{ie}^{l} and movement of the l-frame over Earth's curvature ω_{el}^{l} must be subtracted from the measured specific force f^{b}. The mechanization algorithm provides the position, velocity and attitude components of the moving platform in the following format • The position in geodetic (curvilinear) coordinates (φ, λ, h) • The velocities along the east, north and up directions $(V_e; V_n; V_u)$ • The attitude angles as roll, pitch and yaw. Mechanization in the l-frame is more intuitive for navigation on or near the Earth's surface because the position of the moving platform is provided in familiar map coordinates (latitude, longitude and altitude) and its attitude is given as angles in the familiar roll, pitch and yaw scheme. Also, the gravity model for the l-frame is *simpler*.

2.9.1 Raw Measurement Data

The output of inertial sensors can sometimes (and especially for low cost sensors) be the angular rates and specific forces rather than incremental values. Because we require incremental values for our algorithms the angular rates and specific forces must be changed to their incremental counterparts as follows

$$\Delta\tilde{v}^{b} = \tilde{f}^{b}\,\Delta t \tag{2.67}$$

$$\Delta\overset{\sim}{\theta}_{ib}^{b} = \overset{\sim}{\omega}_{ib}^{b}\Delta t \tag{2.68}$$

$\tilde{f}^{b}$ is the specific force (i.e. the output of the accelerometer) (m/sec^2)

$\overset{\sim}{\omega}_{ib}^{b}$ is the rotation rate of the body frame with respect to the inertial frame, resolved in the body frame (i.e. the output of the gyroscope) $(radian/sec)$

$\Delta\tilde{v}^{b}$ is the change in specific force during the time interval t (i.e. the velocity) (m/s)

$\Delta\overset{\sim}{\theta}_{ib}^{b}$ is the change in angular rate during the time interval t (i.e. an angle) (in radians)

Δt is the sampling interval (i.e. the reciprocal of the sampling frequency) (sec)

2.9.2 Correction of the Measurement Data

Although inertial sensors are calibrated in the factory they are usually recalibrated in the laboratory, as a result of this calibration the biases and scale factors of the sensors are computed and

subsequently compensated for in the raw measurements in order to obtain corrected measurements using the following relationship

$$\Delta\theta_{ib}^{b} = \frac{\tilde{\Delta\theta}_{ib}^{b} - b_{gyro}\Delta t}{1 + S_{gyro}} \tag{2.69}$$

$$\Delta v^{b} = \frac{\tilde{\Delta v}^{b} - b_{acc}\Delta t}{1 + S_{acc}} \tag{2.70}$$

where

b_{gyro} is the drift of the gyroscope (radians/sec)

S_{gyro} is the gyroscope scale factor (in ppm)

b_{gyro} is the bias of the accelerometer (m/sec^2)

S_{gyro} is the accelerometer scale factor (in ppm)

$\Delta\theta_{ib}^{b}$ the corrected incremental gyroscope output (in radians/sec)

Δv_{ib}^{b} is the corrected incremental accelerometer output (in m/s)

2.9.3 Calculation and Updating of Rotation Matrix

In l-frame mechanization the updated rotation matrix R_b^l transforms the sensor outputs from the body frame to the l-frame, which requires a determination of the angular increment θ_{lb}^{b} of the body with respect to the l-frame.

Computation of Angular Increment of Body Rotation

The angular rate of the body with respect to the l-frame ω_{ib}^{b} is

$$\omega_{lb}^{b} = \omega_{ib}^{b} - \omega_{il}^{b} \tag{2.71}$$

$$\omega_{il}^{b} = R_{l}^{b}\omega_{il}^{l} \tag{2.72}$$

$$\omega_{il}^{l} = \omega_{ie}^{l} + \omega_{el}^{l} \tag{2.73}$$

$$\omega_{ie}^{l} = R_{e}^{l}\omega_{ie}^{e} \tag{2.74}$$

$$\tag{2.75}$$

$$\omega_{ie}^{l} = \begin{bmatrix} -sin\lambda & \cos\lambda & 0 \\ -\sin\varphi\cos\lambda & -\sin\varphi\sin\lambda & \cos\varphi \\ \cos\varphi\cos\lambda & \cos\varphi\sin\lambda & \sin\varphi \end{bmatrix} \begin{bmatrix} 0 \\ 0 \\ \omega_e \end{bmatrix} = \begin{bmatrix} 0 \\ \omega_e\cos\varphi \\ \omega_e\sin\varphi \end{bmatrix} \tag{2.76}$$

$$\omega_{el}^{l} = \begin{bmatrix} \dot{\varphi} \\ \dot{\lambda}\cos\varphi \\ \dot{\lambda}\sin\varphi \end{bmatrix} = \begin{bmatrix} -\frac{v_n}{M+h} \\ \frac{v_e}{N+h} \\ \frac{v_e \tan\varphi}{N+h} \end{bmatrix} \tag{2.77}$$

After finding the values of the appropriate terms through the above procedure and substituting them into Eq. (2.75), the equation

is integrated for interval Δt obtain the angular increment of the body rotation with respect to the l-frame

$$\theta_{lb}^{b} = \theta_{ib}^{b} - \theta_{il}^{b} \tag{2.78}$$

Updating the Quaternion

The quaternion can be updated by the analytical method. The closed form solution of the quaternion equation is

$$q_{k+1} = q_k + \frac{1}{2}\left[2\left(\cos\frac{\theta}{2} - 1\right)I + \frac{2}{\theta}\sin\frac{\theta}{2}\bar{S}(\omega)\right]q_k \tag{2.79}$$

$$\begin{bmatrix} q_1 \\ q_2 \\ q_3 \\ q_4 \end{bmatrix} q_{k+1} = q_k + \frac{1}{2}\left[2\left(\cos\frac{\theta}{2} - 1\right)I + \frac{2}{\theta}\sin\frac{\theta}{2}\bar{S}(\omega)\right]q_k \tag{2.80}$$

Chapter 3

Simulation of Strapdown Inertial Navigation System

Many navigation books and papers on inertial navigation system (INS) provide readers with the basic principle of INS. Some also superficially describe simulation methods and rarely provide the free code which can be used by new INS users to help them understand the theory and develop INS applications. Commercial simulation software is available but is not free. The objective of this paper is to develop an easy-to-understand step-by-step development method for simulating INS. Here we consider the most popular INS which is the strapdown inertial navigation system (SINS). The mathematical operations required in our work are mostly matrix manipulations and more generally basic linear algebra [9]. In this paper,Matlab [10] and Mathematica [11] are chosen as the simulation environments. It is a popular computing environment to perform complex matrix calculations and to produce sophisticated graphics in a relatively easy manner. A large collection of Matlab scripts are now available for a wide variety of applications and are often used for university courses.Matlab is also becoming more and more popular in industrial research centers in the design and simulation stages. The main purposes of this work are to develop a comprehensive Matlab implementations for SINS.

In this work, we choose the p-frame as the navigation frame for vehicle trajectory calculation, for the following reason. In the local geographic navigation frame mechanization, the n-frame is required to rotate continuously as the system moves over the surface of the Earth in order to keep its P_{yN} axis pointing to the true north. In order to achieve this condition worldwide, the n-frame must rotate at much greater rates about its P_{zN} axis as the navigation system

moves over the surface of the Earth in the polar regions, compared to the rates required at lower latitudes. It is clear that near the polar areas the local geographic navigation frame must rotate about its P_{zN} axis rapidly in order to maintain the P_{yN}axis pointing to the pole. The heading direction will abruptly change by 180° when moving past the pole. In the most extreme case, the turn rate becomes infinite when passing over the pole. One way of avoiding the singularity, and also providing a navigation system with worldwide capability, is to adopt a wander azimuth mechanization in which the z-component of ω_{ep}^{p} is always set to zero, that is, $\omega_{ep_z}^{p} = 0$. A wander axis system is a local level frame which moves over the Earth surface with the moving vehicle, as depicted in Figure 3.1. However, as the name implies, the azimuth angle between P_{y_N} axis

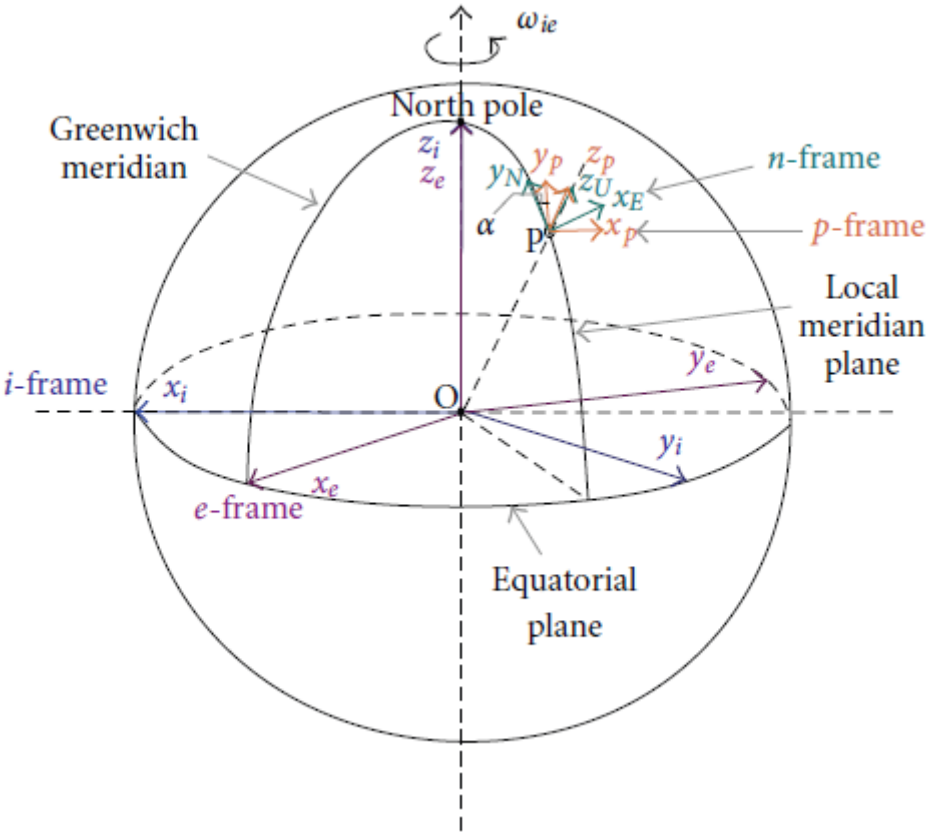

Figure 3.1: The reference frames.

and P_{y_p} axis varies with the vehicle position on Earth equation 2.60. This variation is chosen in order to avoid discontinuities in the orientation of the wander frame with respect to Earth as the vehicle passes over either the north or south pole. below, the main principle of SINS in the p-frame is described. Along the same lines as in [2], a navigation equation for a wander azimuth

system can be constructed as follows:

$$\dot{v}_e^p = C_b^p f^b - \left(2C_e^p \omega_{ie}^e + \omega_{ep}^p\right) v_e^p + g^p \tag{3.1}$$

This matrix propagates in accordance with the following equation:

$$\dot{C}_b^p = C_b^p \Omega_{pb}^b \tag{3.2}$$

Equation 3.2 is integrated to generate estimates of the vehicle speed in the wander azimuth frame, v_e^p.This is then used to generate the turn rate of the wander frame with respect to the Earth frame, ω_{ep}^p

$$\dot{C}_p^e = C_p^e \Omega_{ep}^p \tag{3.3}$$

$$(\dot{C}_p^e)^T = -\Omega_{ep}^p (C_p^e)^T \tag{3.4}$$

$$\dot{C}_e^p = -\Omega_{ep}^p C_e^p \tag{3.5}$$

Because the z-component of $\omega_{ep}^p = 0$ the matrix expression of ω_{ep}^p is

$$\omega_{ep}^p = \begin{bmatrix} \omega_{epx}^p \\ \omega_{epy}^p \\ 0 \end{bmatrix} \tag{3.6}$$

. This process is implemented iteratively and enables any singularities to be avoided.

3.1 Cosine Matrices (DCMs)

Vehicle Attitude DCM C_b^p The definition of the rotation sequence from p-frame to b-frame is (see Figure 3.2)

$$x_p y_p z_p \xrightarrow{z_p, \Psi_G} x'_e y'_e z'_e \xrightarrow{y'_e, \theta} x''_e y''_e z''_e \xrightarrow{x''_e, \gamma} x_b y_b z_p \tag{3.7}$$

$$\overset{p}{C}_b = (\overset{b}{C}_p)^T = \begin{bmatrix} \cos\gamma\cos\Psi_G - \sin\gamma\sin\theta\sin\Psi_G & -\cos\theta\sin\Psi_G & \sin\gamma\cos\Psi_G + \cos\gamma\sin\theta\sin\Psi_G \\ \cos\gamma\sin\Psi_G + \sin\gamma\sin\theta\cos\Psi_G & \cos\theta\cos\Psi_G & \sin\gamma\sin\Psi_G - \cos\gamma\sin\theta\cos\Psi_G \\ -\sin\gamma\cos\theta & \sin\theta & \cos\gamma\cos\theta \end{bmatrix} \tag{3.8}$$

We have that

$$\Psi = \Psi_G + \alpha \tag{3.9}$$

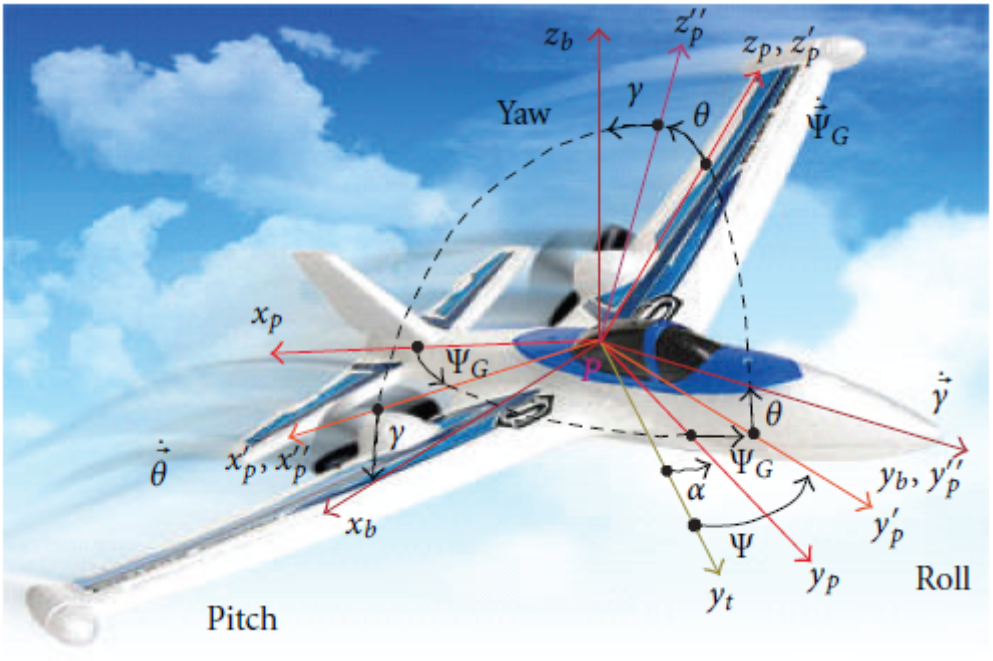

Figure 3.2: The relation between b-frame and p-frame.

, so

$$\overset{n}{C}_b = \begin{bmatrix} \cos\gamma\cos\Psi - \sin\gamma\sin\theta\sin\Psi & -\cos\theta\sin\Psi & \sin\gamma\cos\Psi + \cos\gamma\sin\theta\sin\Psi \\ \cos\gamma\sin\Psi + \sin\gamma\sin\theta\cos\Psi & \cos\theta\cos\Psi & \sin\gamma\sin\Psi - \cos\gamma\sin\theta\cos\Psi \\ -\sin\gamma\cos\theta & \sin\theta & \cos\gamma\cos\theta \end{bmatrix} \tag{3.10}$$

$$\begin{bmatrix} \omega^b_{nbx} \\ \omega^b_{nby} \\ \omega^b_{nbz} \end{bmatrix} = \begin{bmatrix} \cos\gamma\dot{\theta} - \sin\gamma\cos\theta\dot{\psi} \\ \dot{\gamma} + \sin\theta\dot{\psi} \\ \sin\gamma\dot{\theta} + \cos\gamma\cos\theta\dot{\psi} \end{bmatrix} \tag{3.11}$$

Vehicle Position DCM C_e^p Position matrix C_e^p is the DCM from e-frame to p-frame. It has the following rotating sequence (see Figure 3.3):

$$x_e y_e z_e \xrightarrow{z_e,\lambda} x_e' y_e' z_e' \xrightarrow{y_e',90^\circ-\varphi} x_e'' y_e'' z_e'' \xrightarrow{z_e'',90^\circ} x_N y_E z_U \xrightarrow{z_U,\alpha} x_p y_p z_p \tag{3.12}$$

$$\overset{p}{C}_e = \begin{bmatrix} -\sin\alpha\sin\varphi\cos\lambda - \cos\alpha\sin\lambda & -\sin\alpha\sin\varphi\sin\lambda + \cos\alpha\cos\lambda & \sin\alpha\cos\varphi \\ -\cos\alpha\sin\varphi\cos\lambda + \sin\alpha\sin\lambda & -\cos\alpha\sin\varphi\sin\lambda - \sin\alpha\cos\lambda & \cos\alpha\cos\varphi \\ \cos\varphi\cos\lambda & \cos\varphi\sin\lambda & \sin\varphi \end{bmatrix} \tag{3.13}$$

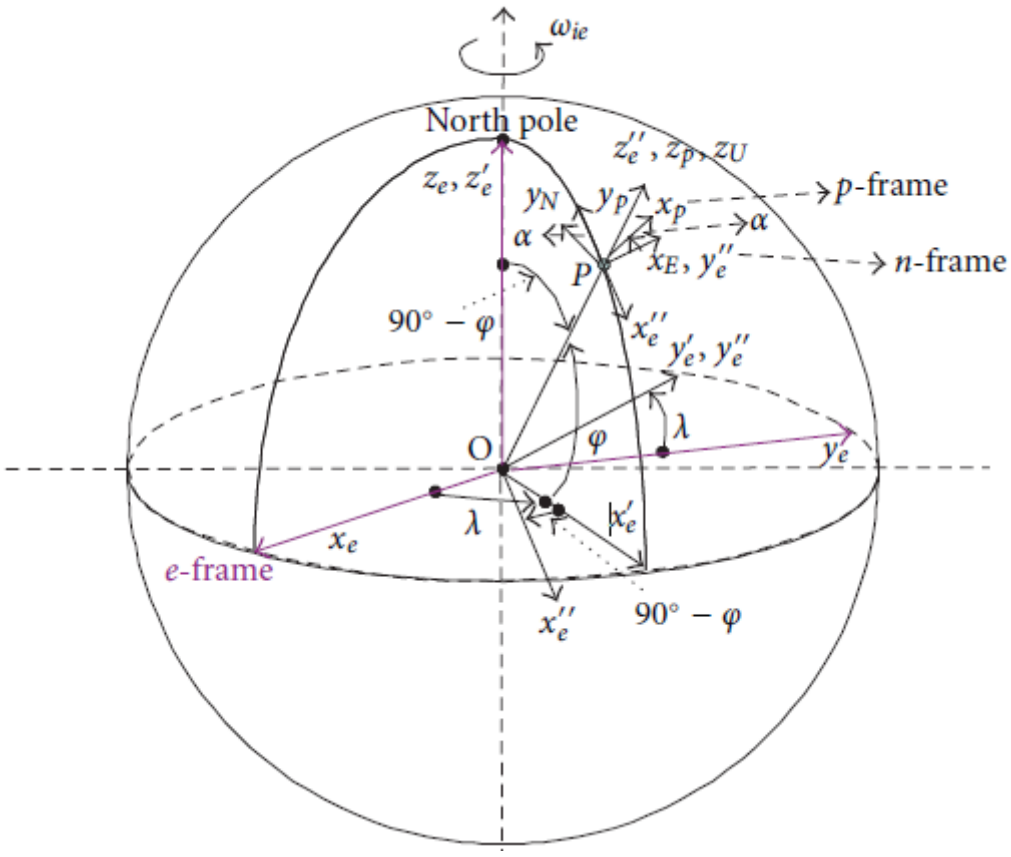

Figure 3.3: The relation between e-frame and p-frame

A trajectory simulation method in the ENU-frame is described step by step to generate sensor data. forward a trajectory and attitude simulator method in the p-frame is described step by step to derive the desired trajectory and attitude from the simulated sensor data or real sensor data; initial parameters and initial data calculation are provided **Sensor Data Generator** The purpose of trajectory simulation is to generate data of the 3 orthogonal gyros and the 3 orthogonal accelerometers according to the designed trajectory. It is mentioned in that p-frame is set up to avoid the singularities when the vehicle passes over either the north or south pole. But in most applications, the SINS systems are seldom operated under this extreme environment. The ENU-frame can be implemented easier than p-frame, so it is chosen as the navigation frame. Figure 3.4 shows the whole process of the SINS principal in the ENU-frame mechanization. First, the vehicle trajectory in the ENU-frame is set. Then, the sensor ideal output is derived using the inverse principle of INS. The sensor simulation data can be obtained by adding noise to the ideal data. Then, we use the simulated sensor data to derive the noise-corrupted simulated trajectory.

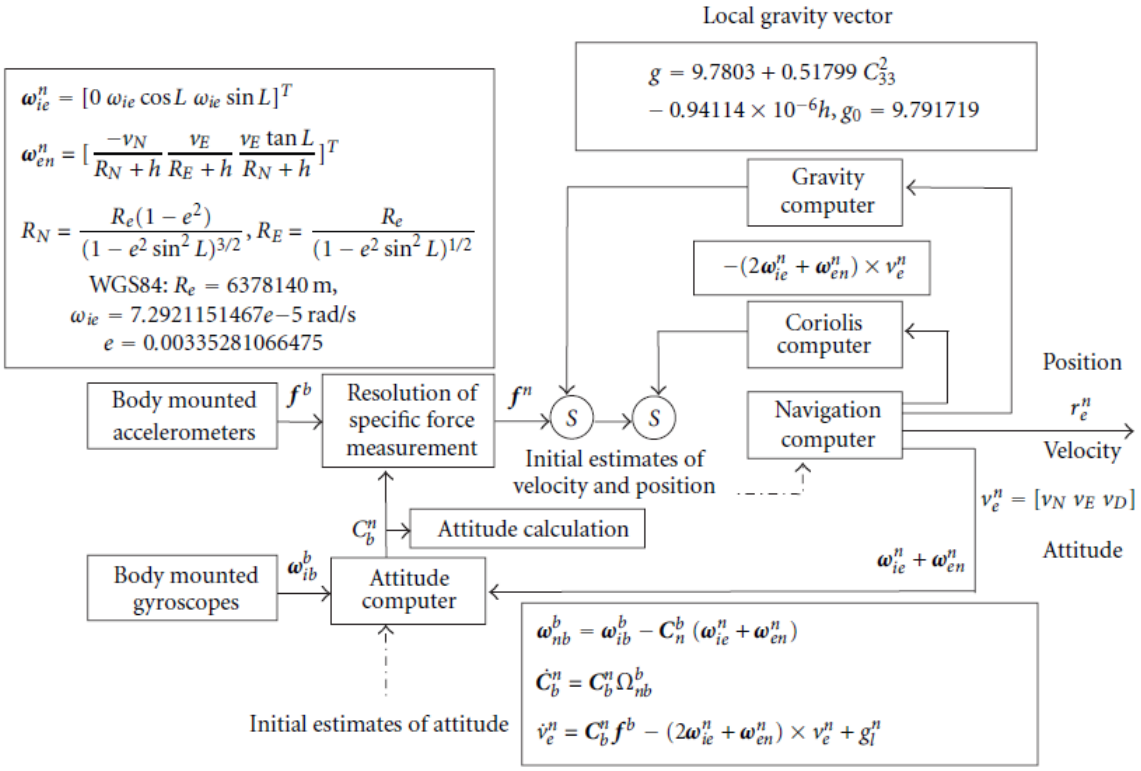

Figure 3.4: SINS ENU-frame mechanization.

Besides, the difference between the ideal and simulated state vectors can be set as the input for the observed measurements in the Kalman filter.

For the designed trajectory, the initial parameters are

- initial position, latitude φ_0, longitude λ_0, height h_0
- initial velocity $v = [v_{E0}, v_{N0}, v_{U0}]$
- the designed variation of acceleration a, which varies with time according to the designed trajectory
- the designed variations of the attitude angles, pitch θ roll γ , and heading ψ, and attitude angle rates, $\dot{\theta}$,$\dot{\gamma}$, and $\dot{\psi}$, which vary with time according to the designed trajectory.

The Update of Velocity . The velocity is updated as

$$v \leftarrow v + a\Delta t \tag{3.14}$$

The Update of Position . The position is updated as

$$L \leftarrow L + \frac{v_N \Delta t}{R_N} \tag{3.15}$$

$$\lambda \leftarrow \lambda + \frac{v_E \Delta t \sec L}{R_E} \tag{3.16}$$

$$h \leftarrow h + v_U \Delta t \tag{3.17}$$

The Update of Attitude. The attitude angles are updated as The Update of Position. The position is updated as

$$\theta \leftarrow \theta + \Delta\theta \tag{3.18}$$

$$\gamma \leftarrow \gamma + \Delta\gamma \tag{3.19}$$

$$\psi \leftarrow \psi + \Delta\psi \tag{3.20}$$

The attitude rates are updated as

$$\dot{\theta} \leftarrow \dot{\theta} + \Delta\dot{\theta} \tag{3.21}$$

$$\dot{\gamma} \leftarrow \dot{\gamma} + \Delta\dot{\gamma} \tag{3.22}$$

$$\dot{\psi} \leftarrow \dot{\psi} + \Delta\dot{\psi} \tag{3.23}$$

The expressions for $\Delta\theta$, $\Delta\gamma$,$\Delta\psi$ and $\Delta\dot{\theta}$, $\Delta\dot{\gamma}$, $\Delta\dot{\psi}$ depend on the designed trajectory. The direction cosine matrix C_b^n can be calculated using matrix expression (3.52).We have that $C_n^b = (C_b^n)^T$

Gyro Data Generator. The output of the gyros is

$$\omega_{ib}^b = (\mathbf{I} - S_g)(C_n^b(\omega_{ie}^n + \omega_{en}^n) + \omega_{nb}^b + \epsilon^b) \tag{3.24}$$

where ω_{ib}^b is the simulated actual output, $\mathbf{I}$ is the 3x3 unit matrix, S_g is the 3×3 diagonal matrix whose diagonal elements correspond to the 3 gyros' scale factor errors, and ϵ^b is the gyro's drift and can be simulated as the sum of a constant noise and a random white noise $\epsilon^b = \epsilon^{b_const} + \epsilon_{random}^b$

$$\omega_{ie}^n = \begin{bmatrix} 0 \\ w_{ie}\cos L \\ w_{ie}\sin L \end{bmatrix} \tag{3.25}$$

In a static base, ω_{nb}^{b} is equal to zero, whereas, in a moving base it is obtained as

$$\omega_{nb}^{b} = \begin{bmatrix} \cos\gamma\dot{\theta} - \sin\gamma\cos\theta\dot{\psi} \\ \dot{\gamma} + \sin\theta\dot{\psi} \\ \sin\gamma\dot{\theta} + \cos\gamma\cos\theta\dot{\psi} \end{bmatrix} \tag{3.26}$$

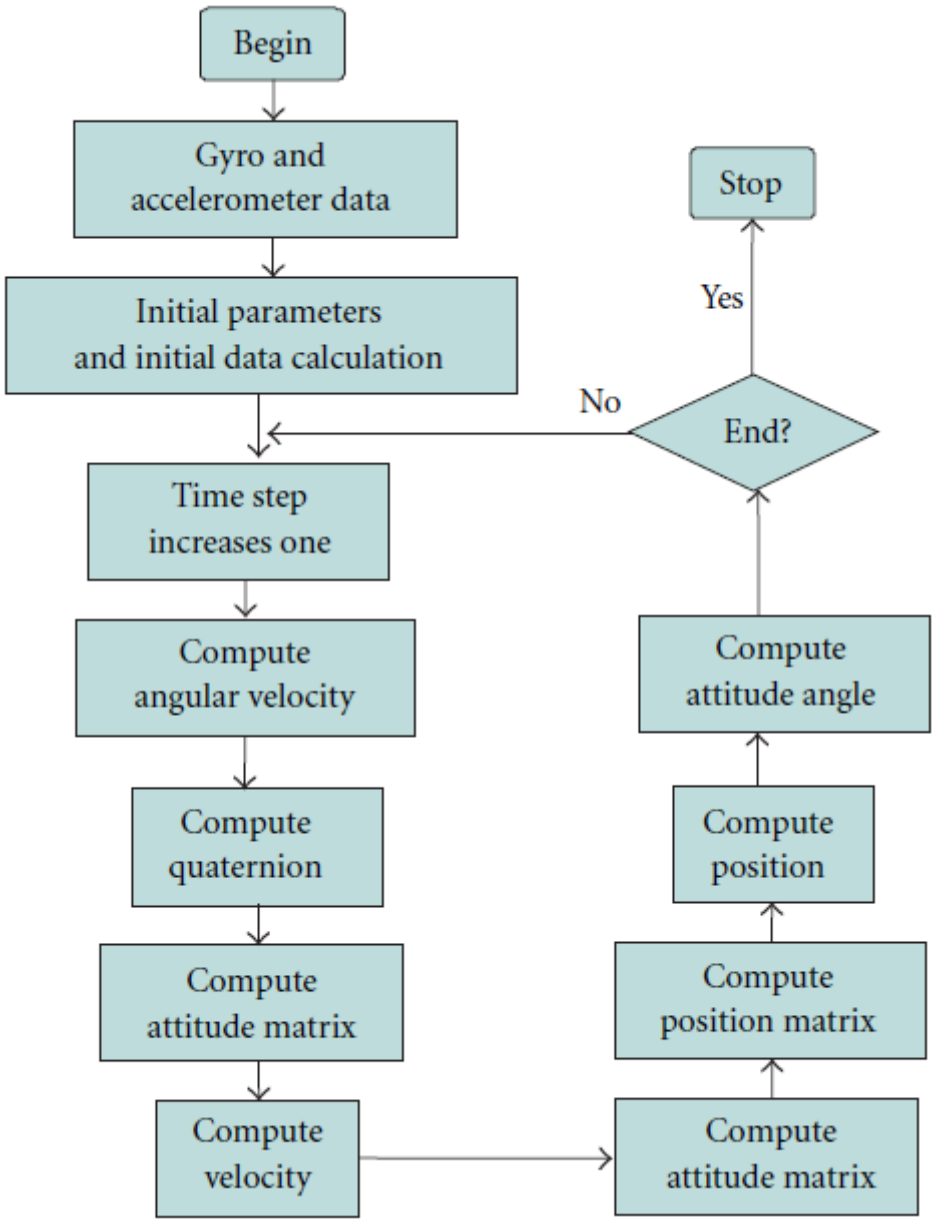

Figure 3.5: SINS. program structure

Accelerometer Data Generator. The measurement of the accelerometer is the specific force:

$$f^b = (\mathbf{I} - S_a)C_n^b f^n + \eta^b \tag{3.27}$$

$$f^n = a + (2\omega_{ie}^n + \omega_{en}^n) \times v - g \tag{3.28}$$

where f^b is the simulated actual output, $\mathbf{I}$ is the 3x3 unit matrix. S_a is the 3x3 diagonal matrix whose diagonal elements correspond to the 3 accelerometers' scale factor errors, $\eta^b$is the bias considered as the sum of a constant noise and a random white noise $\eta^b = \eta^{b_{const}} + \eta_{random}^b$ $g = [0, 0, g]^T]$, and

$$g = 9,7803 + 0,051799\ C_{33}^2 - 0,94114\ 10^{-}6\ h\ \frac{m}{s^2} \tag{3.29}$$

where C_{33} is the 9th element of C_e^p and h is the vehicle altitude.

Examples. For four examples of static, straight line, circle, and s-shape situations, details will be given next under the conditions that the vehicle is moving on the surface of the Earth with no attitude change except for the heading angle,which means that the pitch angle, roll angle, and altitude are constants during the simulation process:

$$\Delta\theta = 0, \tag{3.30}$$

$$\Delta\gamma = 0, \tag{3.31}$$

$$\Delta\dot{\theta} = 0, \tag{3.32}$$

$$\Delta\dot{\gamma} = 0. \tag{3.33}$$

The calculation method for the other parameters for the four situations is described as follows.

- **Static**:

$$\begin{bmatrix} \text{L=constant}, \\ \lambda = constant, \\ v_N = constant, \\ v_E = constant, \\ \Delta\psi = constant, \\ \dot{\psi} = constant. \end{bmatrix} \tag{3.34}$$

- **Straight line**:

$$\begin{bmatrix} a_E = constant, \\ a_N = constant, \\ v_E = v_E + a_E \Delta t, \\ v_N = v_N + a_N \Delta t, \\ \psi = \psi_0 + \arctan \frac{v_E}{v_N} \\ \dot{\psi} = \frac{a_N v_E - a_E v_N}{v_E^2 + v_N^2}. \end{bmatrix} \tag{3.35}$$

- **Circle**:

$$\begin{bmatrix} v_g = constant, \\ a_E = -\frac{2\pi v_g \cos\psi}{T_{circle}}, \\ a_N = -\frac{2\pi v_g \sin\psi}{T_{circle}}, \\ \Delta\dot{\psi} = \frac{2\pi}{T_{circle}}. \end{bmatrix} \tag{3.36}$$

- **S-shape**:

$$\begin{bmatrix} v_g = constant, \\ a_E = -\frac{v_g \cos(\psi_0 + A_{sshape} \sin(\frac{2\pi t}{T_{sshape}}))}{T_{sshape}} \cdot \frac{2\pi A_{sshape} cos(\frac{2\pi t}{T_{sshape}})}{T_{sshape}}, \\ a_N = -\frac{v_g \sin(\psi_0 + A_{sshape} \sin(\frac{2\pi t}{T_{sshape}}))}{T_{sshape}} \cdot \frac{2\pi A_{sshape} cos(\frac{2\pi t}{T_{sshape}})}{T_{sshape}}, \\ \psi = \psi_0 + A_{sshape} \sin(\frac{2\pi t}{T_{sshape}}), \\ \dot{\psi} = \frac{2\pi A_{sshape} \cos(\frac{2\pi t}{T_{sshape}})}{T_{sshape}}. \end{bmatrix} \tag{3.37}$$

3.2 MathematicalModel and Trajectory Calculation Steps

After the gyro and accelerometer data are simulated using the method described in the previous section under the designed scenario, the next step we have to do is to figure out the mathematical model of SINS and the calculation steps to process the sensor data to get the calculated trajectories. Based on the basic principles of strapdown inertial navigation system [12], we draw the mathematical model in the p-frame mechanization in Figure 3.6. The calculation steps are

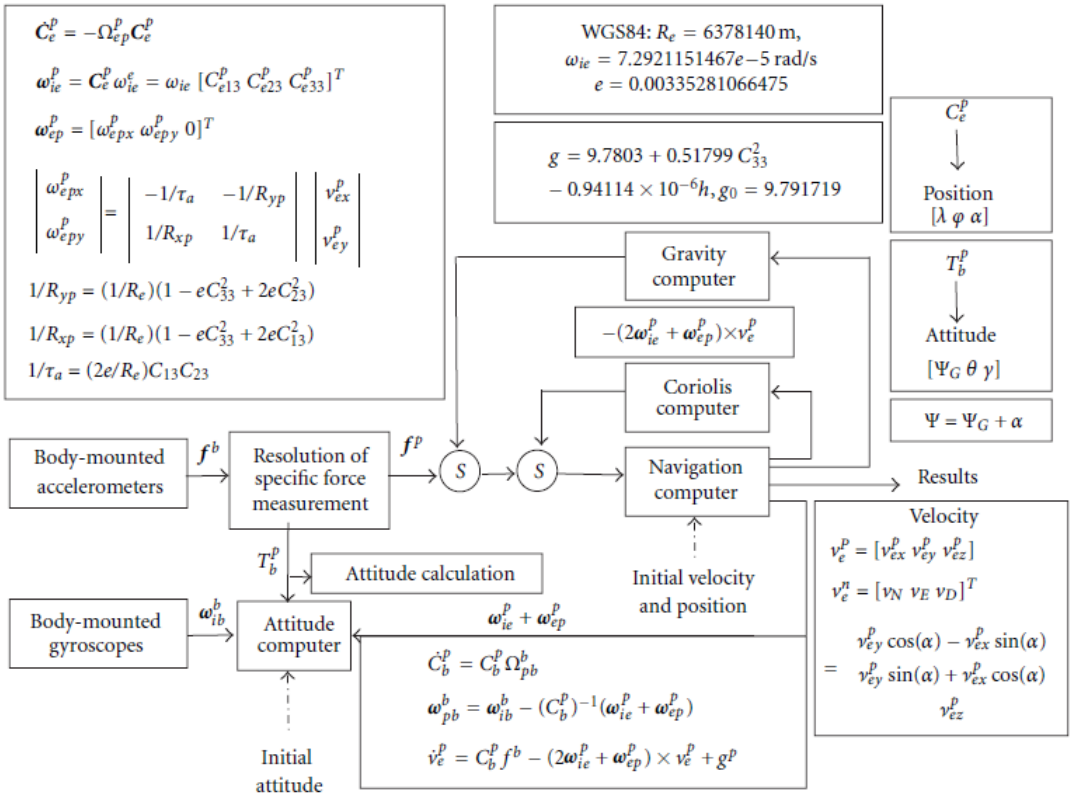

Figure 3.6: SINS p-frame mechanization

described below. Although the situation that the vehicle passes over either the north or south pole seldom happens, the universal p-frame is still chosen instead of the simpler ENU-frame to give a navigation illustration in a different frame.

A. Quaternion Q Update and Optimal Normalization The quaternion formed by a rotating body frame around the platform frame is

$$Q = q_0 + q_1 i_b + q_2 j_b + q_3 k_b \tag{3.38}$$

The update for the quaternion can be obtained by solving the following quaternion differential equation:

$$\begin{bmatrix} \dot{q_0} \\ \dot{q_1} \\ \dot{q_2} \\ \dot{q_3} \end{bmatrix} = \frac{1}{2} \begin{bmatrix} 0 & -\omega_{pbx}^b & -\omega_{pby}^b & -\omega_{pbz}^b \\ \omega_{pbx}^b & 0 & \omega_{pbz}^b & -\omega_{pby}^b \\ \omega_{pby}^b & -\omega_{pbz}^b & 0 & \omega_{pbx}^b \\ \omega_{pbz}^b & \omega_{pby}^b & -\omega_{pbx}^b & 0 \end{bmatrix} \begin{bmatrix} q_0 \\ q_1 \\ q_2 \\ q_3 \end{bmatrix} \tag{3.39}$$

Based on the Euclide norm minimized indicator [12], the optimal normalization for the quaternion

is

$$Q \leftarrow \frac{Q}{\sqrt{q_0^2 + q_1^2 + q_2^2 + q_3^2}} \tag{3.40}$$

B. C_b^p **Calculation.** is vehicle attitude DCM which transforms the measured angle in the b-frame to the p-frame, with its 9 components T_{ij} , $i, j = 1, 2, 3$. Here we use T_{ij} to distinguish it from the components C_{ij} which is used below.

After obtaining $q_0, q_1, q_2, and q_3$ using, C_b^p can be calculated as

$$R = \begin{bmatrix} T(1,1) & T(1,2) & T(1,3) \\ T(2,1) & T(2,2) & T(2,3) \\ T(3,1) & T(3,2) & T(3,3) \end{bmatrix} = \begin{bmatrix} q_1^2 - q_2^2 - q_3^2 + q_4^2 + & 2(q_1q_2 - q_3q_4) & 2(q_1q_3 + q_2q_4) \\ 2(q_1q_2 + q_3q_4) & -q_1^2 + q_2^2 - q_3^2 + q_4^2 & 2(q_2q_3 - q_1q_4) \\ 2(q_1q_3 - q_2q_4) & 2(q_2q_3 + q_1q_4) & -q_1^2 - q_2^2 + q_3^2 + q_4^2 \end{bmatrix} \tag{3.41}$$

C. Specific Force Transformation from f^b **in** b**-Frame to** f^p **in** p**-Frame.**

$$f^p = C_b^p f^b \tag{3.42}$$

D. Velocity v_e^p **Calculation.**

$$\dot{v_e^p} = f^p - (2\omega^p ie + \omega_{ep}^p) \times v_e^p + g^p \tag{3.43}$$

E. The ground speed is the vehicle velocity projection on the horizontal plane:

$$v_g = \sqrt{v_x^2 + v_y^2} \tag{3.44}$$

F. Position Matrix C_e^p **Update.**

$$\dot{C_e^p} = -\Omega_{ep}^p C_e^p \begin{bmatrix} \dot{C_{11}} & \dot{C_{12}} & \dot{C_{13}} \\ \dot{C_{21}} & \dot{C_{22}} & \dot{C_{23}} \\ \dot{C_{31}} & \dot{C_{32}} & \dot{C_{33}} \end{bmatrix} = \begin{bmatrix} 0 & 0 & -\omega_{epy}^p \\ 0 & 0 & \omega_{epx}^p \\ \omega_{epy}^p & -\omega_{epx}^p & 0 \end{bmatrix} \begin{bmatrix} C_{11} & C_{12} & C_{13} \\ C_{21} & C_{22} & C_{23} \\ C_{31} & C_{32} & C_{33} \end{bmatrix} \tag{3.45}$$

G. Position Angular Velocity ω_{ep}^p **Update.** we have $\omega_{ep}^p = 0$, and

$$\begin{bmatrix} \omega_{epx}^p \\ \omega_{epy}^p \end{bmatrix} = \begin{bmatrix} -\frac{1}{\tau_a} & -\frac{1}{R_{yp}} \\ \frac{1}{R_{xp}} & \frac{1}{\tau_a} \end{bmatrix} \begin{bmatrix} v_{ex}^p \\ v_{ey}^p \end{bmatrix} \tag{3.46}$$

$$\frac{1}{R_{yp}} = \frac{1}{R_e}(1 - eC_{33}^2 + 2eC_{23}^2) \tag{3.47}$$

$$\frac{1}{R_{xp}} = \frac{1}{R_e}(1 - eC_{33}^2 + 2eC_{13}^2) \tag{3.48}$$

$$\frac{1}{\tau_a} = \frac{2e}{R_e}C_{13}C_{23} \tag{3.49}$$

where the elements of position matrix C_e^p can be obtained using (3.45).

H. Earth Angular Velocity ω_{ie}^p and Attitude Angular Velocity ω_{pb}^b Calculation.

$$\omega_{ie}^p = C_e^p \omega_{ie}^e = \begin{bmatrix} \omega_{ie}C_{13} \\ \omega_{ie}C_{23} \\ \omega_{ie}C_{33} \end{bmatrix} \tag{3.50}$$

$$\omega_{pb}^b = \omega_{ib}^b - \omega_{ip}^b = \omega_{ib}^b - (C_b^p)^{-1}(\omega_{ie}^p + \omega_{ep}^p) \tag{3.51}$$

I. Attitude Angle Calculation.

$$\overset{p}{C}_b = (\overset{b}{C}_p)^T = \begin{bmatrix} \cos\gamma\cos\Psi_G - \sin\gamma\sin\theta\sin\Psi_G & -\cos\theta\sin\Psi_G & \sin\gamma\cos\Psi_G + \cos\gamma\sin\theta\sin\Psi_G \\ \cos\gamma\sin\Psi_G + \sin\gamma\sin\theta\cos\Psi_G & \cos\theta\cos\Psi_G & \sin\gamma\sin\Psi_G - \cos\gamma\sin\theta\cos\Psi_G \\ -\sin\gamma\cos\theta & \sin\theta & \cos\gamma\cos\theta \end{bmatrix} \tag{3.52}$$

Thus, the principal values of ψ, θ, and γ are

$$\theta_{principal} = \sin^{-1} T_{32} \tag{3.53}$$

$$\gamma principal = \tan^{-1}\left(\frac{-T_{32}}{T_{32}}\right) \tag{3.54}$$

$$\psi G principal = \tan^{-1}\left(\frac{-T_{12}}{T_{22}}\right) \tag{3.55}$$

Considering the defined range of the angles, the expressions of the real values of ψ , θ , and γ are

$$\theta \leftarrow \theta_{principal} \tag{3.56}$$

$$\gamma \leftarrow \left\{ \begin{array}{l} \gamma_{principal} \text{ if } T_{33} > 0, \\ \gamma_{principal} + 180 \text{ if } T_{33} < 0, \gamma_{principal} < 0, \\ \gamma_{principal} - 180 \text{ if } T_{33} < 0, \gamma_{principal} > 0, \end{array} \right\} \tag{3.57}$$

$$\psi \leftarrow \left\{ \begin{array}{l} \psi_{Gprincipal} \text{ if } T_{22} > 0, \\ \psi_{Gprincipal} + 180 \text{ if } T_{22} < 0, \psi_{Gprincipal} < 0, \\ \psi_{Gprincipal} - 180 \text{ if } T_{22} < 0, \psi_{Gprincipal} > 0, \end{array} \right\} \tag{3.58}$$

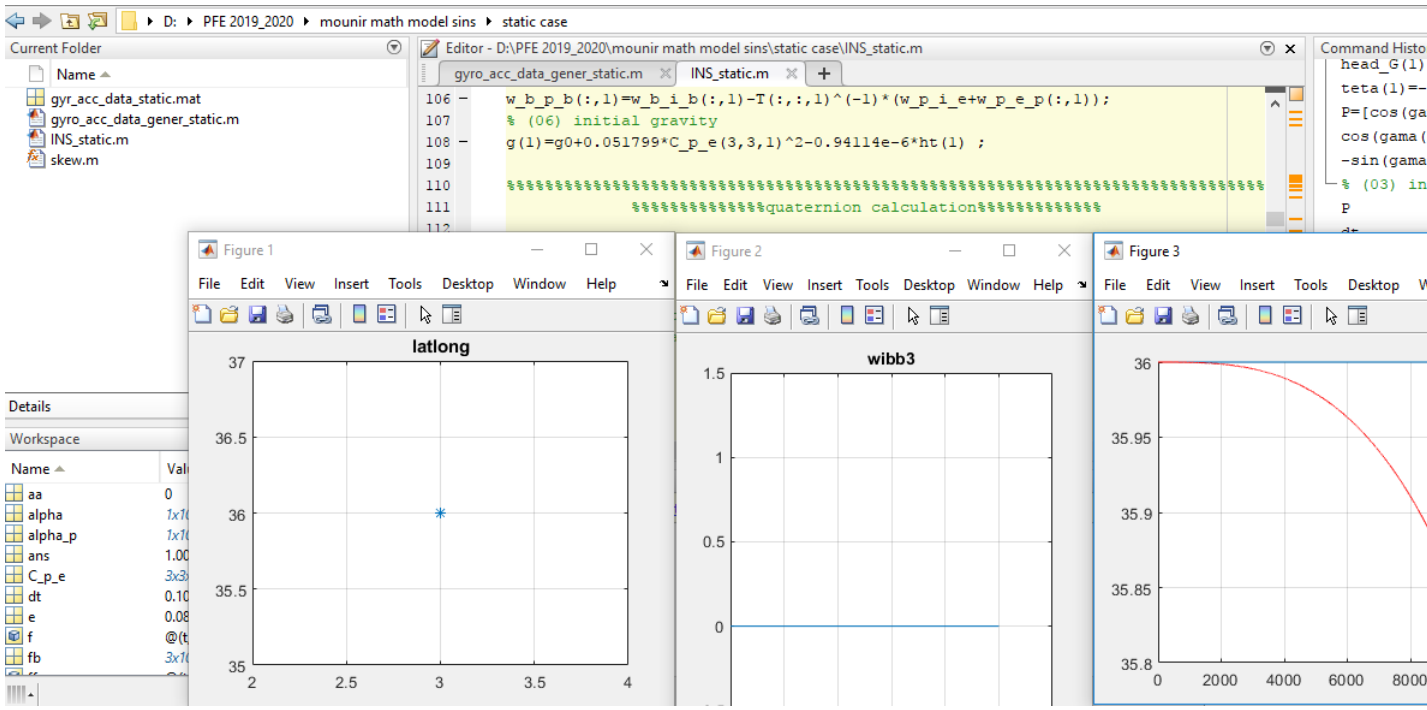

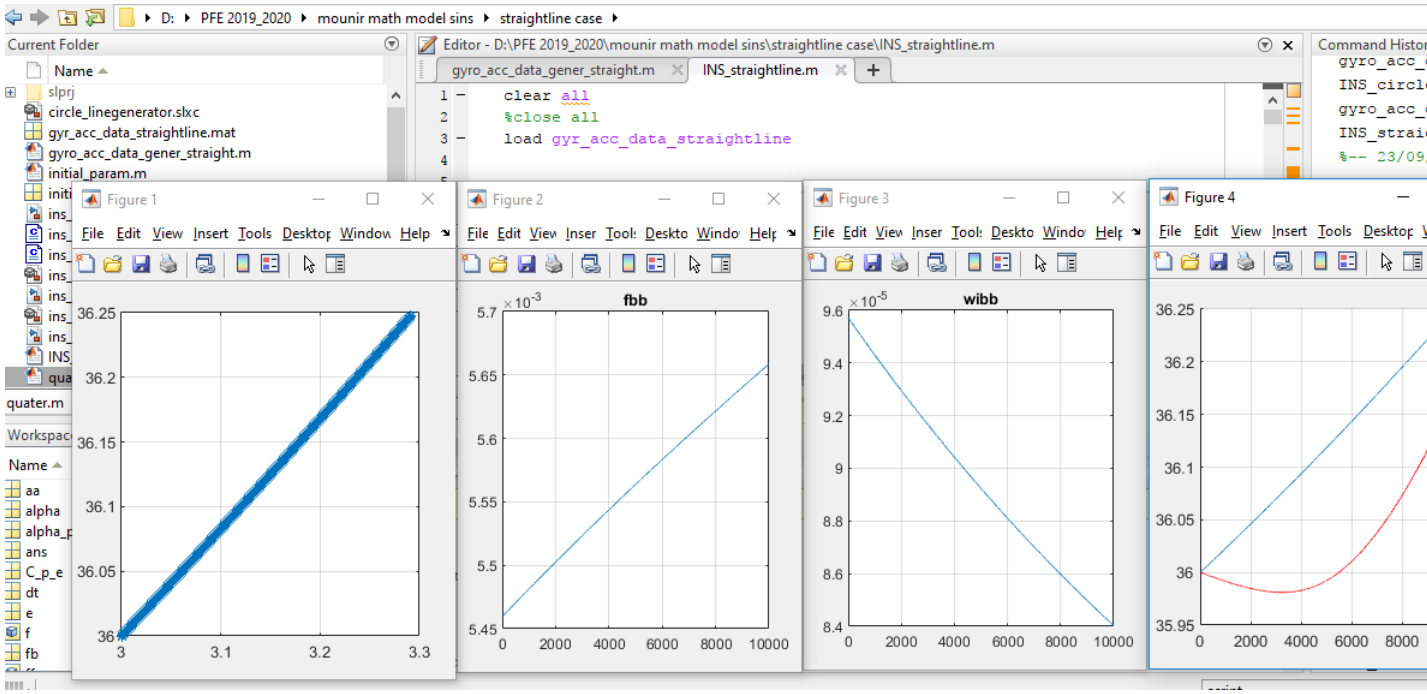

Chapter 3. Simulation of Strapdown Inertial Navigation System

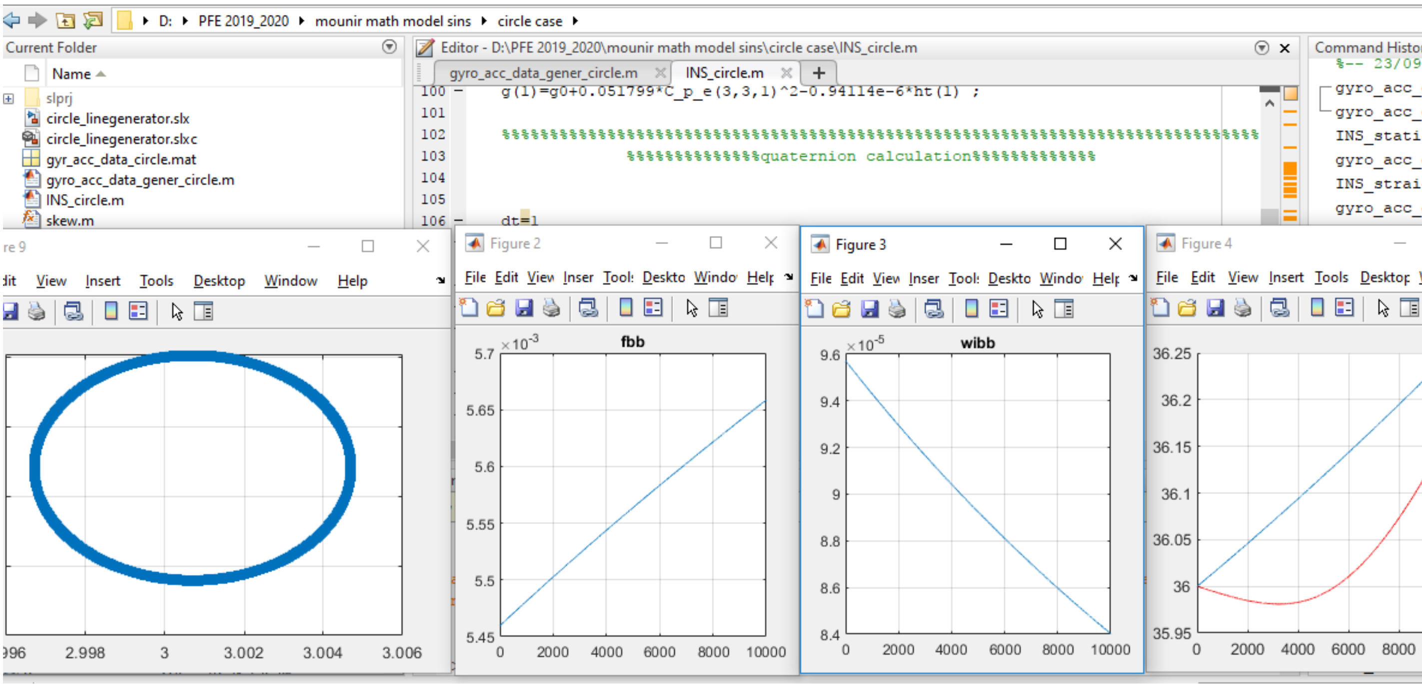

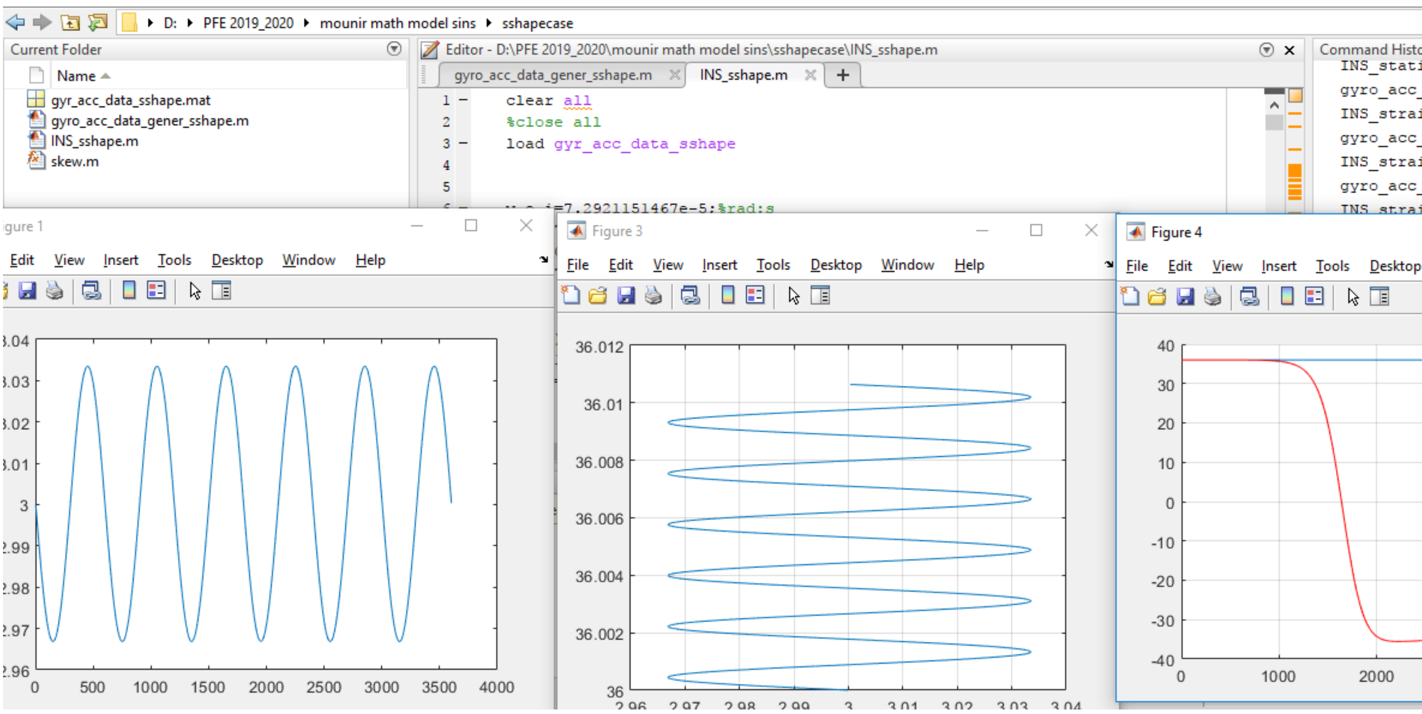

Chapter 4

Simulation of a Strap-Down Inertial Navigation System' Errors

4.1 Introduction

Inertial navigation is a dead reckoning positioning method based on the measurement and mathematical processing of the vehicle absolute acceleration and angular speed in order to estimate its attitude, speed and position related to different reference. Due to the specific operation principle, the positioning errors for this method result from the imperfection of the initial conditions knowledge, from the errors due to the numerical calculation in the inertial system, and from the accelerometers and gyros errors. Therefore, the inertial sensors performances play a main role in the establishment of the navigation system precision, and should be considered in its design phase frames [4]

The RLG (Ring Laser Gyros) has excellent scale-factor stability and linearity, negligible sensitivity to acceleration, digital output, fast turn-on, excellent stability and repeatability across the range, and no moving parts. Present day RLG's is considered a matured technology and its development efforts are to reduce costs more than to increase its performance [13] The studies provide that the developments in solid-state optics and fiber technology could lead to $0.001 - deg/h$ performance in miniature design. Although, gyros and accelerometers are yet too voluminous, the miniaturization seems feasible in the near future and is developing [14].

The aerospace industry tendencies to realize unmanned aircraft (UAV), micro and nanosatellites, easy to launch in space and with the performances analogous with the actual satellites, imposed

a nimble(khafif) rhythm to the expansion of the NEMS (Nano-Electro-Mechanical- Systems) and MEMS (Micro-Electro-Mechanical-Systems) technologies in the domain of the acceleration and rotation sensors, used especially in the inertial navigation systems. The use of such miniaturized sensors creates the premises (mukadimat mantiqia) to have redundant strap-down inertial navigation systems through the miscellaneous dedicated architectures and at the low-costs comparatively with the case of non-miniaturized and very precise inertial sensors use. On the other way, the use of these miniaturization technologies for the inertial sensors allows the implementation of the entire inertial navigation system in a single chip, including here the sensors and all circuits for the signals proccessing [15].

From the other point of view, these miniaturized sensors have some disadvantages due to the performances decrease with the miniaturization degree increase. They are quite noises, because at the great majority of the acceleration sensors the noise density is between $100\mu g/Hz^{\frac{1}{2}}$ and a few hundreds of $\mu g/Hz^{\frac{1}{2}}$, for the bandwidths between 100Hz and 2500Hz, and at the gyro sensors it is between $\mathbf{0.001}\left(\deg/s/Hz^{\frac{1}{2}}\right)$ & $\mathbf{0.1}\left(\deg/s/Hz^{\frac{1}{2}}\right)$, for the pass bandwidths between 50Hz and 100Hz. Also, for the same type of sensors the noise density can vary from one sensor to the other with 20% of the catalogue value. The filtering of the noise it is not recommended because it is possible to be altered the useful signal and, so, the sensor output doesn't reflect exactly the signal applied at the input of the sensor. Beside the noise increase, through miniaturization appear negative influences on the stability and value of bias, on the scale factor calibration, on the cross-axis sensitivity for the accelerometers and on the sensitivity at the accelerations applied along any given axis for the gyros. For all of these the data sheets of the MEMS and NEMS products stipulate maximal values relatively high, without be able to specify exactly their value to be corrected [16]. To test the influences of the sensors errors on the solution of navigation of strap-down inertial navigators we realized Matlab/Simulink models for the acceleration and rotation sensors based on the sensors data sheets and on the IEEE equivalent models for the inertial sensors. for the accelerometers was obtained the model in figure 4.1

The model has as inputs the acceleration a_i, applied along of the sensitive axis, and the cross-axis acceleration a_c, and as output the perturbed acceleration a. The analytic form of the model is:

$$a = (a_i + Na_i + B + k_c a_c + \nu)\left(1 + \frac{\Delta K}{K}\right) \tag{4.1}$$

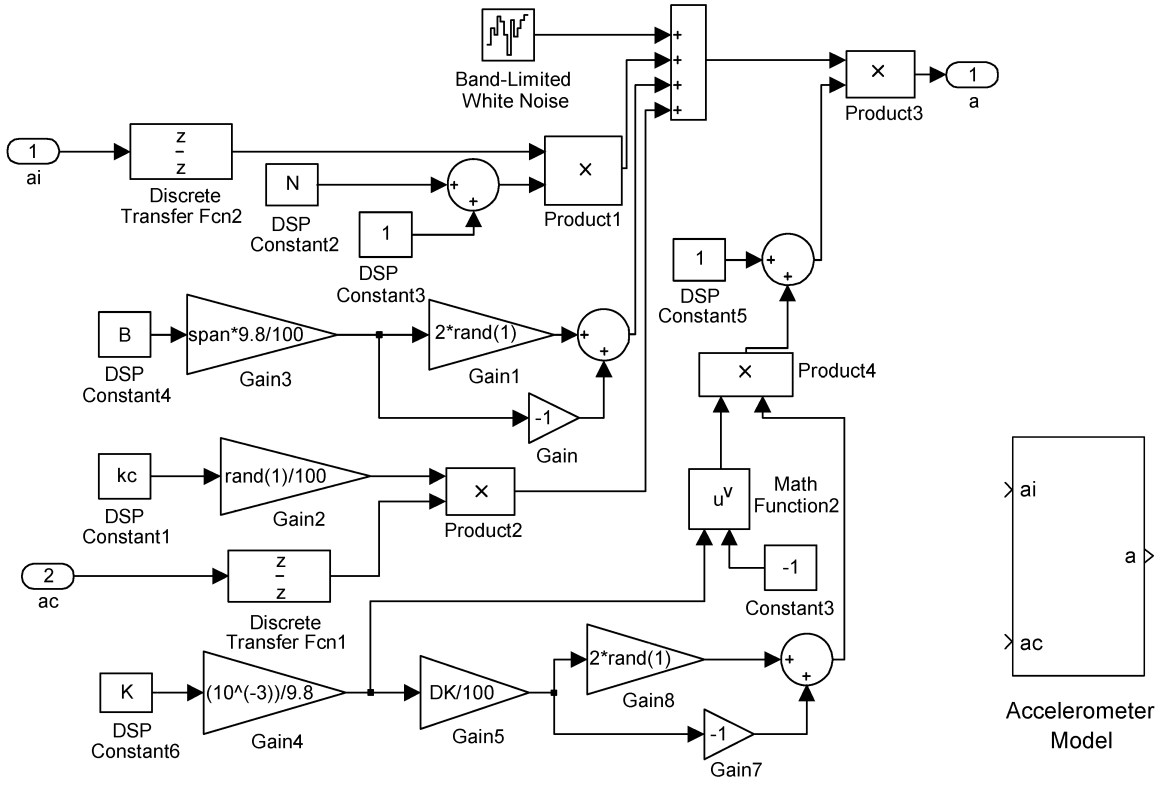

Figure 4.1: Accelerometers Matlab/Simulink model and its interface.

Table 4.1: Gyroscopes Error Model

Measurement range (span)[g]	25
Scale factor [mV/g]	160
Bandwidth [Hz]	1500
Noise density [μg/Hz$^{\frac{1}{2}}$]	25
Bias [% from Span]	2
Scale factor error [% from Scale factor]	2
Crossaxis sensitivity [% from a_c]	3
Sensitivity axis misalignment [rad]	0
Sample time [s]	0.01

where N is sensitivity axis misalignment (in radians), B-bias (expressed in percent of span), k_c-crossaxis sensitivity (expressed in percent of a_c), ν-sensor noise (given by its density ν_d expressed in μg/Hz$^{\frac{1}{2}}$, K-scale factor (expressed in mV/g), and ΔK-scale factor error (percents of K), and a,

a_i, a_c expressed in m/s^2. The model was built for few miniaturized acceleration sensors and covers theirs main errors: bias, scale factor error, sensitivity axis misalignment, cross axis sensitivity and noise. The model related to the gyro sensors was implemented in Matlab/Simulink figure 4.2

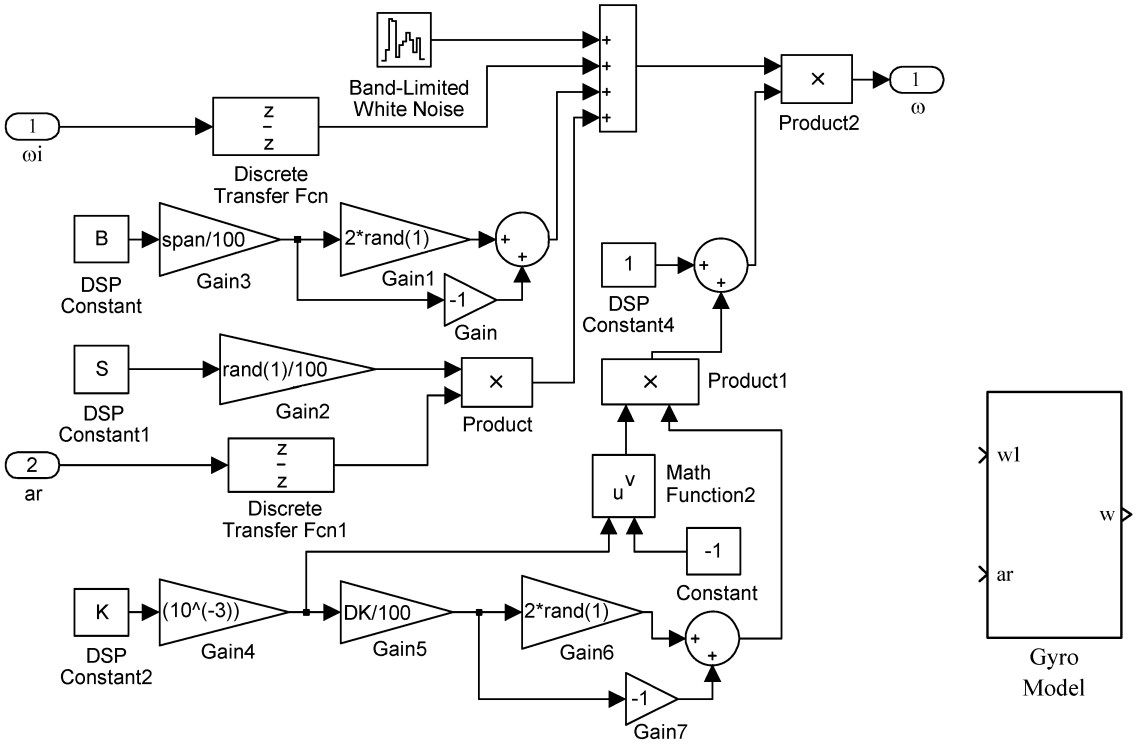

Figure 4.2: Gyros Matlab/Simulink model and its interface.

starting from the equation

$$\omega = (\omega_i + Sa_r + B + \nu)\left(1 + \frac{\Delta K}{K}\right) \tag{4.2}$$

ω-sensors output angular speed (disturbed signal) expressed in deg/s, ω_i-applied angular speed (deg/s), S-sensitivity to the acceleration a_r applied on an arbitrary direction ((deg/s)/g), B-bias (expressed in percents of span), ν-sensor noise (given by its density ν_d expressed in (deg $/s/\text{Hz}^{\frac{1}{2}}$), K-scale factor (expressed in $mV/(deg/s)$), ΔK-scale factor error (percents of K).

The models have the advantages to work independent with each of the sensor errors and to study in this way their influence on the inertial navigator positioning solution. Although sensors data sheets specifications are not related to the components of noise, for a more detailed study of the navigators' errors, the sensors' models can be completed with some noise terms starting from theirs Allan variance definitions. Allan's variance results are related to the seven noise terms. Five

Table 4.2: Accelerometers Error Model

Measurement range (span)$[drg/s]$	500
Scale factor [mV/drg/s]	10
Bandwidth [Hz]	60
Noise density [μdrg/s/Hz$^{\frac{1}{2}}$]	0.0035
Bias [% from Span]	0.1
Scale factor error [% from Scale factor]	1
Sensitivity of acceleration $[drg/s/g]$	0.02
Sample time [s]	0.01

noise terms are basic terms: angle random walk, rate random walk, bias instability, quantization noise and drift rate ramp, while the other two are the sinusoidal noise and exponentially correlated (Markov) noise [16]

This section deals with solving of a navigation problem relative to terrestrial non-inertial reference frames by using attitude matrices to calculate the vehicle attitude. Once it is highlighted the general equation of inertial navigation, a numerical algorithm is developed for determining the position and speed of the vehicle based on this equation. The algorithm provides position and vehicle speed in horizontal local reference frame (ENU) and its global coordinates (latitude, longitude and altitude). For the presented algorithm is developed an error model that highlights the dependencies of the vehicle positioning, velocity and attitude errors by the strap-down inertial sensor errors used to detect acceleration and angular speed. In the development of the error model the small perturbation technique is used. Following is conducted a study of the dependence of the inertial navigator outputs errors by the errors of the used inertial sensors based on the Matlab/Simulink models built for acceleration and gyro sensors.

4.2 Navigation algorithm

The output $\vec{f}$ of an accelerometer is influenced by the gravitational field, it is a combination between the vehicle kinematic acceleration $\vec{a}$ and the gravitational acceleration $\vec{g}$ i.e. $\vec{f} = \vec{a} - \vec{g}$

In literature, f is very well known as specific force according to the Coriolis formula we have:

$$\left.\frac{d\vec{r}}{dt}\right|_I = \left.\frac{d\vec{r}}{dt}\right|_P + \vec{\Omega} \times \vec{r} = \vec{v} + \vec{\Omega} \times \vec{r} \tag{4.3}$$

from where

$$\vec{a} = \frac{d}{dt}\left[\left.\frac{d\vec{r}}{dt}\right|_I\right]_I = \frac{d}{dt}\left[\vec{v} + \vec{\Omega} \times \vec{r}\right]_I = \left.\frac{d\vec{v}}{dt}\right|_I + \vec{\Omega} \times \left.\frac{d\vec{r}}{dt}\right|_I = \left.\frac{d\vec{v}}{dt}\right|_I + \vec{\Omega} \times \vec{v} + \vec{\Omega} \times \left(\vec{\Omega} \times \vec{r}\right) \tag{4.4}$$

$\vec{r}$ is the position vector of the monitored vehicle in inertial frame I, $\vec{v}$-the vehicle speed relative to the ECEF (Earth Centered Earth Fixed) reference frame (denoted with P), and $\vec{\Omega}$ -Earth rotation speed around its axis. Denoting with $\vec{\omega}_N$ the absolute angular speed of the navigation reference frame N, then the Coriolis formula applied to the $\left.\frac{d\vec{v}}{dt}\right|_I$ term implies:

$$\left.\frac{d\vec{v}}{dt}\right|_I = \left.\frac{d\vec{v}}{dt}\right|_N + \vec{\Omega}_N \times \vec{v} \tag{4.5}$$

where $\left.\frac{d\vec{v}}{dt}\right|_N$ is the derivative of v relative to the navigation frame. Therefore

$$\vec{a} = \left.\frac{d\vec{v}}{dt}\right|_N + \vec{\omega}_N \times \vec{v} + \vec{\Omega} \times \vec{v} + \vec{\Omega} \times \left(\vec{\Omega} \times \vec{r}\right) \tag{4.6}$$

and the specific force can be rewritten as:

$$\vec{f} = \left.\frac{d\vec{v}}{dt}\right|_N + \vec{\omega}_N \times \vec{v} + \vec{\Omega} \times \vec{v} + \vec{\Omega} \times \left(\vec{\Omega} \times \vec{r}\right) - \vec{g} \tag{4.7}$$

Considering $\vec{g}_a = \vec{g} - \vec{\Omega} \times \left(\vec{\Omega} \times \vec{r}\right)$

$$\vec{f} = \left.\frac{d\vec{v}}{dt}\right|_N + \vec{\omega}_N \times \vec{v} + \vec{\Omega} \times \vec{v} - \vec{g}_a \tag{4.8}$$

which is known as **general equation of the inertial navigation**.

The position and the speed of a vehicle may be obtained by the numerical integration of the eq. 4.8 relative to the navigation frame. In the inertial navigation systems with stable platform, the axes of the acceleration sensors are kept parallel with the navigation frame axes, and, as a consequence, the components of the specific force are obtained directly in this frame. If a strap-down architecture is used for the inertial measurement unit (IMU), then the components of the specific force in the navigation frame should be calculated starting from the specific force components in the vehicle frame (SV); the acceleration sensors in IMU are fixed directly on the

vehicle rigid structure. In this situation the coordinate change between the vehicle frame and navigation frame is made by using the rotation matrix describing the vehicle attitude relative to the navigation frame. By choosing as navigation frame the local horizontal frame ENU (East-North-Up) it results $\vec{\omega_N} = \vec{\omega_l}$ (index l denotes the ENU frame). The scalar components of the eq.4.8 in this frame are:

$$\begin{aligned} f_{xl} &= \frac{dv_{xl}}{dt} + \omega_{yl}v_{zl} - \omega_{zl}v_{yl} + \Omega_{yl}v_{zl} - \Omega_{zl}v_{yl} - g_{axl} \\ f_{yl} &= \frac{dv_{yl}}{dt} + \omega_{xl}v_{zl} - \omega_{zl}v_{xl} + \Omega_{xl}v_{zl} - \Omega_{zl}v_{xl} - g_{ayl} \\ f_{zl} &= \frac{dv_{zl}}{dt} + \omega_{xl}v_{yl} - \omega_{yl}v_{xl} + \Omega_{xl}v_{yl} - \Omega_{yl}v_{xl} - g_{azl} \end{aligned} \tag{4.9}$$

where f_{xl}, f_{yl}, f_{zl} are the components of the specific force in ENU frame; v_{xl}, v_{yl}, v_{zl}components of the vehicle speed relative to ECEF frame in ENU frame;$\omega_{xl}, \omega_{yl}, \omega_{zl}$-components of the ENU frame absolute angular speed $\vec{\omega_l}$ on its own axes; $\Omega_{xl}, \Omega_{yl}, \Omega_{zl}$-components of $\vec{\Omega}$ in ENU frame; g_{xl}, g_{yl}, g_{zl}-components of the apparent gravitational acceleration in ENU frame

$$g_{xl} \cong 0, g_{yl} \cong 0, g_{zl} \cong 9.7803 + 0.0519\sin^2\phi - 3.08 \cdot 10^6 \cdot h \tag{4.10}$$

With these considerations we have

$$\left[\vec{\Omega}\right]_l = [\Omega_{xl}\ \Omega_{yl}\ \Omega_{zl}]^T = [0\ \Omega\cos\phi\ \Omega\sin\phi]^T \tag{4.11}$$

$$\left[\vec{\omega_l}\right]_l = [\omega_{xl}\ \omega_{yl}\ \omega_{zl}]^T = \left[-\frac{v_{yl}}{R_\phi + h}, \frac{v_{xl}}{R_\lambda + h} + \Omega\cos\phi, \frac{v_{xl}}{R_\lambda + h}\tan\phi + \Omega\sin\phi\right]^T \tag{4.12}$$

$$R_\phi = a\frac{1 - e^2}{\left(1 - e^2\sin^2\phi\right)^{\frac{2}{3}}} \tag{4.13}$$

$$R_\lambda = \frac{a}{\left(1 - e^2\sin^2\phi\right)^{\frac{1}{2}}} \tag{4.14}$$

The angular speed$\vec{\omega}_r$, relative to the ECEF reference frame, has in ENU frame the next components:

$$\left[\vec{\omega_r}\right]_l = [\omega_{rxl}\ \omega_{ryl}\ \omega_{rzl}]^T = \left[-\frac{v_{yl}}{R_\phi + h}, \frac{v_{xl}}{R_\lambda + h}, \frac{v_{xl}}{R_\lambda + h}\tan\phi\right]^T \tag{4.15}$$

Therefore, equations 4.2 become:

$$\frac{dv_{xl}}{dt} = f_{xl} + \frac{v_{xl}v_{yl}}{R_\lambda + h}\tan\phi + 2\Omega\sin\phi v_{yl} - v_{zl}\left(\frac{v_{xl}}{R_\lambda + h} + 2\Omega\cos\phi\right) + + g_{axl}$$
$$\frac{dv_{yl}}{dt} = f_{yl} - \frac{v_{xl}^2}{R_\lambda + h}\tan\phi - 2\Omega\sin\phi v_{xl} - v_{zl}\frac{v_{yl}}{R_\phi + h} + g_{ayl} \tag{4.16}$$
$$\frac{dv_{zl}}{dt} = f_{zl} + \frac{v_{yl}^2}{R_\phi + h} + \frac{v_{xl}^2}{R_\lambda + h} + 2\Omega\cos\phi v_{xl} + g_{azl}$$

To integrate these equations we need to know the initial values of ϕ,λ ,h, v_{xl},v_{yl},v_{zl} and, $\vec{f}$ also, the components of f and $\vec{g}$ in ENU frame. Because the IMU of the strap-down inertial navigation system contains three accelerometers and three gyros, its inputs will be the components of the vehicle absolute acceleration and angular speed in the vehicle frame:

$$\left[\vec{f}\right]_v = [f_{xv}\ f_{yv}\ f_{zv}]^T$$

$$\left[\vec{\omega_v}\right]_v = [\omega_{xv}\ \omega_{yv}\ \omega_{zv}]^T$$

The components of the specific force in ENU can be determinate by using the relation:

$$\left[\vec{f}\right]_l = R^l{}_v \left[\vec{f}\right]_v \tag{4.17}$$

where

$$\dot{R}^l{}_v = R^l{}_v\widetilde{\omega}_v - \widetilde{\omega}_l R^l{}_v \tag{4.18}$$

where

$$\widetilde{\omega}_v = \begin{bmatrix} 0 & -\omega_{zv} & \omega_{yv} \\ \omega_{zv} & 0 & -\omega_{xv} \\ -\omega_{yv} & \omega_{xv} & 0 \end{bmatrix} \tag{4.19}$$

$$\widetilde{\omega}_l = \begin{bmatrix} 0 & -\omega_{zl} & \omega_{yl} \\ \omega_{zl} & 0 & -\omega_{xl} \\ -\omega_{yl} & \omega_{xl} & 0 \end{bmatrix} \tag{4.20}$$

Can be easily observed that eq. 4.18 has the general form:

$$\dot{X} = XA - BX \tag{4.21}$$

with $A = \widetilde{\omega}_v$and $B = \widetilde{\omega}_l$. Considering that for a short period of time Δt, between t_n and t_{n+1} times, the angular speeds ω_{xv}, ω_{yv},ω_{zv}, and ω_{xl}, ω_{yl},ω_{zl}, are constant, we obtains:

$$\begin{aligned}
\Delta\phi_{xv} &= \int_{t_n}^{t_{n+1}} \omega_{xv} dt = \omega_{xv}\Delta t \\
\Delta\phi_{yv} &= \int_{t_n}^{t_{n+1}} \omega_{yv} dt = \omega_{yv}\Delta t \\
\Delta\phi_{zv} &= \int_{t_n}^{t_{n+1}} \omega_{zv} dt = \omega_{zv}\Delta t \\
\Delta\phi_{xl} &= \int_{t_n}^{t_{n+1}} \omega_{xl} dt = \omega_{xl}\Delta t \\
\Delta\phi_{yl} &= \int_{t_n}^{t_{n+1}} \omega_{yl} dt = \omega_{yl}\Delta t \\
\Delta\phi_{zl} &= \int_{t_n}^{t_{n+1}} \omega_{zl} dt = \omega_{zl}\Delta t
\end{aligned} \tag{4.22}$$

$\Delta\phi_{xv}, \Delta\phi_{yv}, \Delta\phi_{zv}$ are the increments of the angular rotations measured around the roll, pitch and yaw axes,$\Delta\phi_{xl}, \Delta\phi_{yl}, \Delta\phi_{zl}$ the increments of the angular rotations around the ENU frame axes calculated by the navigation processor In this way, the value provided for the X matrix at the tn+1 time is given by:

$$X_{n+1} = X_n + \dot{X}_n\Delta t = X_n + X_n A\Delta t - B\Delta t X_n \tag{4.23}$$

$$X_{n+1} = X_n\left(I + A\Delta t\right) - B\Delta t X_n = X_n A_n - B_n X_n \tag{4.24}$$

with

$$A_n = \begin{bmatrix} 1 & -\Delta\phi_{zv} & \Delta\phi_{yv} \\ \Delta\phi_{zv} & 1 & -\Delta\phi_{xv} \\ -\Delta\phi_{yv} & \Delta\phi_{xv} & 1 \end{bmatrix} \tag{4.25}$$

$$B_n = \begin{bmatrix} 0 & -\Delta\phi_{zl} & \Delta\phi_{yl} \\ \Delta\phi_{zl} & 0 & -\Delta\phi_{xl} \\ -\Delta\phi_{yl} & \Delta\phi_{xl} & 0 \end{bmatrix} \tag{4.26}$$

Therefore, the solution of the eq. 4.18 has the form:

$$R_v^l\big|_{n+1} = R_v^l\big|_n A_n - B_n R_v^l\big|_n \tag{4.27}$$

Through the numerical integration of the equations 4.2 are obtained the components of the relative speed $\vec{v}$ in ENU frame:v_{xl}, v_{yl},v_{zl}. With the equations

$$\dot{\phi} = \frac{v_{yl}}{R_\phi + h} \tag{4.28}$$

$$\dot{\lambda} = \frac{v_{xl}}{(R_\phi + h)\cos\phi} \tag{4.29}$$

$$\dot{h} = v_{zl} \tag{4.30}$$

the geographic coordinated of the vehicle are calculated using:

$$\phi(t) = \phi(0) + \int_0^t \frac{v_{yl}}{R_\phi + h} dt \tag{4.31}$$

$$\lambda(t) = \lambda(0) + \int_0^t \frac{v_{xl}}{(R_\lambda + h)\cos\phi} dt \tag{4.32}$$

$$h(t) = h(0) + \int_0^t v_{zl} dt \tag{4.33}$$

By using the rotation matrix between ENU and ECEF frames

$$[R_l^p]^T = R_p^l = \begin{bmatrix} -\sin\lambda & \cos\lambda & 0 \\ -\sin\phi\cos\lambda & -\sin\phi\sin\lambda & \cos\phi \\ \cos\phi\cos\lambda & \cos\phi\sin\lambda & \sin\phi \end{bmatrix} \tag{4.34}$$

the components of the relative speed $\vec{v}$ in ECEF frame result with equation:

$$\left[\vec{v}\right]_p = R_l^p \left[\vec{v}\right]_l \tag{4.35}$$

numerical integration of the relative speed $\left[\vec{v}\right]_p$ yields $\left[\vec{r}\right]_p$

$$\left[\vec{r}\right]_p = \left[\vec{r(0)}\right]_p + \int_0^t \left[\vec{v}\right]_p dt = [x_p, y_p, z_p]^T \tag{4.36}$$

with the model of the gravitational field for ECEF reference frame (Radix, 1993),

$$\left[\vec{g_a}\right]_p = \begin{bmatrix} g_{axp} \\ g_{ayp} \\ g_{azp} \end{bmatrix} = \begin{bmatrix} A_1 \frac{x_p}{r^3}\left(1 + \frac{A_2}{r^2}\left(\frac{5z_p^2}{r^2} - 1\right)\right) + \Omega^2 \cdot x_p \\ A_1 \frac{y_p}{r^3}\left(1 + \frac{A_2}{r^2}\left(\frac{5z_p^2}{r^2} - 1\right)\right) + \Omega^2 \cdot y_p \\ A_1 \frac{z_p}{r^3}\left(1 + \frac{A_2}{r^2}\left(\frac{5z_p^2}{r^2} - 3\right)\right) \end{bmatrix} \tag{4.37}$$

$A_1 = -3.986005 \cdot 10^{14} \cdot m3/s^2$, $A_2 = -6.66425 \cdot 10^{10} \cdot m^2$ (Radix, 1993). Components of $\vec{g}_a$ in ENU frame, starting from the model (33), are calculated by using the inverse transform ECEF to ENU:

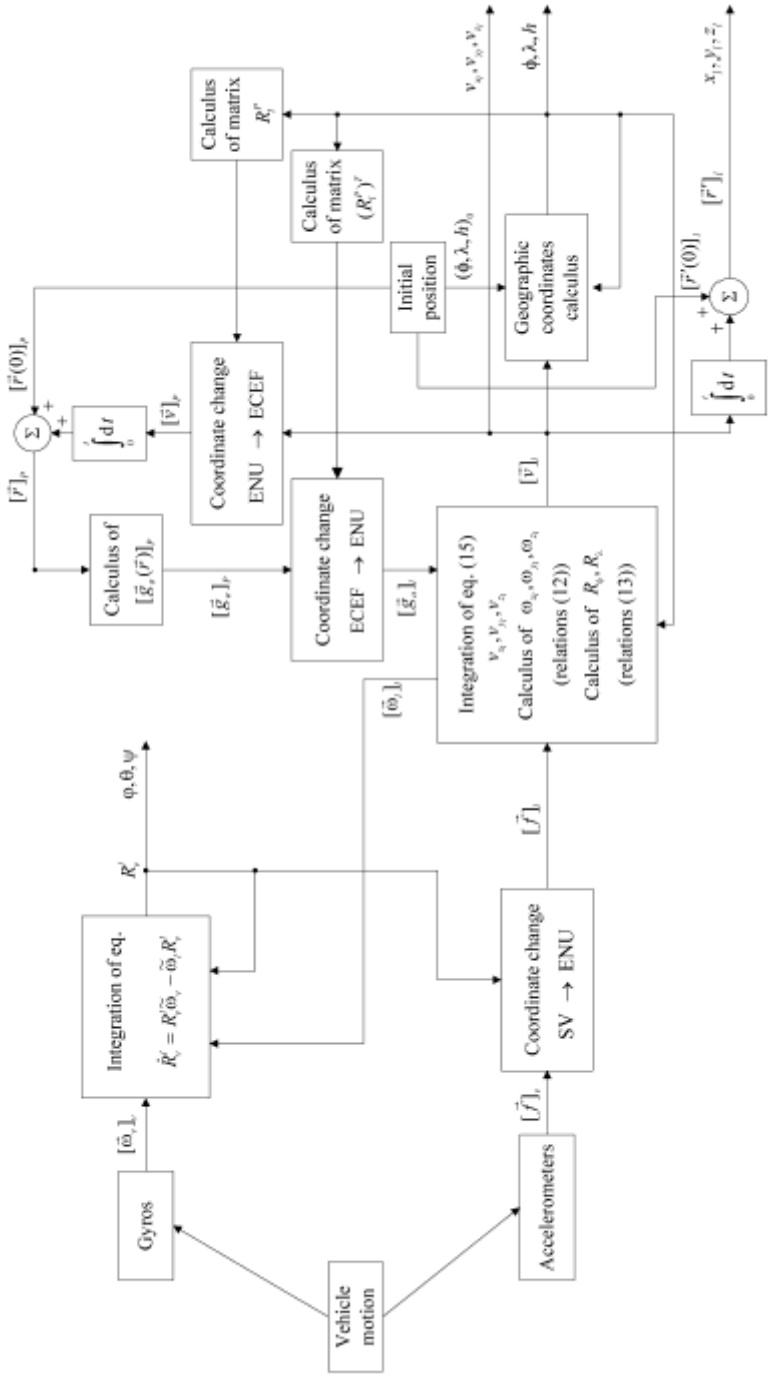

Figure 4.3: Block diagram of the navigation algorithm.

$$\left[\vec{g_a}\right]_l = R_p^l \left[\vec{g_a}\right]_p \tag{4.38}$$

Finally, the vehicle coordinates in ENU are obtained with the equation:

$$\left[\vec{r}\right]_l = \left[r(\vec{0})\right]_l + \int_0^t \left[\vec{v}\right]_l dt = [x_l, y_l, z_l]^T \tag{4.39}$$

where $\left[\vec{r}\right]$ is the vehicle position vector in ENU reference frame. From the mathematical description of the algorithm, yields the block diagram in figure 4.3

4.3 Error model of the navigation algorithm

The quality of the inertial navigator depends on the precision of the used sensors and on the numerical algorithms implemented in the navigation processor. For the error model developed in this subchapter are taken into account only the errors of the inertial sensors, considering that the numerical algorithm implemented in the navigation processor works free of errors. Thus, the model highlights the dependence of the position, velocity and attitude errors by the errors of the accelerometers and gyros in strap-down IMU.

Denoting with m the ideal value of a measurement and with $\widehat{m}$ its real value, given by the measurement system, the measurement error is calculated with the relation:

$$\delta m = m - \widehat{m} \tag{4.40}$$

Starting from this expression

$$\delta f_{xv} = f_{xv} - \widehat{f_{xv}}; \delta f_{yv} = f_{yv} - \widehat{f_{yv}}; \delta f_{zv} = f_{zv} - \widehat{f_{zv}} \tag{4.41}$$

$$\delta \omega_{xv} = \omega_{xv} - \widehat{\omega_{xv}}; \delta \omega_{yv} = \omega_{yv} - \widehat{\omega_{yv}}; \delta \omega_{zv} = \omega_{zv} - \widehat{\omega_{zv}} \tag{4.42}$$

Similarly can be defined the errors of the attitude angles(ϕ, θ, ψroll, pitch and yaw),errors of the vehicle position over the ENU frame axes (x_l, y_l, z_l), and the errors of the vehicle linear speed $(v_x l, v_y l, v_z l)$:

$$\delta\phi = \phi - \widehat{\phi}; \delta\theta = \theta - \widehat{\theta}; \delta\psi = \psi - \widehat{\psi}; \tag{4.43}$$

$$\delta x_l = x_l - \widehat{x_l}; \delta y_l = y_l - \widehat{y_l}; \delta z_l = z_l - \widehat{z_l}; \tag{4.44}$$

$$\delta v_{xl} = v_{xl} - \widehat{v_{xl}}; \delta v_{yl} = v_{yl} - \widehat{v_{yl}}; \delta v_{zl} = v_{zl} - \widehat{v_{zl}}; \tag{4.45}$$

Starting from the errors of the attitude angles may be deduced the errors affecting the attitude matrices. Thus, with the equations expressing the elements of the rotation matrix R_l^v (ENU to SV) and considering $\delta\phi \cdot \delta\theta = \delta\phi \cdot \delta\psi = \delta\psi \cdot \delta\theta = 0$

$$R_l^v = \widehat{R_l^v} \begin{bmatrix} 1 & -\delta\psi & \delta\theta \\ \delta\psi & 1 & -\delta\phi \\ -\delta\theta & \delta\phi & 1 \end{bmatrix} = \widehat{R_l^v} \left(I + \widetilde{R} \right) \tag{4.46}$$

with

$$\widetilde{R} = \begin{bmatrix} 0 & -\delta\psi & \delta\theta \\ \delta\psi & 0 & -\delta\phi \\ -\delta\theta & \delta\phi & 0 \end{bmatrix} \tag{4.47}$$

where R_l^v is the ideal matrix, and $\widehat{Rv}_l$ the matrix provided by the navigation system (real). From eq. 4.46 we have:

$$R_v^l = (R_l^v)^T = \left(I + \widetilde{R} \right)^T \cdot \left(\widehat{R_l^v} \right)^T = \left(I - \widetilde{R} \right) \cdot \widetilde{R_v^l} \tag{4.48}$$

In similar way, for the R_p^lmatrix (ECEF to ENU), in which are considered the latitude and longitude errors:

$$\delta\lambda = \lambda - \widehat{\lambda}; \delta\phi = \phi - \widehat{\phi}; \delta h = h - \widehat{h}; \tag{4.49}$$

$$R_p^l = \left(I - \widetilde{P} \right) \cdot \widehat{R_p^l} \tag{4.50}$$

where R_p^l is the ideal matrix, and $\widehat{R_p^l}$ the matrix provided by the navigation system (real). and $\widetilde{P}$ has the form:

$$\widetilde{P} = \begin{bmatrix} 0 & -\delta p_z & \delta p_y \\ \delta p_z & 0 & -\delta p_x \\ -\delta p_y & \delta p_x & 0 \end{bmatrix} \tag{4.51}$$

with: $\delta p_x = -\delta\phi, \delta p_y = \cos(\widehat{\phi}) \cdot \delta\lambda, \delta p_z = \sin(\widehat{\phi}) \cdot \delta\lambda$ One of the form of the attitude Poisson equation is

$$\dot{R_l^v} = R_l^v \cdot \widetilde{\omega_l} - \widetilde{\omega_v} \cdot R_l^v \tag{4.52}$$

where $\widetilde{\omega}_l$ and $\widetilde{\omega}_v$ have the expressions given by equations 4.19. Due to the erroneous measurements, the inertial system integrates the next equation:

$$\dot{\widehat{R}}_l^v = \widehat{R}_l^v \cdot \widehat{\widetilde{\omega}}_l - \widehat{\widetilde{\omega}}_v \cdot \widehat{R}_l^v \tag{4.53}$$

Thus, it results:

$$\dot{\widehat{R}}_l^v = \widehat{R}_l^v \cdot \left(\widetilde{\omega}_l - \delta\widetilde{\omega}_l\right) - \left(\widetilde{\omega}_v - \delta\widetilde{\omega}_v\right) \cdot \widehat{R}_l^v \tag{4.54}$$

with

$$\delta\widetilde{\omega}_v = \begin{bmatrix} 0 & -\delta\omega_{zv} & \delta\omega_{yv} \\ \delta\omega_{zv} & 0 & -\delta\omega_{xv} \\ -\delta\omega_{yv} & \delta\omega_{xv} & 0 \end{bmatrix} \tag{4.55}$$

$$\delta\widetilde{\omega}_l = \begin{bmatrix} 0 & -\delta\omega_{zvl} & \delta\omega_{yl} \\ \delta\omega_{zl} & 0 & -\delta\omega_{xl} \\ -\delta\omega_{yl} & \delta\omega_{xl} & 0 \end{bmatrix} \tag{4.56}$$

From eq. 4.47 we obtain:

$$R_l^v - \widehat{R}_l^v = \widehat{R}_l^v \cdot \widetilde{R} \tag{4.57}$$

which, through derivation, implies:

$$\dot{R}_l^v - \dot{\widehat{R}}_l^v = \dot{\widehat{R}}_l^v \cdot \widetilde{R} + \widehat{R}_l^v \cdot \dot{\widetilde{R}} \tag{4.58}$$

so

$$\widehat{R}_l^v \cdot \dot{\widetilde{R}} = \dot{R}_l^v - \dot{\widehat{R}}_l^v \cdot \left(I + \widetilde{R}\right) \tag{4.59}$$

Substituting and rearanging above relations we get:

$$\dot{\widetilde{R}} = \left\{\widetilde{R} \cdot \widetilde{\omega}_l - \widetilde{\omega}_l \cdot \widetilde{R}\right\} + \left\{\delta\widetilde{\omega}_l\right\} - \left\{\left(\widehat{R}_l^v\right)^T \cdot \delta\widetilde{\omega}_v \cdot \widehat{R}_l^v\right\} \tag{4.60}$$

With formulas (4.61) and (4.30) it results:

$$\begin{aligned} \left[\vec{\omega_l}\right]_l = [\omega_{xl}\ \omega_{yl}\ \omega_{zl}]^T &= \left[-\frac{v_{yl}}{R_\phi + h}, \frac{v_{xl}}{R_\lambda + h} + \Omega\cos\phi, \frac{v_{xl}}{R_\lambda + h}\tan\phi + \Omega\sin\phi\right]^T = \\ &= \left[-\dot{\phi}, \dot{\lambda}\cos\phi + \Omega\cos\phi, \dot{\lambda}\sin\phi + \Omega\sin\phi\right]^T \end{aligned} \tag{4.61}$$

Evaluating the terms of differential equation (4.60), we obtain:

$$\widetilde{R}\cdot\widetilde{\omega}_l-\widetilde{\omega}_l\cdot\widetilde{R}=\begin{bmatrix}0 & -(\omega_{yl}\delta\phi-\omega_{xl}\delta\theta) & \omega_{xl}\delta\psi-\omega_{zl}\delta\phi\\ \omega_{yl}\delta\phi-\omega_{xl}\delta\theta & 0 & -(\omega_{zl}\delta\theta-\omega_{yl}\delta\psi)\\ -(\omega_{xl}\delta\psi-\omega_{zl}\delta\phi) & \omega_{zl}\delta\theta-\omega_{yl}\delta\psi & 0\end{bmatrix} \tag{4.62}$$

$$[\delta\omega_l]_l=\begin{bmatrix}\delta\omega_{xl}\\ \delta\omega_{yl}\\ \delta\omega_{zl}\end{bmatrix}=\begin{bmatrix}-\dot{\delta\phi}\\ -\sin\phi\cdot\dot{\lambda}\cdot\delta\phi+\cos\phi\cdot\delta\dot{\lambda}-\Omega\cdot\sin\phi\cdot\delta\phi\\ +\cos\phi\cdot\dot{\lambda}\cdot\delta\phi+\sin\phi\cdot\delta\dot{\lambda}+\Omega\cdot\cos\phi\cdot\delta\phi\end{bmatrix} \tag{4.63}$$

and for the product $\left[\left(\widehat{R_l^v}\right)^T\cdot\delta\widetilde{\omega}_v\cdot\widehat{R_l^v}\right]$ are given by the following matrix elements expressions

Therefore, the elements of the matrix $\dot{\widetilde{R}}$ from equation 4.60 are calculated by using relations of

$a_{11}=a_{22}=a_{33}=$	0
$a_{21}=-a_{12}=$	$-\sin\widehat{\theta}\cdot\delta\omega_{xv}-\sin\widehat{\phi}\cdot\cos\widehat{\theta}\cdot\delta\omega_{yv}+\cos\widehat{\phi}\cdot\cos\widehat{\theta}\cdot\delta\omega_{zv}$
$a_{13}=-a_{31}=$	$+\cos\widehat{\theta}\cdot\sin\widehat{\phi}\cdot\delta\omega_{xv}+\left(\sin\widehat{\phi}\cdot\sin\widehat{\theta}\cdot\sin\widehat{\psi}+\cos\widehat{\phi}\cdot\cos\widehat{\psi}\right)\cdot\delta\omega_{yv}+$
	$+\left(\cos\widehat{\phi}\cdot\sin\widehat{\theta}\cdot\sin\widehat{\psi}-\sin\widehat{\phi}\cdot\cos\widehat{\psi}\right)\cdot\delta\omega_{zv}$
$a_{13}=-a_{31}=$	$+\cos\widehat{\theta}\cdot\cos\widehat{\phi}\cdot\delta\omega_{xv}+\left(\sin\widehat{\phi}\cdot\sin\widehat{\theta}\cdot\cos\widehat{\psi}-\cos\widehat{\phi}\cdot\sin\widehat{\psi}\right)\cdot\delta\omega_{yv}+$
	$+\left(\cos\widehat{\phi}\cdot\sin\widehat{\theta}\cdot\cos\widehat{\psi}+\sin\widehat{\phi}\cdot\sin\widehat{\psi}\right)\cdot\delta\omega_{zv}$

the form:

$r_{11}=r_{22}=r_{33}=$	0
$r_{21}=-r_{12}=$	$(\omega_{yl}\delta\phi-\omega_{xl}\delta\theta)-a_{21}+\delta\omega_{zl}$
$r_{13}=-r_{31}=$	$(\omega_{xl}\delta\psi-\omega_{zl}\delta\phi)-a_{13}+\delta\omega_{yl}$
$r_{32}=-r_{23}=$	$(\omega_{zl}\delta\theta-\omega_{yl}\delta\psi)-a_{32}+\delta\omega_{xl}$

Taking into account that:

$$\left[\delta\vec{\omega_v}\right]_v=[\delta\omega_{xv},\delta\omega_{yv},\delta\omega_{zv}]^T \tag{4.64}$$

can be quickly demonstrated that the elements described by formulas 4.3 come from a product by the form $\left\{\left(\widehat{R_l^v}\right)^T\cdot\left[\delta\vec{\omega_v}\right]_v\right\}$ Thus, denoting with:

$$\left[\vec{\Phi}\right]_l=[\deg\phi,\delta\theta,\delta\psi]^T \tag{4.65}$$

the vector having the components equal with the errors of the attitude angles, it appears that:

$$\begin{bmatrix} \omega_{zl}\delta\theta - \omega_{yl}\delta\psi \\ \omega_{xl}\delta\psi - \omega_{zl}\delta\phi \\ \omega_{yl}\delta\phi - \omega_{xl}\delta\theta \end{bmatrix} = -\left[\vec{\omega}_l \times \vec{\Phi}\right]_l \tag{4.66}$$

and the matrix equation 4.60 can be transfigured as:

$$\left[\dot{\vec{\Phi}}\right]_l = -\left[\vec{\omega}_l \times \vec{\Phi}\right]_l - \left[\left(\widehat{R_l^v}\right)^T \cdot \left[\delta\vec{\omega_v}\right]\right]_v + \left[\delta\vec{\omega_l}\right]_l \tag{4.67}$$

where $\left[\left(\widehat{R_l^v}\right)^T \cdot \left[\delta\vec{\omega_v}\right]\right]_v$ represents the errors due to gyro measurements in ENU frame, and $\left[\delta\vec{\omega_l}\right]_l$ contains the errors of the angular velocities assessment committed by navigation processor. Equation 4.67 is the differential equation of the attitude error. the equation that characterizes the speed error evolution in time is as follow:

$$\left[\delta\dot{\vec{v}}\right]_l = -\left[\vec{\Phi}\right]_l \cdot \left[\vec{f}\right]_v + \widehat{R_v^l} \cdot \left[\delta\vec{f}\right]_v + \left[\delta\vec{g_a}\right]_l - \left[\left(\vec{\omega}_l + \Omega\right) \times \delta\vec{v}\right]_l - \left[\left(\delta\vec{\omega}_l + \delta\Omega\right) \times \vec{v}\right]_l \tag{4.68}$$

$$\left[\delta\vec{g_a}\right]_l \simeq \left[0, 0, -2\frac{g}{a} \cdot \delta h\right] \tag{4.69}$$

$$\left[\delta\vec{\Omega}\right]_l \simeq [0,\ -\Omega \cdot \sin\phi \cdot \delta\phi,\ \Omega \cdot \cos\phi \cdot \delta\phi]^T \tag{4.70}$$

from the next equation:

$$\begin{aligned} v_{xl} &= (R_\lambda + h) \cdot \cos\phi \cdot \dot{\lambda} \\ v_{yl} &= (R_\phi + h) \cdot \dot{\phi} \\ v_{zl} &= \dot{h} \end{aligned} \tag{4.71}$$

we obtain the positioning errors on the axes of the ENU frame:

$$\begin{aligned} \delta x_l &= (R_\lambda + h) \cdot \cos\phi \cdot \delta\lambda \\ \delta y_l &= (R_\phi + h) \cdot \delta\phi \\ \delta z_l &= \delta h \end{aligned} \tag{4.72}$$

By derivation with respect to time, equations 4.73 imply after rearrangement we get:

$$\begin{aligned}
\delta\dot{x}_l &= \delta v_{xl} - (R_\phi + h)\cdot\sin\phi\cdot\left[\dot{\phi}\cdot\delta\lambda - \dot{\lambda}\cdot\delta\phi\right] + \cos\phi\cdot\left[\delta\dot{\lambda} - \dot{\lambda}\cdot\delta h\right] \\
\delta\dot{x}_l &= \delta v_{yl} + \dot{h}\cdot\delta\phi - \dot{\phi}\cdot\delta h \\
\delta\dot{x}_l &= \delta v_{zl}
\end{aligned} \tag{4.73}$$

If we denote:

$$\left[\vec{p}\right]_l = [\delta p_x,\ \delta p_y,\ \delta p_z]^T = \left[-\delta\phi,\ \cos\widehat{\phi}\cdot\delta\lambda,\ \sin\widehat{\phi}\cdot\delta\lambda\right]^T \tag{4.74}$$

and we denote

$$\left[\dot{\vec{r}}\right]_l = \left[\delta\dot{x}_l, \delta\dot{y}_l, \delta\dot{z}_l\right] \tag{4.75}$$

the equation characterizing the evolution in time of the positioning error (eq. (83)) becomes:

$$\left[\delta\dot{\vec{r}}\right]_l = \left[\delta\vec{v}\right]_l + \left[\vec{p}\times\vec{v}\right]_l - \left[\vec{\omega_r}\times\delta\vec{r}\right]_l \tag{4.76}$$

In conclusion, the error model of the navigation algorithm in terrestrial non-inertial reference frames by using attitude matrices is described by next equations:

$$\begin{cases}
\left[\dot{\vec{\Phi}}\right]_l = -\left[\vec{\omega_l}\times\vec{\Phi}\right]_l - \left[\left(\widehat{R_l^v}\right)^T\cdot\left[\delta\vec{\omega_v}\right]\right]_v + \left[\delta\vec{\omega_l}\right]_l \\
\left[\delta\dot{\vec{v}}\right]_l = -\left[\vec{\Phi}\right]_l\left[\vec{f}\right]_v + \widehat{R_v^l}\left[\delta\vec{f}\right]_v + \left[\delta\vec{g_a}\right]_l - \left[\left(\vec{\omega_l} + \Omega\right)\times\delta\vec{v}\right]_l - \left[\left(\delta\vec{\omega_l} + \delta\Omega\right)\times\vec{v}\right]_l \\
\left[\dot{\vec{r}}\right]_l = \left[\delta\vec{v}\right]_l + \left[\vec{p}\times\vec{v}\right]_l - \left[\vec{\omega_r}\times\delta\vec{r}\right]_l
\end{cases} \tag{4.77}$$

The resulting model consists of a system of coupled differential equations and contains nine variables: three variables are errors in the determination of the attitude angles $(\delta\phi, \delta\theta, \delta\psi)$, three variables are errors in the determination of the speed $(\delta v_{xl}, \delta v_{yl}, \delta v_{zl})$ and three variables are errors in determination of the position $(\delta x_l, \delta y_l, \delta z_l)$. The input variables of the model are the errors of the six inertial sensors used in the strap-down inertial navigation system. In addition to the nine variables, in the error model are involved the global positioning errors of the vehicle $(\delta\lambda, \delta\varphi, \delta h)$, linking the nine differential equations. Numerical integration of the error model is rather difficult due to the couplings between its equations, but also due to the time evolution considered for inertial sensors errors. It can be performed, however, some numerical simulations, for different

sources of error affecting the inertial sensors, in order to highlight their influence on the final errors of the navigation algorithm.

4.4 Numerical simulations

The validation of the navigation algorithm and of its error model is achieved by building Matlab/Simulink models for them followed by numerical simulation of these models for several navigation particular cases. Following is conducted a study of the dependence of the inertial navigator outputs errors by the errors of the used inertial sensors. For this purpose, the Matlab/Simulink models built for acceleration and gyro sensors are used; on the inertial navigator inputs are considered three miniaturized optical integrated accelerometers (MOEMS) and three fiber optic gyros with the associated errors according to their data sheets. Due to the fact that the accelerometer and gyro software developed models allow users to work independently with each sensor error in the theoretical model, are studied the influences of the noise, bias and scale factor sensors errors on the navigation solution components. Simulations are performed for three different navigation cases, the vehicle having the same initial position in all three cases: 1) the vehicle is immobile, 2) the vehicle runs at $0.1g$ acceleration on the x-axis, 3) The vehicle is subjected to turning with angular velocity $0.1 degree/s$, while running on the track with acceleration $0.1g$ along x-axis, which means the sensing of an acceleration of -0.0516 m/s^2 ($-0.0053g$) along y-axis.

Thus, starting from the navigation algorithm block scheme in Fig. 4.3 the Matlab/Simulink model in Fig.4.4 is obtained. Also, the software implementation of the navigator error model leads to the Matlab/Simulink model in Fig.4.5.

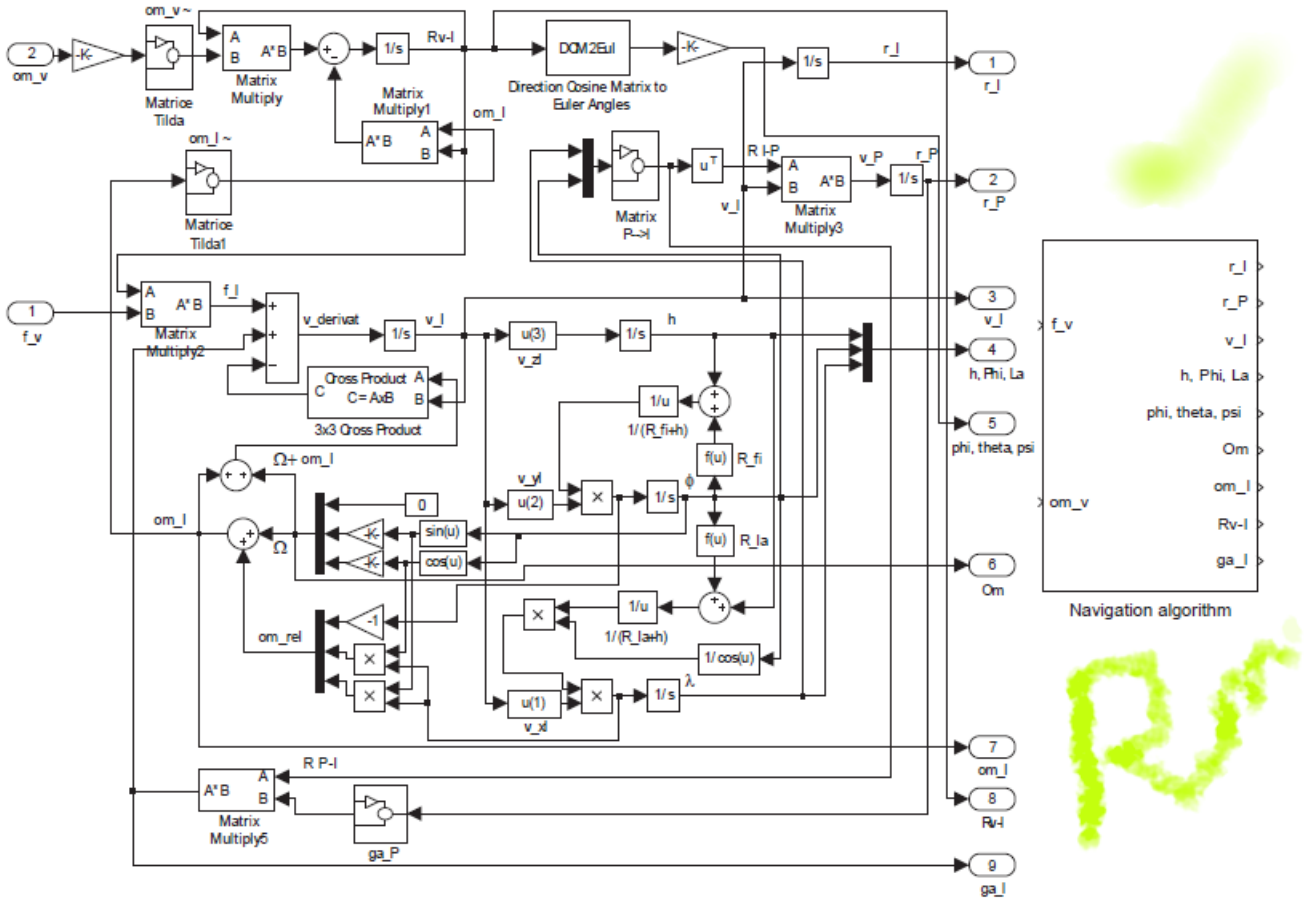

Figure 4.4: Matlab/Simulink model of the navigation algorithm.

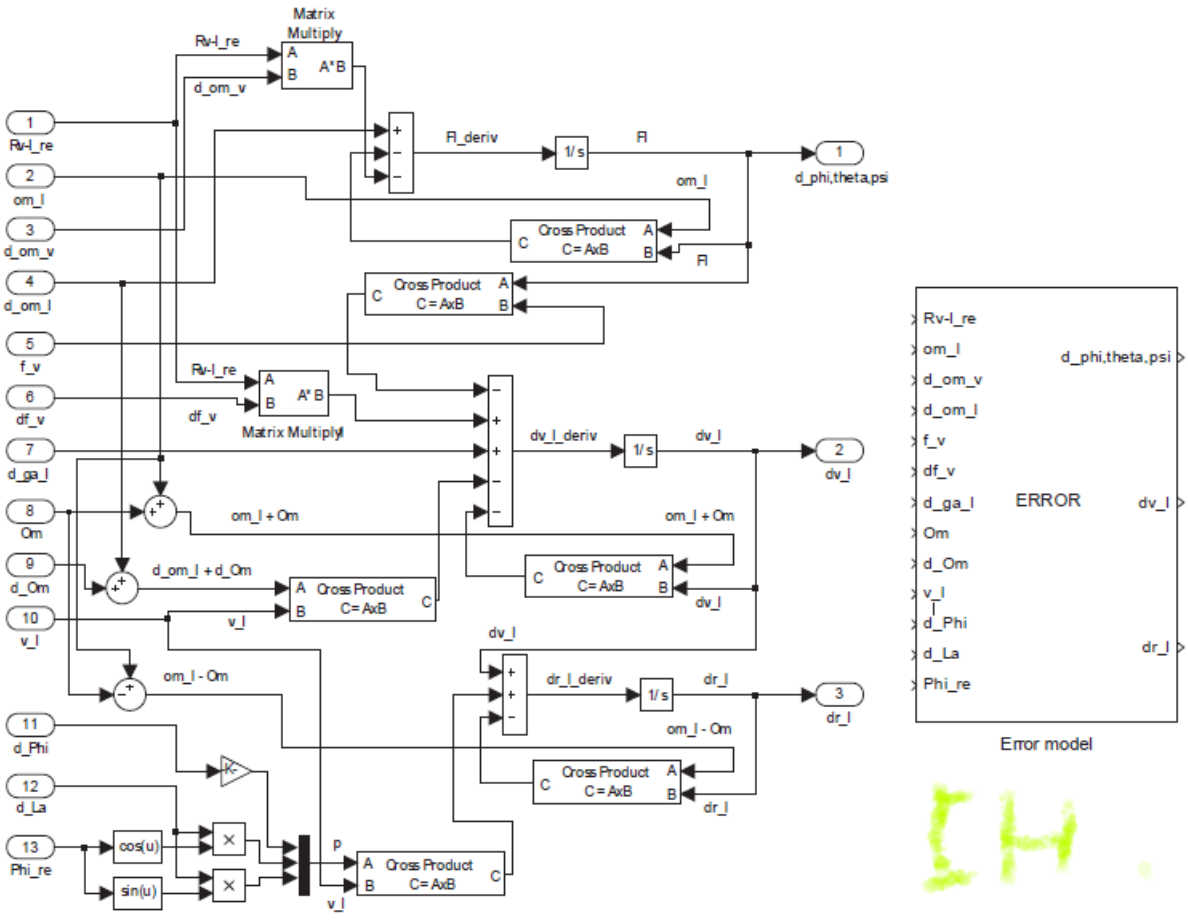

Figure 4.5: Matlab/Simulink implementation of the inertial navigator error model.

Figure 4.6: Matlab Simulink validation model.

With these two models it results the validation model in Fig. 4.4; "REAL" and "IDEAL" are blocks modelling the navigation algorithm (as in Fig. 4.4), having as inputs accelerations and angular speeds signals disturbed by the errors of strap-down inertial sensors, respectively undisturbed by the errors of strap-down inertial sensors. "ERROR" is a block by the form in Fig. 4.5. The input blocks "Acc" and "Gyro" are accelerometers and gyros models as in Fig. 4.1 and Fig. 4.2, and theirs outputs are applied to the "REAL" block. The values of the input constants are considered to be ideal signals, un-disturbed by the acceleration and rotation sensors, these being applied to the "IDEAL" block. Modelling and Simulation Based Matlab/Simulink of a Strap-Down Inertial Navigation System... The error model validation is realized through the comparison of the differences between the outputs of the "IDEAL" and "REAL" blocks with the outputs of the error model. In Fig. ========== a. are depicted the attitude angles errors, the first column containing the differences between the outputs of the "IDEAL" and "REAL" blocks, and the second column-the outputs of the error model. In the same mode are built Fig. ========== b. (for the positioning errors in ENU reference frame) and Fig. ========== c. (for the speed errors in ENU reference frame).

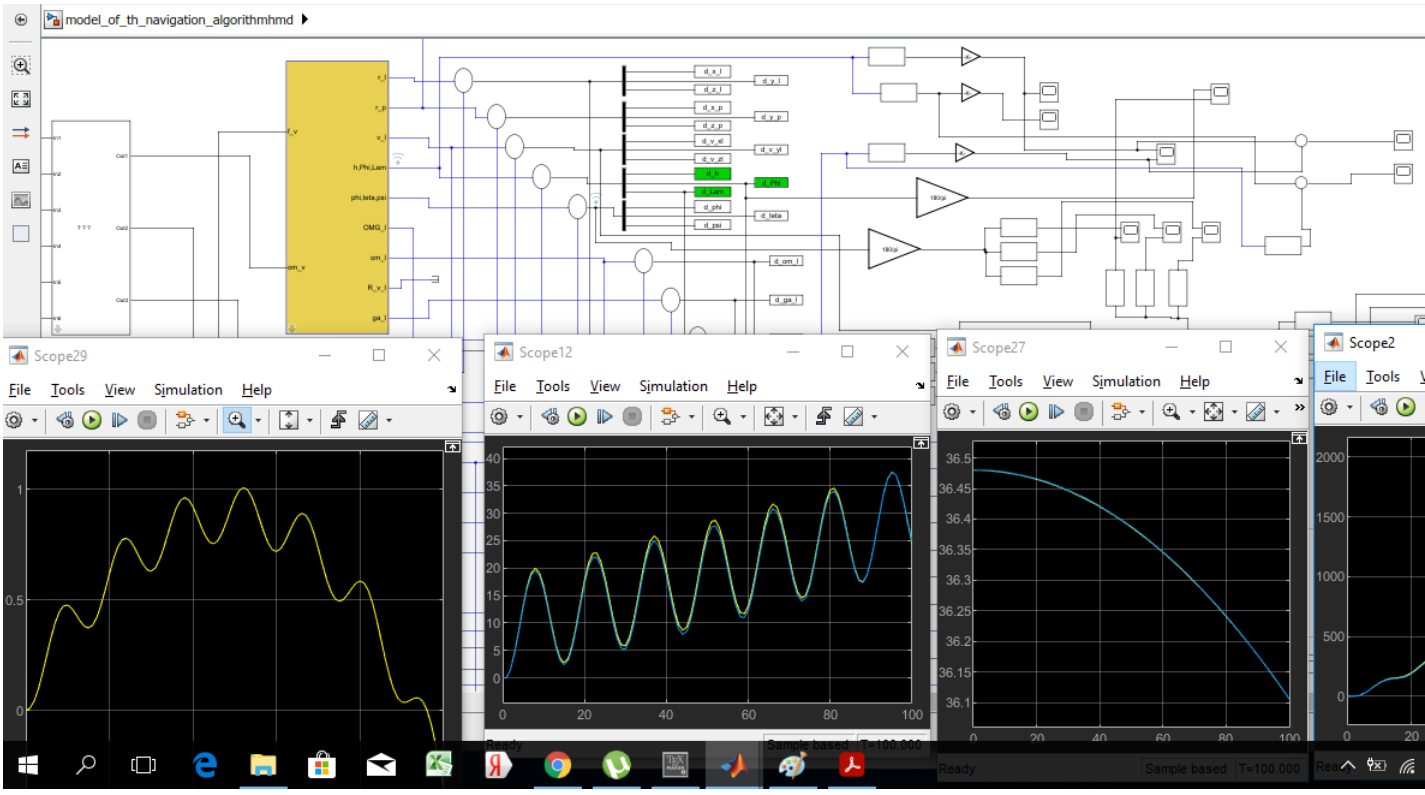

CONCLUSION

Main objectives of this work are to model and examine a model of an inertial navigation unit. The research in this work led to the following contributions: Development of a simulation method, which can be used to estimate the quality of a strapdown INS in a laboratory before its using in practice. The development of the mechanization of an inertial unit. The creation of a simulink interface that allows the determination of the various parameters of the inertial navigation. During the achievement of this work we were able to learn the method of mechanizing. Much difficulty have been presented in the creation of the simulink interface, and at the level of the very complicated that we gave a lot of time to figure it out. By now we have been familiar with this method and we have been able to set up the simulation of the position (latitude and longitude) velocity attitude and errors associated with those parameters. Finally. We hope that this document will be of assistance to new exploiters in this area.

Appendix A

the first appendix

A.1 Inertial Sensor Performance Characteristics

To assess an inertial sensor for a particular application, numerous characteristics must be considered.

- **Repeatability**: The ability of a sensor to provide the same output for repeated applications of the same input, presuming all other factors in the environment remain constant. It refers to the maximum variation between repeated measurements in the same conditions over multiple runs.
- **Stability**: This is the ability of a sensor to provide the same output when measuring a constant input over a period of time. It is defined for single run.
- **Drift**: The term drift is often used to describe the change that occurs in a sensor measurement when there is no change in the input. It is also used to describe the change that occurs when there is zero input.

A.2 Solution to Transformation Matrix

The time rate of change of a transformation matrix from the body frame into a computational frame k is where R is the transformation matrix from the body frame to the computational frame, and X is the skew-symmetric matrix associated with the angular velocities xx;xy;xz of the

body frame with respect to the computational frame Equation (5.75) requires the solution of nine differential equations in order to obtain the transformation matrix from the angular velocity data. A closed form solution of this equation will now be discussed. Assuming the angular velocity x is constant over the small time interval Dt, then the small incremental angular changes of the rotation of the body frame with respect to the computation frame k is

A.3 Solutions of the Quaternion Equation

DiscretDuring a short interval of time Dt, the angular velocity of the rotation x can be presumed constant, and the closed form of the discrete solution to the quaternion Eq. (5.91) ise Closed form (Analytical) Solution

Numerical Integration Methods If the rotation rate is slow, then standard numerical integration algorithms can also be used to solve the differential Eqs. (5.75) and (5.91). Euler's Method For a first-order differential equation

Bibliography

[1] Wen Zhang, Mounir Ghogho, and Baolun Yuan. Mathematical model and matlab simulation of strapdown inertial navigation system. *Modelling and Simulation in Engineering*, 2012, 2012.

[2] JL Weston and DH Titterton. Strapdown inertial navigation technology. *Institution of Electrical Engineers and American Institute of Aeronautics and Astronautics*, 2004.

[3] kvh2020. https://www.kvh.com/fog-and-inertial-systems/fiber-optic-gyros. 2020.

[4] Esmat Bekir. *Introduction to modern navigation systems*. World Scientific, 2007.

[5] JH Kwon and Ch Jekeli. A new approach for airborne vector gravimetry using gps/ins. *Journal of Geodesy*, 74(10):690–700, 2001.

[6] Jack B Kuipers. *Quaternions and rotation sequences: a primer with applications to orbits, aerospace, and virtual reality*. Princeton university press, 1999.

[7] Robert M Rogers. *Applied mathematics in integrated navigation systems*. American Institute of Aeronautics and Astronautics, 2007.

[8] *Matrices and Linear Algebra, Dover Publications,*. 1989.

[9] Amos Gilat. *MATLAB: An introduction with Applications*. John Wiley & Sons, 2009.

[10] Marian Mureşan. *Introduction to Mathematica® with applications*. Springer, 2017.

[11] Z Chen. Strapdown inertial navigation system principles. *Beijing: Astronautics Press*, 19:24, 1986.

[12] Neil Barbour and George Schmidt. Inertial sensor technology trends. *IEEE Sensors journal*, 1(4):332–339, 2001.

[13] Rachele Fermani, Tobias Mueller, Bo Zhang, Michael J Lim, and Rainer Dumke. Heating rate and spin flip lifetime due to near-field noise in layered superconducting atom chips. *Journal of Physics B: Atomic, Molecular and Optical Physics*, 43(9):095002, 2010.

[14] Amitava Bose, Somnath Puri, and Paritosh Banerjee. *Modern inertial sensors and systems*. PHI Learning Pvt. Ltd., 2008.

[15] Lucian T Grigorie and Ruxandra M Botez. Modeling and numerical simulation of an algorithm for the inertial sensors errors reduction and for the increase of the strap-down navigator redundancy degree in a low cost architecture. *Transactions of the Canadian Society for Mechanical Engineering*, 34(1):1–16, 2010.

If the rotation rate is slow, then standard numerical integration algor

This is a **tcolorbox**.